2015-06-01

Analysis of Multiple Collision-Based Periodic Orbits in Dimension Higher than One

Skyler C. Simmons
Brigham Young University - Provo

Analysis of Multiple Collision-Based Periodic Orbits in Dimension Higher than One

Skyler C. Simmons

A dissertation submitted to the faculty of
Brigham Young University
in partial fulfillment of the requirements for the degree of

Doctor of Philosophy

Lennard Bakker, Chair
Todd Fisher
Chris Grant
Ben Webb
Jared Whitehead

Department of Mathematics

Brigham Young University

June 2015

ABSTRACT

Analysis of Multiple Collision-Based Periodic Orbits in Dimension Higher than One

Skyler C. Simmons
Department of Mathematics, BYU
Doctor of Philosophy

We exhibit multiple periodic, collision-based orbits of the Newtonian n-body problem. Many of these orbits feature regularizable collisions between the masses. We demonstrate existence of the periodic orbits after performing the appropriate regularization. Stability, including linear stability, for the orbits is then computed using a technique due to Roberts. We point out other interesting features of the orbits as appropriate. When applicable, the results are extended to a broader family of orbits with similar behavior.

Keywords: Newtonian n-body problem, collision, regularization, stability, linear stability, Sitnikov problem

ACKNOWLEDGMENTS

I wish to thank my advisor, Dr. Bakker, for his support over the past years. I am again indebted very much to my family for their ever-constant love and encouragement.

The God who placed the planets in their orbits placed people in ours.

-Neal A. Maxwell

...All things denote there is a God; yea, even the earth, and all things that are upon the face of it, yea, and its motion, yea, and also all the planets which move in their regular form do witness that there is a Supreme Creator.

-Alma 30:44

CONTENTS

LIST OF FIGURES

CHAPTER 1. INTRODUCTION

Mathematically, the study of determining the motion of n point masses in space whose motion is governed by Newton's gravitational law is known as the Newtonian n-body problem. Notationally, if $\{q_1, q_2, ..., q_n\}$ represent the positions of the bodies in $\mathbb{R}^k$ ($k = 1, 2$, or 3) with masses $\{m_1, m_2, ..., m_n\}$ respectively, then their motion is governed by the system of differential equations

$$m_i \ddot{q}_i = \sum_{i \neq j} \frac{m_i m_j (q_j - q_i)}{|q_i - q_j|^3}, \tag{1.1}$$

where the dot represents the derivative with respect to time. Despite hundreds of years of study and the relatively recent development of computer ODE solvers, many open questions about the n-body problem remain.

Linearly stable symmetric periodic orbits are one aspect of the n-body problem. Recently, Roberts [1] desribed an analytic-numerical method for determining the linear stability of a symmetric periodic orbit of a Hamiltonian system. He applied this method to the time-reversible collision-free figure-eight orbit in the equal mass three-body problem numerically discovered by Moore [2] and whose existence was proven by Chenciner and Montgomery [3]. (Other such *choreographic solutions*, in which all bodies trace out the same curve in space with a time shift between them, were found numerically by Simó [4].) Roberts' method shows that the figure eight orbit is linearly stable. The method uses the symmetries to factor a matrix similar to the monodromy matrix for the periodic orbit into an integer power of the product of two involutions. One of the two involutions depends on the linearized dynamics along only a part of the periodic orbit. For the figure eight this part is one-tweltfth of the full orbit since it has a symmetry group isomorphic to the group $D_3 \times \mathbb{Z}_2$ of order 12. (Here the dihedral group D_k is the group of symmetries of the regular k-gon.) The eigenvalues of the product of the two involutions are then reduced to the numerical computation of a few real numbers. (This technique will be outlined and applied in many examples in this work.)

One aspect of the n-body problem that has been getting much attention of late are orbits in-

volving collision singularities. A *collision singularity* occurs when $q_i = q_j$ for some $i \neq j$. In the equations governing the motion, this results in a zero denominator in one or more terms in the sum. Under certain conditions, these collisions can be *regularized* and the solutions can be continued past collision. Binary collisions, triple collisions, etc., are discussed at length in [5] (see especially Ch. 1, section 6). The Simultaneous Binary Collision (SBC) problem has been widely studied as well, both analytically and numerically. Simó [6] showed that the block regularization in the cases of the n-body problem which reduce to one-dimensional problems is differentiable, but the map passing from initial to final conditions (in suitable choices of transversal sections) is exactly $C^{8/3}$. Ouyang and Yan [7] give another approach for the regularization and analyze some properties of SBC solutions in the collinear four-body problem. Elbialy [8] studied the nature of the collision-ejection orbits associated to SBC.

Schubart [9] numerically discovered a singular periodic orbit in the collinear equal mass three-body problem. The orbit alternates between binary collisions. Hénon [10] extended Schubart's numerical investigations to the case of unequal masses. Venturelli [11] and Moeckel [12] proved the existence of the Schubart orbit when the outer masses are equal and the inner mass is arbitrary. Shibiyama [13] recently demonstrated the existence of the arbitrary-mass version. The linear stability of the Schubart orbit was determined numerically by Hietarinta and Mikkola [14] revealing that linear stability occurs for some but not all of the choices of the three masses. Sweatman ([15] and [16], see also [17]) numerically found and determined the linear stability of a Schubart-like orbit in the symmetric collinear four-body problem with outer bodies having mass 1, and the inner pair having mass m. This Schubart-like periodic orbit alternates between simultaneous binary collisions (SBC) and inner binary collisions. Ouyang and Yan [18] proved the existence of this orbit. In the regularized setting, this periodic orbit has a symmetry group isomorphic to D_2, of which both of the generators are time-reversing symmetries. The regularization of these singular periodic orbits is achieved by a generalized Levi-Civita type transformation and an appropriate scaling of time, as adapted from Aarseth and Zare [19]. (See also [20].) Non-Schubart-like linearly stable periodic orbits in the collinear three-body problem were found by Saito and Tanikawa for certain

choices of the masses [21], [22], [23].

Planar orbits with regularizable collisions have also been studied. Among the first of these is the rhomboidal four-body orbit, which features two pairs of bodies: one pair on the x-axis and the second on the y-axis. The pairs collide at the origin in an alternating fashion. This orbit was shown to exist analytically in multiple independent papers (by Yan in [24] and Martinez in [25] for equal masses, [13] for symmetric masses). Additionally, Yan showed that for equal masses, the orbit is linearly stable.

Other planar orbits with singularities have also been studied. A planar four-body orbit featuring simultaneous binary collisions was described in [26] (Chapter 4 of this work). The orbit was shown to be linearly stable in [27] (Chapter 5). It was later shown that this orbit could be numerically extended to symmetric masses in [28] (see also [29] and Chapter 6), and linear stability for this extension was shown for an interval of certain mass ratios in [30] (Chapter 7).

A different planar orbit was discussed in [31] (also Chapter 8). This orbit is known as the rhomboidal symmetric-mass orbit. This orbit itself is another solution of the Caledonian problem (see, for example, [32] and [33]) which features regularized collisions between pairs of bodies. In a separate study of the rhomboidal four-body problem, Waldvogel [34] notes that "sufficiently simple systems may bear the chance of permitting theoretical advances," and identifies the rhomboidal problem as one such system.

More generally, analytic existence of many families of orbits with two degrees of freedom and regularizable singularities was recently proven by Shibayama in [13] and Martinez in [25]. The rhomboidal four-body orbit and the equal-mass planar SBC orbits are special cases of one of the many orbits presented in each.

This work is a compilation of multiple results related to stable, periodic, collision-based orbits. Specifically, each of Chapters 4 through 9 were published in various journals, and shed some light on this problem as a whole. (As a historical note, the work corresponding to Chapters 4 through 6 was done during my undergraduate years at BYU. Chapter 7 was done while earning my MS, and Chapters 8 and 9 were done during my time as a PhD student.) Although reasonable attempts

to make the notation consistent have been made, it will be helpful to the reader to consider all variables as re-defined at the beginning of each new chapter.

The remainder of the paper is as follows: In Chapter 2, we review some of the relevant principles of the n-body problem, Hamiltonian systems, and stability theory. Chapter 3 demonstrates some essential results from Roberts' stability calculation technique, which will be used in multiple instances. Chapters 4 through 7 are all results related to a symmetric, planar, four-body orbit that were developed over a few years. Specifically, Chapter 4 establishes the existence of the orbit. Chapter 5 demonstrates its linear stability. Chapter 6 shows the extension of the orbit beyond the equal-mass case. Chapter 7 gives the linear stability in the extended case. Next, Chapter 8 gives similar results for another orbit, called the rhomboidal orbit. It will be noted that much of the analysis in that chapter is much simpler than that of 4 - 7, due mostly to the relative simplicity of the orbit considered. Lastly, Chapter 9 gives an interesting result that arose from considering the limiting ($m \to 0$) case of the rhomboidal orbit in Chapter 8. This result provides a connection between the rhomboidal orbit and the so-called Sitnikov problem, which will be introduced in Chapter 9.

CHAPTER 2. BACKGROUND

2.1 THE n-BODY PROBLEM

In the *Principia Mathematica* [35], published in 1687, Newton outlined many governing principles of the motion of physical objects. Among the most well-known are his three laws of motion. Explicitly, we have

1. An object in motion will remain in motion unless acted upon by an outside force. An object at rest will remain at rest unless acted upon by an outside force.

2. Force equals mass times acceleration, or $F = ma$.

3. To every action there is an equal and opposite reaction.

Furthermore, Newton's law of universal gravitation states that for two objects of mass m_1 and m_2 separated by a distance r, the force due to gravity between them is given by

$$F_{\text{grav}} = \frac{Gm_1m_2}{r^2},$$

where G is some constant depending on the units chosen. In SI units, with r in meters, m_i in kilograms, and F_{grav} in Newtons, G has the value $6.673 \times 10^{-11}\ N(m/kg)^2$.

In the n-body problem, we consider an isolated system of n point masses with mass m_i in $\mathbb{R}^d$. Most often, $d = 2$ or 3. Assuming that gravity is the sole force acting on the particles, combining the laws $F = ma$ with the law of universal gravitation gives a system of differential equations that govern the motion of the particles. Specifically, if q_i represents the position of the ith particle, then its acceleration is $\ddot{q}_i$, where the dot represents the derivative with respect to time. The force due to gravity is simply the sum of the gravitational forces exerted by the remaining bodies:

$$F_i = \sum_{i \neq j} \frac{m_i m_j}{|q_i - q_j|^2},$$

where units are chosen so that $G = 1$. Since $F_i = m_i \ddot{q}_i$, and q_i is a vector quantity, we then have

$$m_i \ddot{q}_i = \sum_{i \neq j} \frac{m_i m_j}{|q_i - q_j|^2} \left(\frac{(q_j - q_i)}{|q_i - q_j|} \right) = \sum_{i \neq j} \frac{m_i m_j (q_j - q_i)}{|q_i - q_j|^3}, \tag{2.1}$$

where the extra terms constitute a unit vector in the direction from the ith point mass to the jth point mass. This is then a system of nd second-order differential equations. The standard technique is to split this further into a system of $(2 \times n \times d)$ first-order differential equations by introducing a new set of variables p_i that are related to the quantities $\dot{q}_i$. In the n-body problem, this is traditionally done by

$$\dot{q}_i = \frac{p_i}{m_i}, \quad \dot{p}_i = \sum_{i \neq j} \frac{m_i m_j (q_j - q_i)}{|q_i - q_j|^3}.$$

Physically, the new variables p_i give the momentum of the point masses, and the quantity p_i/m_i is the velocity.

2.2 Hamiltonian Dynamics

A *Hamiltonian System* is a system of $2n$ differential equations that arise from a function (called a *Hamiltonian*) of the form $H(q_1, ..., q_n, p_1, ..., p_n)$. The variables q_i and p_i evolve according to the ODEs

$$\frac{dq_i}{dt} = \frac{\partial H}{\partial p_i}, \quad \frac{dp_i}{dt} = -\frac{\partial H}{\partial q_i}.$$

The function H is called the *Hamiltonian* for the resulting system of differential equations. For the n-body problem, if we define functions K and U by

$$K = \sum_{i=1}^{n} \frac{p_i^2}{2m_i} \quad U = \sum_{i \neq j} \frac{m_i m_j}{|q_j - q_i|},$$

setting $H = K + U$ gives the n-body problem as a Hamiltonian system. Note that K here is simply the sum of terms of the form $mv^2/2$, the familiar equation for kinetic energy from physics. Similarly, U is the potential energy for the system, which is only dependent upon masses and positions.

Mathematically, this gives differential equations $\dot{q}_i$ and $\dot{p}_i$ which depend only upon q_i and p_i.

It may be the case that the function H depends on quantities other than q_i and p_i. The most common extra non-constant quantity is time. In this case, we may still take the same partial derivatives as above, and the resulting derivatives for q_i and p_i will also depend upon time. In this circumstance, we say we have a *time-dependent Hamiltonian system*. This will be the case in Chapter 9.

Hamiltonian systems, time-dependent or not, have a number of highly desirable and useful properties. The most relevant will be explained in the following sections.

2.3 Conserved Quantities

Let $H(q_i, p_i)$ generate a Hamiltonian system. Then there are a number of time-invariant quantities, called *first integrals*, for the resulting system. The first of these is H itself. This is easy to show, as

$$\begin{aligned}\frac{dH}{dt} &= \sum_{i=1}^{n} \frac{\partial H}{\partial q_i}\frac{\partial q_i}{\partial t} + \frac{\partial H}{\partial p_i}\frac{\partial p_i}{\partial t} \\ &= \sum_{i=1}^{n} \frac{\partial H}{\partial q_i}\frac{\partial H}{\partial p_i} - \frac{\partial H}{\partial p_i}\frac{\partial H}{\partial q_i} \\ &= 0.\end{aligned}$$

Note that this is true for Hamiltonian systems in general, so long as they are not time-dependent. The remaining fixed quantities apply specifically to the n-body problem. Using the same notations as in Section 2.2, there are three extra first integrals:

1. Net momentum: $\sum_{i=1}^{n} p_i$,
2. Center of mass: $\sum_{i=1}^{n} m_i q_i$,
3. Angular momentum: $\sum_{i=1}^{n} m_i (q_i \times \dot{q}_i)$.

(For angular momentum, when working in $\mathbb{R}^2$, simply treat each point as a vector in $\mathbb{R}^3$ with zero z component.) Evaluating the derivative for net momentum, we get

$$\sum_{i=1}^{n} \dot{p}_i = \sum_{i=1}^{n} \sum_{i \neq j} \frac{m_i m_j (q_j - q_i)}{|q_i - q_j|^3}.$$

Each of these terms cancels in pairs, as the $q_j - q_i$ term is precisely the negative of the $q_i - q_j$ term, which occurs when the values of i and j are reversed in the summations. Hence, the net momentum for the system is constant. If we assume that the net momentum is zero (which is physically sensible from a proper reference frame), we can then show that

$$\sum_{i=1}^{n} m_i \dot{q}_i = \sum_{i=1}^{n} p_i = 0,$$

so the center of mass is constant as well. (In practice, this is often set to be at the origin.) The angular momentum can be similarly evaluated, and results in positive and negative versions of the same terms appearing in a summation, similar to the evaluation of net momentum. (We omit the lengthy calculations here.) It can also be shown (see Chapter 5 of [5], also [36]) that there are no additional algebraic integrals of the n-body problem. More specifically, there are no other simple algebraic expressions whose derivatives are zero.

2.4 CHANGE OF VARIABLES

It is common practice to introduce a change of variables when studying the n-body problem that are more natural to the system being studied. In particular, exploiting the above conserved quantities can reduce the number of equations that need to be studied. Changing the variables being used also requires a change in the equations as well. As a simple example, consider the differential equation

$$\dot{y} = y.$$

If we make the change of variables $x = y^3$, then we have (after solving for x)

$$\dot{x} = (dx/dy)(dy/dt) = (3y^2)(y) = 3y^3 = 3x.$$

More complicated changes of variables (e.g. involving multiple variables) follow along the same line, but involve more algebra.

An important class of variable transformations in Hamiltonian systems is the class of *canonical transformations*. These are transformations that preserve a Hamiltonian structure. Namely, if $H(q_i, p_i)$ is a Hamiltonian system, and $Q_i = Q_i(q_i, p_i)$ and $P_i = P_i(q_i, p_i)$ is a coordinate transformation, then the transformation is canonical if

$$\dot{Q}_i = \frac{\partial H(Q_i, P_i)}{\partial P_i}, \quad \dot{P}_i = -\frac{\partial H(Q_i, P_i)}{\partial Q_i}.$$

It may be the case that the value of $H(q_i, p_i)$ and $H(Q_i, P_i)$ are different for corresponding points. In this case, there is some number ε for which $H(q_i, p_i) = \varepsilon H(Q_i, P_i)$ for all time. Then the transformation is called *canonical with multiplier* ε. When $\varepsilon = 1$, the transformation is usually simply referred to as *canonical*.

Canonical transformations themselves arise from taking derivatives of other functions, called *generating functions*. If F is a function of $2n$ variables $F(q_i, P_i)$ with $Q_i(q_i, p_i) = \partial F/\partial P_i$ and $p_i(Q_i, P_i) = \partial F/\partial q_i$, then the resulting change of variables is canonical. The coordinates can then be transformed when the equations for Q_i have been inverted. (Full details of this, in terms of symplectic forms, is given in Chapter 6 of [37].)

2.5 Collisions and Regularization

A *collision singularity* of the n-body problem occurs at a time when $q_i = q_j$ for some $i \neq j$. This causes a zero-denominator to appear in Equation 2.1. Physically, this corresponds to a collision of two (or more) of the point masses at some point in space. (The term *collision singularity* is used as there are other types, called *non-collision singularities*, which will not be discussed in this work.

The work by Xia [38] is the chief example.)

It is possible to *regularize* certain collisions in the n-body problem so that the system can be continued past collision. *Regularization* involves a change of spatial (q_i and p_i) variables, as well as a re-scaling of time that results in the velocity at collision being finite. Under appropriate regularizations, the behavior of the bodies before and after collision corresponds to a perfectly elastic bounce.

A standard technique for regularization of collisions involving two bodies (the so-called *binary collision*) is given by Levi-Civita in [39] and has been modified by many since then. The particular details of the coordinate transformations depend on the orbit being studied.

As a simple example, consider the two-body collinear configuration with two bodies of mass 1 located at $(\pm q, 0)$. Their conjugate momenta is given by $p = 2\dot{q}$. The Hamiltonian in this setting is then given by

$$H = \frac{1}{4}p^2 - \frac{1}{2q}.$$

Collisions at the origin can be regularized via

$$q = Q^2, \quad P = 2qp.$$

This is a canonical transformation arising from the generating function $F = \sqrt{q}P$. Hence,

$$Q = \frac{\partial F}{\partial P} = \sqrt{q} \text{ and } p = \frac{\partial F}{\partial q} = \frac{P}{2\sqrt{q}}.$$

Solving for p and substituting yields

$$\begin{aligned}\tilde{H} &= \frac{1}{4}\left(\frac{P^2}{4Q^2}\right) - \frac{1}{2Q^2} \\ &= \frac{P^2}{16Q^2} - \frac{1}{2Q^2}.\end{aligned}$$

Since the change of variables was canonical, $\tilde{H}$ still yields a Hamiltonian system. Consequently, the value of $\tilde{H}$ is some fixed constant E, which can be determined after initial conditions have been

chosen. Then the value of $\tilde{H} - E$ is zero along the orbit. The Hamiltonian function $\tilde{H}$ is defined at all points except those for which $Q = q = 0$, namely, collision at the origin. The final step in regularization is to introduce a new time variable s that dynamically depends upon the conditions in the orbit. In this case, clearing the Q^2 terms in the denominator would remove the singularity, so we define s to satisfy $dt/ds = Q^2$. Then the final regularized Hamiltonian is denoted Γ and is given by

$$\begin{aligned}\Gamma &= \frac{dt}{ds}(\tilde{H} - E) \\ &= Q^2\left(\frac{P^2}{16Q^2} - \frac{1}{2Q^2}\right) - E \\ &= \frac{P^2}{16} - \frac{1}{2} - Q^2E.\end{aligned}$$

Note that at collision ($Q = 0$), assuming $\Gamma = 0$, we find $P = \sqrt{8}$. The collision has therefore been regularized as claimed, and the point $Q = 0$ does not correspond to an equilibrium point. Thus the orbit continues past the collision.

Introducing the quantities E and s into the Hamiltonian Γ equation yields *extended phase space*, which is an extension of the original phase space defined by q_i and p_i that includes the extra variables E and s. (Concretely, this is the space $\mathbb{R}^{2n} \times \mathbb{R}^2$, where $\mathbb{R}^{2n}$ is spanned by $\{q_i\}$, $\{p_i\}$, and E and s yield $\mathbb{R}^2$.) Moreover, this new system can also be considered as Hamiltonian, as

$$\frac{dE}{dt} = 0, \quad \frac{ds}{dt} = -\frac{\partial \Gamma}{\partial E}.$$

2.6 Poincaré Sections

Let $\phi(t, x_0) : \mathbb{R} \times \mathbb{R}^n \mapsto \mathbb{R}^n$ denote the solution to a system of differential equations at time t with initial conditions x_0. Let Σ be a subset of $\mathbb{R}^n$ of dimension $n-1$. (For simplicity, this may be considered to be a linear subspace, as will be the case in this work.) Let $\rho : \Sigma \to \Sigma$ be given by

$$\rho(x_0) = \phi(\tau(x_0), x_0),$$

where $\tau(x_0)$ is the smallest value of $t > 0$ for which $\phi(t, x_0) \in \Sigma$ if such a t exists. (If no such time exists, then ρ is undefined.) In other words, to find the image of $\rho(x_0)$, simply take the initial conditions at x_0 and evolve them according to the differential equations until Σ is crossed again. Then ρ is called the *return map*, and Σ is called a *Poincaré Section*. This introduces a discretized version of the differential equation flow and is often useful for qualitatively describing certain global behaviors of the system.

If x_0 is a point on a periodic orbit, then $\rho^n(x_0) = x_0$ for some $n \in \mathbb{N}$. If care is taken in choosing the section, then $n = 1$. Moreover, ρ is a continuous map, as both the flow and the return time are continuous functions in x_0 by standard arguments.

For many of the examples that will be presented in this work, the differential equations will be given by a Hamiltonian system $H(q_1, q_2, p_1, p_2)$. Given initial values for the variables q_1, q_2, p_1, and p_2, the constant value of H for the entire orbit can be determined. Since H is constant and known, then one of these four variables can be written in terms of the other three. Hence, we may consider the resulting system of non-independent differential equations on $\mathbb{R}^3$. Poincaré sections are then two-dimensional slices (often planes or half-planes) of $\mathbb{R}^3$.

One important property of a Poincaré section in a Hamiltonian system is that ρ preserves the Lebesgue measure of sets on Σ.

2.7 Stability, Stability, Stability, and Stability

Let $O(x_0)$ denote the *orbit* (set of all points under forward and reverse time) of the point x_0 in a given system of differential equations, and $\phi(t, y_0)$ the point on the solution to the differential equation at time t with initial condition y_0 as before. Suppose that x_0 is a point on a periodic orbit (perhaps a fixed point). Then $O(x_0)$ is a (perhaps trivial) closed loop. There are multiple notions of *stability* for this periodic orbit. The general idea of *stability* is that orbits that start close (in terms of initial conditions as points in phase space) should stay close as time progresses.

The orbit $O(x_0)$ is called *asymptotically stable* if there is an open set U about x_0 such that if $y_0 \in U$, then the distance $d(\phi(t, y_0), O(x_0)) \to 0$ as $t \to \infty$. (Here, $d(\cdot, \cdot)$ denotes the distance.) An

important distinction of asymptotic stability is that we only consider forward time. It is usually the case that asymptotically stable orbits do not satisfy this relation in reverse time. In the case of Hamiltonian systems, preservation of area by ρ implies that a periodic orbit cannot be asymptotically stable.

The orbit $O(x_0)$ is called *Lyapunov stable* if for any $\varepsilon > 0$ there is a $\delta > 0$ so that if $d(x_0, y_0) < \delta$, then $d(\phi(t, y_0), \phi(t, x_0)) < \varepsilon$ for *all* t, not strictly positive t.

The orbit $O(x_0)$ is called *Poincaré stable* if for any $\varepsilon > 0$ there is a $\delta > 0$ so that if $d(x_0, y_0) < \delta$, then $d(\phi(t, y_0), O(x_0)) < \varepsilon$ for *all* t, not strictly positive t. (Here, the distance is taken to be the minimum difference between the point and the compact set $O(x_0)$, where again x_0 is a point on a periodic orbit.) By definition, any Lyapunov stable orbit is automatically Poincaré stable.

Some examples will help to distinguish the multiple definitions. To begin, the simple autonomous system $y' = -y$ has the stationary orbit $y = 0$ is stable in forward time (all solutions are of the form $y = ce^{-t}$), but this is not Lyapunov stable or Poincaré stable as reverse-time solutions diverge away from 0.

On the other hand, consider the system given in polar coordinates by

$$\dot{r} = 0, \quad \dot{\theta} = f(r),$$

where $f(r)$ is some monotonically non-decreasing function. Then each point belongs to some periodic orbit, as all orbits are circles about the origin. Certainly the origin is not asymptotically stable, as no point's forward trajectory moves it closer to the origin. If $f(r) = 1$, then any point orbits in 2π time, as the system corresponds to rigid rotation of the plane. So any orbit is both Lyapunov stable and Poincaré stable. On the other hand, if $f(r) = r$, then a point on the $r = r_0$ circle returns to its initial position in $2\pi/r_0$ time. Each constant r circle still remains close to other nearby circles, so this system is still Poincaré stable. However, the system is not Lyapunov stable: Let x and y be any two distinct points on the line $\theta = \theta_0$ for some θ_0. If r_x and r_y are the radii of the circles on which those points lie, then at time $t_0 = \pi/|r_x - r_y|$, the θ values of $\phi(t_0, x)$ and $\phi(t_0, y)$ differ by π. Since x and y can be made arbitrarily close, the system cannot be Lyapunov stable, as

no δ can guarantee that a point δ-close to x will remain in a ball of radius $r_x/2$ about x.

Most often in celestial mechanics (and certainly in this work) when we refer to "stability" we will refer to Poincaré stability. There is an important connection between Poincaré stability and Poincaré sections. Specifically, if x_0 is a fixed point on a 2-dimensional Poincaré section Σ in $\mathbb{R}^3$, and there are is a closed loop S_ε lying within a distance ε of x_0 on Σ such that $\rho(S_\varepsilon) = S_\varepsilon$, then the image of S_ε in the ambient space forms a closed torus, separating $\mathbb{R}^3$ into an "interior" and "exterior". By uniqueness of solutions to ODEs, it must then be the case that an orbit which starts within that torus remains in that torus. If such a loop exists for each $\varepsilon > 0$, then the orbit containing x_0 is Poincaré stable.

Verifying the existence of such loops for a general map is quite difficult, and depends on certain number-theoretic properties. Without loss of generality, suppose $(0,0)$ is a fixed point of a map $\mathbb{R}^2 \to \mathbb{R}^2$ by $(x,y) \mapsto (f(x,y), g(x,y))$, where f and g are analytic functions expressed as power series. Then certain technical conditions must be satisfied by the coefficients of the power series expansions for both f and g in order for these loops to exist. The full details of this are given in [5].

There is one additional type of stability, called *linear stability*, that is a necessary but insufficient condition for Poincaré stability. This depends only on the eigenvalues of the linearized map given by f and g. Linear stability, however, is verifiable numerically. Moreover, the numerical calculation can be made rigorous due to some results of Roberts (see [1]). The specifics of linear stability will be discussed shortly.

2.8 Symplectic Matrices

Let J be the $2n \times 2n$ matrix

$$J = \begin{bmatrix} 0 & I \\ -I & 0 \end{bmatrix},$$

where I and 0 denote the $n \times n$ identity and zero matrices, respectively. It is straightforward to show that $J^{-1} = J^T = -J$. This matrix arises frequently in Hamiltonian systems. In particular, if

H is a Hamiltonian function, and

$$\gamma = (q_1, ..., q_n, p_1, ..., p_n)^T,$$

then the system can be written as

$$\gamma' = JDH(\gamma),$$

where $DH(\gamma)$ represents the vector of partial derivatives of H evaluated at γ.

A $2n \times 2n$ matrix A is called *symplectic* if $A^T JA = J$. If $A^T JA = \mu J$, then A is called *symplectic with multiplier* μ. Since J is non-singular, any symplectic matrix A is also non-singular. Also, it can be shown (see [37]) that if A is symplectic and

$$A = \begin{bmatrix} A_{11} & A_{12} \\ A_{21} & A_{22} \end{bmatrix},$$

where each A_{ij} is an $n \times n$ block then

$$A^{-1} = \begin{bmatrix} A_{22}^T & -A_{12}^T \\ -A_{21}^T & A_{11}^T \end{bmatrix}.$$

Suppose A is a symplectic matrix with eigenvalue λ and eigenvector $\eta = [\eta_1^T \ \eta_2^T]^T$, where η_1 and η_2 are n-element column vectors. That is to say,

$$A \begin{bmatrix} \eta_1 \\ \eta_2 \end{bmatrix} = \lambda \begin{bmatrix} \eta_1 \\ \eta_2 \end{bmatrix}.$$

Then, since $A^T JA = J$, we have

$$\begin{aligned}
A^T JA \begin{bmatrix} \eta_1 \\ \eta_2 \end{bmatrix} &= J \begin{bmatrix} \eta_1 \\ \eta_2 \end{bmatrix} \\
A^T J\lambda \begin{bmatrix} \eta_1 \\ \eta_2 \end{bmatrix} &= \begin{bmatrix} \eta_2 \\ -\eta_1 \end{bmatrix} \\
A^T \lambda \begin{bmatrix} \eta_2 \\ -\eta_1 \end{bmatrix} &= \begin{bmatrix} \eta_2 \\ -\eta_1 \end{bmatrix}, \\
A^T \begin{bmatrix} \eta_2 \\ -\eta_1 \end{bmatrix} &= \frac{1}{\lambda} \begin{bmatrix} \eta_2 \\ -\eta_1 \end{bmatrix},
\end{aligned}$$

and so $1/\lambda$ is also an eigenvalue for A. Consequently, real eigenvalues of A come in reciprocal pairs, and complex eigenvalues of A come in complex "quartets".

2.9 Linear Stability

Let $X(t)$ be a fundamental matrix solution to

$$\xi' = JD^2H(\gamma)\xi,$$

where γ is a T-periodic solution to the Hamiltonian system (e.g. each component of γ is T-periodic), and $X(0) = I$. Then the matrix $X(T)$ is symplectic, and is called the *monodromy matrix* for the orbit γ. The linear stability of γ is determined by the eigenvalues of $X(T)$. Each conserved quantity from Section 2.3 results in $X(T)$ having an eigenvalue equal to 1. The orbit γ is *linearly stable* if $X(T)$ has all eigenvalues of modulus 1 and the only repeated eigenvalues are those resulting from these conserved quantities. As mentioned in Section 2.7, linear stability is necessary for Poincaré stability. The proof of this is lengthy (see [5]).

2.10 SYMMETRIES

Let γ be a T-periodic orbit of some (not necessarily Hamiltonian) system of differential equations, and let S be a matrix. Then S is said to be a *time-preserving symmetry* of γ if there exists some $0 < t_0 < T$ such that $S\gamma(t) = \gamma(t + t_0)$ for all t. On the other hand, S is called a *time-reversing symmetry* of γ if there exists some $0 < t_0 < T$ such that $S\gamma(t) = \gamma(t_0 - t)$ for all t.

As a simple example, let

$$\gamma = \begin{bmatrix} \sin(t) \\ \cos(t) \end{bmatrix},$$

and let

$$S_1 = \begin{bmatrix} 1 & 0 \\ 0 & -1 \end{bmatrix}.$$

Then it holds that

$$\gamma(\pi - t) = \begin{bmatrix} \sin(\pi - t) \\ \cos(\pi - t) \end{bmatrix} = \begin{bmatrix} -\sin(t) \\ -\cos(\pi - t) \end{bmatrix} = S_1\gamma,$$

and so S_1 is a time-reversing symmetry for γ. Similarly,

$$S_2 = \begin{bmatrix} 0 & 1 \\ 1 & 0 \end{bmatrix}$$

satisfies $\gamma(\pi/2 - t) = S_2\gamma$, and so S_2 is another time-reversing symmetry for γ. An outstanding conjecture by Roberts (see [40]) states that any linearly stable periodic orbit of the n-body problem must have a time-reversing symmetry.

CHAPTER 3. ROBERT'S SYMMETRY-REDUCTION TECHNIQUE

We will make frequent use of a technique developed by Roberts to aid in our evaluation of linear stability for various periodic orbits. The material in this chapter is all given by Roberts in [1] and is duplicated here for reference and convenience. The first four results involve solutions to the matrix differential equation

$$\dot{\xi} = JD^2H(\gamma)\xi \tag{3.1}$$

with various initial conditions.

Lemma 3.1. *Suppose that $\gamma(t)$ is a T-periodic solution of a Hamiltonian system with Hamiltonian H and symmetry matrix S such that*

1. *For some $N \in \mathbb{N}$, $\gamma(t+T/N) = S\gamma(t)$ for all t,*
2. *$H(Sx) = H(x)$,*
3. *$SJ = JS$,*
4. *S is orthogonal.*

Then the fundamental matrix solution $X(t)$ to (3.1) with $\xi(0) = I$ satisfies

$$X(t+T/N) = SX(t)S^TX(T/N).$$

(Here, S^T means the transpose of S.)

Proof. Let $A = X(T/N)$, $Y(t) = X(t+T/N)$, and $Z(t) = SX(t)S^TX(T/N)$. Consider the differential equation

$$\dot{\xi} = SJD^2H(\gamma(t))S^T\xi, \quad \xi(0) = A. \tag{3.2}$$

Then

$$\dot{Y} = \dot{X}(t+T/N) = JD^2H(\gamma(t+T/N))X(t+T/N) = SJD^2H(\gamma(t))S^TY(t)$$

by properties 1-3 of S. On the other hand,

$$\dot{Z} = SJD^2H(\gamma(t))X(t)S^TA = SJD^2H(\gamma(t))S^TZ(t)$$

using the fact that S is orthogonal. Thus both $Y(t)$ and $Z(t)$ satisfy (3.2) with the same initial condition $Y(0) = Z(0) = A$. By uniqueness, $Y(t) = Z(t)$ as required. □

Corollary 3.2. *Under the hypotheses of Lemma 3.1, the fundamental matrix solution $X(t)$ satisfies*

$$X(kT/N) = S^k(S^TX(T/N))^k$$

for any $k \in \mathbb{N}$.

Proof. This follows from Lemma 3.1 by induction on k. □

Alternate initial conditions can also be considered. If $Y(t)$ is the fundamental matrix solution to (3.1) with $\xi(0) = Y_0$, a similar argument shows that

$$Y(t+T/N) = SY(t)Y_0^{-1}S^TY(T/N)$$

and so

$$Y(kT/N) = S^kY_0(Y_0^{-1}S^TY(T/N))^k.$$

The reason for considering these alternate initial conditions as follows: If Y is the fundamental matrix solution of

$$\xi' = JD^2\Gamma(\gamma(s))\xi, \quad \xi(0) = Y_0 \tag{3.3}$$

for some invertible matrix Y_0, then by definition of $X(s)$, $Y(s) = X(s)Y_0$, implying $X(T) = Y(T)Y_0^{-1}$. Then we have

$$X(T) = Y(T)Y_0^{-1} = Y_0(Y_0^{-1}Y(T))Y_0^{-1}$$

and so $X(T)$ and $Y_0^{-1}Y(T)$ are similar, and linear stability can be determined by the eigenvalues of either.

Lemma 3.3. *Suppose that $\gamma(t)$ is a T-periodic solution of a Hamiltonian system with Hamiltonian H and symmetry matrix S such that*

1. *For some $N \in \mathbb{N}$, $\gamma(-t+T/N) = S\gamma(t)$ for all t,*
2. *$H(Sx) = H(x)$,*
3. *$SJ = JS$,*
4. *S is orthogonal.*

Then the fundamental matrix solution $X(t)$ to 3.1 with $\xi(0) = I$ satisfies

$$X(-t+T/N) = SX(t)S^T X(T/N). \tag{3.4}$$

Proof. Let $A = X(T/N)$, $Y(t) = X(-t+T/N)$, and $Z(t) = SX(t)S^T X(T/N)$. Consider the differential equation

$$\dot{\xi} = SJD^2H(\gamma(t))S^T\xi, \quad \xi(0) = A. \tag{3.5}$$

Then

$$\dot{Y} = \dot{X}(-t+T/N) = -JD^2H(\gamma(-t+T/N))X(-t+T/N) = SJD^2H(\gamma(t))S^TY(t)$$

by properties 1-3 of S. On the other hand,

$$\dot{Z} = SJD^2H(\gamma(t))X(t)S^TA = SJD^2H(\gamma(t))S^TZ(t)$$

using the fact that S is orthogonal. Thus both $Y(t)$ and $Z(t)$ satisfy (3.2) with the same initial condition $Y(0) = Z(0) = A$. By uniqueness, $Y(t) = Z(t)$ as required. □

Corollary 3.4. *Under the hypotheses of Lemma 3.3, the fundamental matrix solution $X(t)$ satisfies*

$$X(T/N) = SB^{-1}S^T B$$

where $B = X(T/2N)$.

Proof. Evaluating (3.4) at $= T/2N$ gives $B = SBS^T X(T/N)$. Solving for $X(T/N)$ gives the result. □

Alternate initial conditions can also be considered. If $Y(t)$ is the fundamental matrix solution to (3.1) with $\xi(0) = Y_0$, a similar argument shows that

$$Y(-t+T/N) = SY(t)Y_0^{-1}S^T Y(T/N)$$

and so

$$Y(T/N) = SY_0B^{-1}S^T B$$

where $B = Y(T/2N)$.

An appropriate choice of Y_0 and applications of Corollaries 3.2 and 3.4 allow the monodromy matrix to be written as a power of a another matrix W, which itself is a product of powers of Y_0, S, B, $Y(T/N)$ for various N, and their inverses. The particular form of this product varies depending on the system being studied. Specific details will be discussed later with the accompanying orbits. A particular form of W helps in performing the stability analysis.

Lemma 3.5. *Suppose W is a symplectic matrix that satisfies*

$$\frac{1}{2}(W + W^{-1}) = \begin{bmatrix} K^T & 0 \\ 0 & K \end{bmatrix}. \tag{3.6}$$

Then W has all eigenvalues on the unit circle if and only if all the eigenvalues of K are real and in the interval $[-1,1]$.

Proof. Suppose that $\mathbf{v}$ is an eigenvector for W with eigenvalue λ. Then

$$\frac{1}{2}(W+W^{-1})\mathbf{v} = \frac{1}{2}(\lambda+\lambda^{-1})\mathbf{v}$$

from which it follows that $\frac{1}{2}(\lambda+\lambda^{-1})$ is an eigenvalue of K. Note that the map $f:\mathbb{C}\to\mathbb{C}$ given by $f(\lambda)=\frac{1}{2}(\lambda+\lambda^{-1})$ takes the unit circle onto the real interval $[-1,1]$ while mapping the exterior of the unit disk homeomorphically onto $\mathbb{C}\setminus[-1,1]$.

Suppose that all eigenvalues of K lie in the real interval $[-1,1]$. If W has an eigenvalue λ of modulus other than 1, then either λ or $1/\lambda$ has modulus greater than 1. But then K would have an eigenvalue outside of $[-1,1]$.

On the other hand, let μ be an eigenvalue of K. Then $k\mathbf{u}=\mu\mathbf{u}$ implies that

$$\frac{1}{2}(W+W^{-1})\begin{bmatrix}0\\ \mathbf{u}\end{bmatrix} = \mu\begin{bmatrix}0\\ \mathbf{u}\end{bmatrix}.$$

Therefore μ is an eigenvalue of $\frac{1}{2}(W+W^{-1})$ and so must be real and in $[-1,1]$. □

Appropriate choices of Y_0 and applications of Lemmas 3.1-3.5 allow the monodromy matrix of a periodic solution to then be evaluated by evaluating the eigenvalues of K. This is highly desirable numerically, as determining if the real eigenvalues of K lie in an interval is much more feasible than proving that a complex number has modulus exactly equal to 1.

CHAPTER 4. THE EQUAL-MASS PLANAR ORBIT

In this chapter, we present the analytic existence of a family of singular symmetric periodic planar orbits in the four-body equal mass problem. The initial conditions of these orbits are symmetric in both positions and velocities, which lead to periodic simultaneous binary collisions with each of the four masses alternating between collisions with its two nearest neighbors. Due to the abundance of symmetries present in the initial conditions, we can reduce the number of variables needed to just four – two for representing position and two for representing momentum. In contrast to its one-dimensional counterparts (see [7] and [18]), the proof for existence of this orbit is surprisingly simple. We begin in Section **4.1.1** by giving a description of the proposed orbit and prove its existence. In Section **4.1.2** we present the numerical methods used to produce the initial conditions that will lead to this orbit. In Section **4.2**, we consider variants on this orbit, giving a family of orbits with singularities for an even number of equal masses.

The results presented in this chapter were originally published as [26].

4.1 THE PROPOSED ORBIT

4.1.1 Analytical Description. We focus on finding a symmetric, periodic SBC orbit for four equal masses in two dimensions. After appropriate rescaling, we assume that the orbit begins with the four bodies lying at $(\pm 1, 0)$ and $(0, \pm 1)$ with initial velocities $(0, \pm v)$ and $(\pm v, 0)$, respectively, where $v \in (0, +\infty)$. For convenience throughout the rest of the chapter, we number the bodies 1 to 4 as in Figure 4.1.

Due to the symmetry of the initial conditions and the equations governing the motion of the bodies, the symmetry that is present in the initial conditions is maintained for all time.

Theorem 4.1 (Main Theorem)**.** *Let $E = K - U$ be the total energy and m be the mass for each of the four bodies. For any $E < 0$ and $m > 0$, there exists a symmetric, periodic, four-body orbit with SBC in $\mathbb{R}^2$, as pictured in Figure 4.1.*

By an appropriate rescaling of units, we can assume $m = 1$ and the initial positions are as

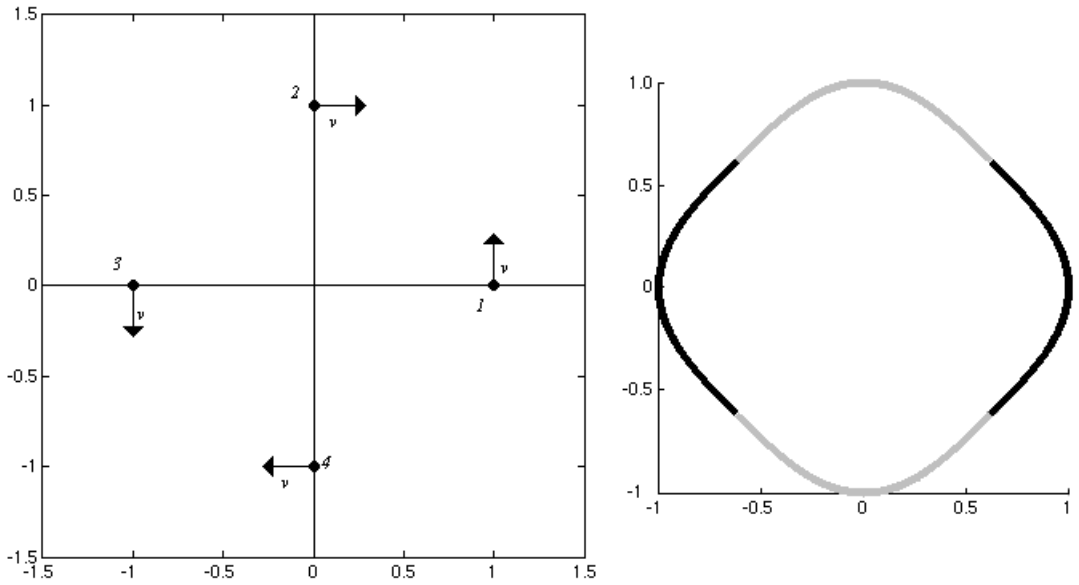

Figure 4.1: On the left, we illustrate the initial conditions leading to the four-body two-dimensional periodic SBC oribt. On the right, the orbit is shown. The darker curves show the orbit of the first and third bodies, and the lighter curves show the orbit of the second and fourth.

illustrated in Figure 4.1. The proof of existence will be given at the end of this section.

Let t_0 be the time of first SBC. For $t \in [0,t_0)$, let the coordinate of body 1 be (x_1,x_2). By symmetry, the coordinates of bodies 2, 3, and 4 are (x_2,x_1), $(-x_1,-x_2)$ and $(-x_2,-x_1)$, respectively. Using equation (2.1), the acceleration of a body at point (x_1,x_2) is given by:

$$(\ddot{x_1},\ddot{x_2}) = -\left[\frac{(x_1-x_2,x_2-x_1)}{(2(x_1-x_2)^2)^{\frac{3}{2}}} + \frac{(2x_1,2x_2)}{(4x_1^2+4x_2^2)^{\frac{3}{2}}} + \frac{(x_1+x_2,x_1+x_2)}{(2(x_1+x_2)^2)^{\frac{3}{2}}}\right] \tag{4.1}$$

We now perform the regularization of the system. The system has the Hamiltonian:

$$H = \frac{1}{8}(w_1^2+w_2^2) - \frac{\sqrt{2}}{x_1-x_2} - \frac{\sqrt{2}}{x_1+x_2} - \frac{1}{\sqrt{x_1^2+x_2^2}} \tag{4.2}$$

where $w_1 = 4\dot{x}_1$ and $w_2 = 4\dot{x}_2$ are the conjugate momenta to x_1 and x_2. Note that SBC happens

when $x_1 = \pm x_2$. We introduce a new set of coordinates:

$$q_1 = x_1 - x_2, \qquad q_2 = x_1 + x_2.$$

Their conjugate momenta p_i are given by using a generating function $F = (x_1 - x_2)p_1 + (x_1 + x_2)p_2$:

$$w_1 = p_1 + p_2, \qquad w_2 = p_2 - p_1.$$

The Hamiltonian corresponding to the new coordinate system is

$$H = \frac{1}{4}(p_1^2 + p_2^2) - \frac{\sqrt{2}}{q_1} - \frac{\sqrt{2}}{q_2} - \frac{\sqrt{2}}{\sqrt{q_1^2 + q_2^2}}. \tag{4.3}$$

Following the work of Sweatman [15], we introduce another canonical transformation:

$$q_i = Q_i^2, \qquad P_i = 2Q_i p_i \qquad (i = 1, 2)$$

with $Q_i > 0$. We also introduce a new time variable s, which satisfies $\frac{dt}{ds} = q_1 q_2 = Q_1^2 Q_2^2$. This produces a regularized Hamiltonian in extended phase space:

$$\Gamma = \frac{dt}{ds}(H - E)$$

$$= \frac{1}{16}(P_1^2 Q_2^2 + P_2^2 Q_1^2) - \sqrt{2}(Q_1^2 + Q_2^2) - \frac{\sqrt{2} Q_1^2 Q_2^2}{\sqrt{Q_1^4 + Q_2^4}} - Q_1^2 Q_2^2 E \tag{4.4}$$

where E is the total energy of the Hamiltonian H.

The regularized Hamiltonian gives the following differential equations of motion:

$$Q_1' = \frac{1}{8} P_1 Q_2^2, \tag{4.5}$$

$$Q_2' = \frac{1}{8} P_2 Q_1^2, \tag{4.6}$$

$$P_1' = -\frac{1}{8}P_2^2 Q_1 + 2\sqrt{2}Q_1 + \frac{2\sqrt{2}Q_1Q_2^2}{\sqrt{Q_1^4+Q_2^4}} - \frac{2\sqrt{2}Q_1^5Q_2^2}{(Q_1^4+Q_2^4)^{\frac{3}{2}}} + 2EQ_1Q_2^2, \tag{4.7}$$

$$P_2' = -\frac{1}{8}P_1^2 Q_2 + 2\sqrt{2}Q_2 + \frac{2\sqrt{2}Q_2Q_1^2}{\sqrt{Q_1^4+Q_2^4}} - \frac{2\sqrt{2}Q_2^5Q_1^2}{(Q_1^4+Q_2^4)^{\frac{3}{2}}} + 2EQ_2Q_1^2, \tag{4.8}$$

with initial conditions

$$Q_1(0) = 1, \quad Q_2(0) = 1, \quad P_1(0) = -4v, \quad P_2(0) = 4v, \tag{4.9}$$

where derivatives are with respect to s, and E is the total energy of the Hamiltonian H.

Theorem 4.2. *Let s_0 be the time of the first SBC in the regularized system. Then s_0 is a continuous function with respect to the initial velocity v. Furthermore,*

$$p_2(t_0) = \frac{P_2(s_0, v)}{2Q_2(s_0, v)}$$

is also continuous with respect to v.

Proof. At the first SBC, $Q_1(s_0) = 0$, and $Q_2(s_0) = \sqrt{q_2} = \sqrt{x_1 + x_2} > 0$. Our goal is to show that $p_2(t_0)$ is a continuous function with respect to v.

Because $\Gamma = 0$ at $s = s_0$, $P_1(s_0) = -4\sqrt[4]{2}$ from (4.4). Since Γ is regularized, the solution $P_i = P_i(s, v)$ and $Q_i = Q_i(s, v)$ are continuous functions with respect to the two variables s and v. At time $s = s_0$,

$$0 = Q_1(s_0(v), v).$$

To apply the implicit function theorem, we need to show that

$$\frac{\partial Q_1}{\partial s}(s_0, v) \neq 0.$$

From (4.5)

$$\frac{\partial Q_1}{\partial s}(s_0,v) = \frac{1}{8}P_1Q_2^2\,|_{(s_0,v)} = -\frac{1}{2}\sqrt[4]{2}Q_2(s_0)^2 < 0.$$

So $s_0 = s_0(v)$ is a continuous function of v. Therefore both $P_2(s_0,v)$ and $Q_2(s_0,v)$ are continuous functions of v. Further, since $Q_2(s_0,v) > 0$, $p_2(t_0)$ is also a continuous function of v. □

Theorem 4.3. *There exists a $v = v_0$ such that $\dot{x}_1(t_0)+\dot{x}_2(t_0) = \frac{1}{2}p_2(t_0) = 0$, where t_0 is the time of the first SBC, i.e. the net momentum of bodies 1 and 2 at the first SBC is 0.*

The outline of this proof is as follows: We will show that there exist v_1 and v_2 such that $\dot{x}_1+\dot{x}_2$ is negative at SBC for $v = v_1$ and positive at SBC for $v = v_2$. The result then follows by Theorem 4.2.

Proof. Consider Newton's equation before the time of the first SBC:

$$\ddot{x}_1 = \frac{x_2-x_1}{2\sqrt{2}(x_1-x_2)^3} - \frac{2x_1}{8(x_1^2+x_2^2)^{3/2}} - \frac{x_1+x_2}{2\sqrt{2}(x_1+x_2)^3}, \tag{4.10}$$

$$\ddot{x}_2 = \frac{x_1-x_2}{2\sqrt{2}(x_1-x_2)^3} - \frac{2x_2}{8(x_1^2+x_2^2)^{3/2}} - \frac{x_1+x_2}{2\sqrt{2}(x_1+x_2)^3}. \tag{4.11}$$

Therefore,

$$\ddot{x}_1+\ddot{x}_2 = -\frac{x_1+x_2}{4(x_1^2+x_2^2)^{3/2}} - \frac{1}{\sqrt{2}(x_1+x_2)^2} < 0, \tag{4.12}$$

which means $\dot{x}_1+\dot{x}_2$ is decreasing with respect to t.

At the initial time $t = 0$, $x_1 = 1$, $x_2 = 0$, $\dot{x}_1 = 0$, and $\dot{x}_2 = v$. Note that for $v \in (0,\infty)$, there is no triple collision or total collision for $t \in [0,t_0]$, where t_0 is the time of the first SBC, as a triple collision implies total collapse by symmetry. Also, from the initial time to t_0, $0 \le x_2 \le x_1 \le 1$, $0 < x_1+x_2 < 2$, and $x_1^2+x_2^2 < 4$.

Let $y(t) = x_1(t)+x_2(t)$. Then for any choice of v, $\ddot{y}(t) < 0$ and $0 < y(t) < 2$ hold for any $t \in [0,t_0]$. In other words, $\dot{y}(t)$ is decreasing with respect to t.

First, we will show that there exists v_1 such that $\dot{y}(t_0) < 0$. When $v = 0$ the four bodies form a central configuration and, as a consequence, the motion of the four bodies leads to total collapse.

Consider the time interval $t \in [0, t_0/2)$. In this interval, the differential equations (4.10) and (4.11) have no singularity, and $\ddot{y}(t_0/2) < 0$. By continuous dependence on initial conditions, $\dot{y}(t_0/2) = \dot{x}_1(t_0/2) + \dot{x}_2(t_0/2)$ is a continuous function with respect to the initial velocity v. When $v = 0$, $\dot{x}_1(t_0/2) < 0$, $\dot{x}_2(t_0/2) = 0$, which gives $\dot{y}(t_0/2) < 0$. Therefore, there exists a $\delta > 0$, such that $\dot{y}(t_0/2) < 0$ holds for any $v \in (-\delta, \delta)$.

Choose $v_1 = \delta/2$, then $\dot{y}(t_0/2) < 0$. Because $\dot{y}(t)$ is decreasing with respect to t, $\dot{y}(t_0) \leq \dot{y}(t_0/2) < 0$.

Next we will show that there exists v_2 such that $\dot{y}(t_0) > 0$. Note that as $v \to \infty$,

$$\lim_{v \to \infty} y(t_0) = \lim_{v \to \infty} x_1(t_0) + x_2(t_0) = 2$$

and

$$\lim_{v \to \infty} \dot{y}(t_0) = \infty.$$

(Intuitively, the two bodies collide instantaneously at the point (1,1) with infinite velocity.) Therefore there exists some positive value v_2, such that $\dot{y}(t_0) > 0$. □

Proof of Theorem 4.1. From Theorem 4.3, we know there exists an initial velocity $v = v_0$ such that $\dot{x}_1(t_0) + \dot{x}_2(t_0) = 0$. Let $\{P_1, P_2, Q_1, Q_2\}$ for $s \in [0, s_0]$ be the solution in the regularized system corresponding to the orbit from $t = 0$ to $t = t_0$. Following collision, consider the behavior of the first and second bodies. Assume their velocity was reflected about the $y = x$ line in the plane. In the new coordinate system, this corresponds to a new set of functions

$$\{-P_1(2s_0 - s), -P_2(2s_0 - s), -Q_1(2s_0 - s), -Q_2(2s_0 - s)\}$$

for $s \in [s_0, 2s_0]$. We can easily check that

$$\{-P_1(2s_0 - s), -P_2(2s_0 - s), -Q_1(2s_0 - s), -Q_2(2s_0 - s)\}$$

for $s \in [s_0, 2s_0]$ is also a set of solutions for equations (4.5) through (4.8) with initial conditions at

$s = s_0$. Also, $\{P_1(s), P_2(s), Q_1(s), Q_2(s)\}$ for $s \in [s_0, 2s_0]$ satisfies equations (4.5) through (4.8) with the same initial conditions at $s = s_0$. Note that equations (4.5) through (4.8) with initial conditions at $s = s_0$ have a unique solution for any choice of $v \in (0, \infty)$. Then by uniqueness, the orbit for $s \in [s_0, 2s_0]$ must be the same as the orbit for $s \in [0, s_0]$ in reverse, i.e.

$$P_i(s) = -P_i(2s_0 - s), Q_i(s) = -Q_i(2s_0 - s)$$

for $s \in [0, s_0]$. Therefore at time $s = 2s_0$, bodies 1 and 2 will have returned to their initial positions with velocities $(0, -v)$ and $(-v, 0)$ respectively. Similarly, at time $s = 2s_0$, bodies 3 and 4 will have also returned to their initial positions with velocities $(0, v)$ and $(v, 0)$ respectively.

Next, we use symmetry and uniqueness to show the orbit from $s = 2s_0$ to $s = 4s_0$ and the orbit from $s = 0$ to $s = 2s_0$ will be symmetric with respect to the $y-$axis. Compare the motion of body 2 and body 3 from $s = 2s_0$ to $s = 4s_0$ with the motion of body 2 and body 1 from time $s = 0$ to $s = 2s_0$. The initial conditions of body 3 at $s = 2s_0$ and the initial conditions of body 1 at $s = 0$ are symmetric with respect to the $y-$axis. Also the initial conditions of body 2 at $s = 2s_0$ and the initial conditions of body 4 at $s = 0$ are symmetric with respect to the $x-$axis. Therefore, by uniqueness, the orbit of bodies 2 and 3 from $s = 2s_0$ to $s = 4s_0$ and the orbit of bodies 1 and 2 from $s = 0$ to $s = 2s_0$ must be symmetric with respect to $y-$axis. Therefore, the orbit of bodies 1 and 4 from $s = 2s_0$ to $s = 4s_0$ and and the orbit of bodies 3 and 4 from $s = 0$ to $s = 2s_0$ are symmetric with respect to the $y-$axis. Hence, at $s = 4s_0$, the positions and velocities of the four bodies are exactly the same as at $s = 0$. Therefore, the orbit is periodic with period $s = 4s_0$. □

4.1.2 Numerical Method. As we are searching for a periodic orbit of the n-body problem, we assume the value of the Hamiltonian needs to be negative (see [41], Proposition 4.1). Using the initial positions of the four bodies described earlier, it is not hard to find the potential energy at $t = 0$:

$$U = 2\sqrt{2} + 1.$$

Then, acting under the negative Hamiltonian assumption:

$$2\sqrt{2}+1 \geq \sum_{i=1}^{n} \frac{m_i|v_i|^2}{2}.$$

Since all masses are equal, if we require that the velocities of each body are equal in magnitude, we obtain:

$$v_{max} = \sqrt{\frac{2\sqrt{2}+1}{2}} \tag{4.13}$$

with v_{max} defined to be the value of v such that the value of the Hamiltonian is zero. Define $\theta = \frac{v}{v_{max}}$. This parameter is used in the numerical algorithm.

Since we know suitable bounds on the velocity parameter ($\theta \in (0,1)$), we can search the interval numerically. We use an n-body simulator with the initial positions previously described. The simulation is run until one SBC occurs. For simplicity, we consider only the collision between the first and second bodies in the first quadrant. Summing their velocities immediately before the collision gives a vector running along the line $y = x$ (due to symmetry), with both components having the same sign. The magnitude of this vector is given in Figure 4.2. Negative magnitudes represent vectors with both components less than zero.

Next, a standard bisection method is used to find the amount of energy required to cause the net velocity at collision to be zero. Using the initial interval $\theta \in [0,1]$,cthe correct value of θ was found to be approximately $\theta = 0.464495$.

Numerical simulations also demonstrate that for values of θ near the correct value, the orbit remains for a significant length of time with the paths of the bodies lying in a "fattened" annular region roughly the shape of the original orbit. Near the extreme ends, the orbit experiences near total-collapse and then (numerically) the bodies rapidly shoot off to infinity.

4.2 VARIANTS

4.2.1 Orbits of more than four bodies. The same technique can be adopted to find similar orbits for any arbitrary even number n. A key feature of these orbits will be higher numbers

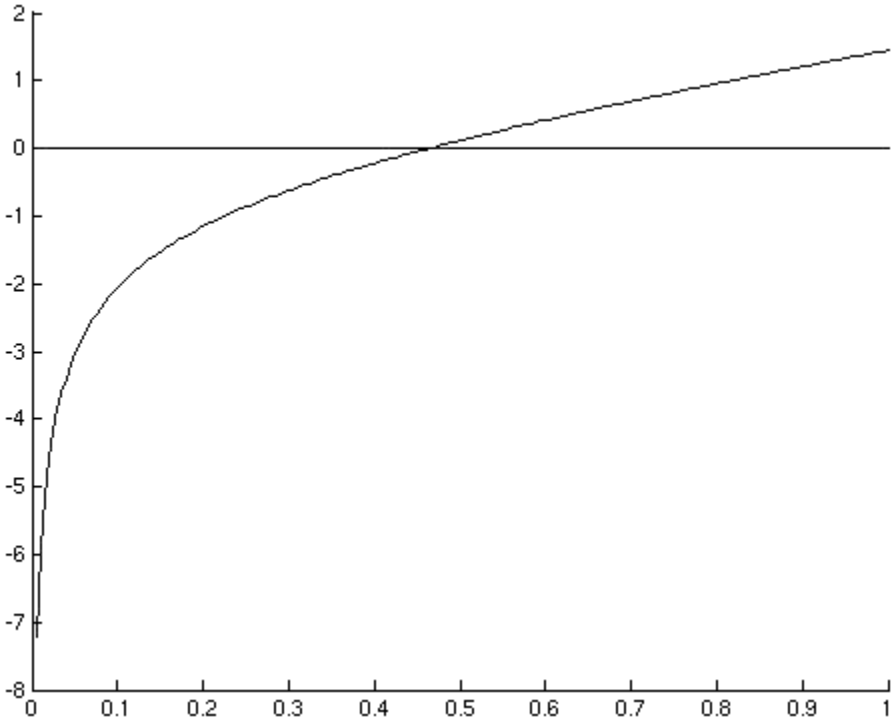

Figure 4.2: The signed magnitude of the net velocity of the first two bodies (vertical axis) at the time of collision for various values of θ (horizontal axis).

of simultaneous binary collisions. For a given value of n, initial positions are given by spacing the bodies evenly about the unit circle. The potential energy (and the value of v_{max}) is found numerically by iterating over each pair of bodies and summing the reciprocal of the distances between them. (Recall that all $m_i = 1$.) Velocities are then assigned to the bodies in alternating counter-clockwise and clockwise directions, initially tangent to the circle. Again we consider the collision between the first and the second bodies. Although the net velocity of the two at collision will not lie along the $y = x$ line, the components of this vector will both have the same sign. The magnitudes of the net velocity between the first two bodies at initial collision are shown in Figure 4.3 for various values of n. Lower curves in the graph correspond to higher values of n. Again, negative magnitudes correspond to both components being negative.

Pictures of the orbit for $n = 6$ and $n = 8$ are shown in Figure 4.4. It is readily seen that as n increases, the shape of the orbit more closely approximates a circle.

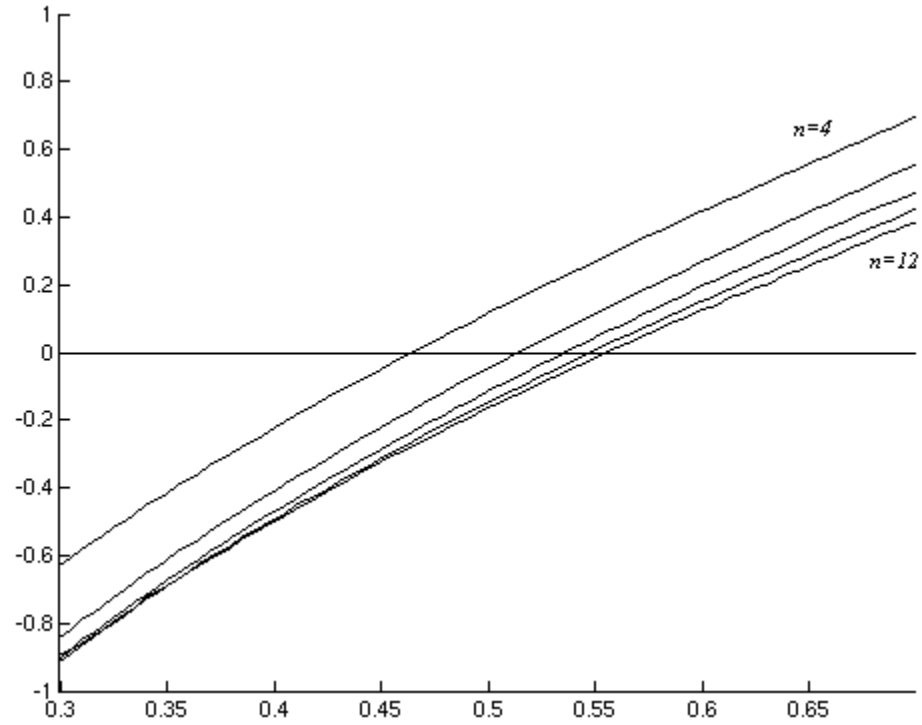

Figure 4.3: Curves showing the magnitude of the net velocity of the first two bodies (vertical axis) at the time of collision for various values of θ (horizontal axis) for $n = 4, 6, 8, 10, 12$.

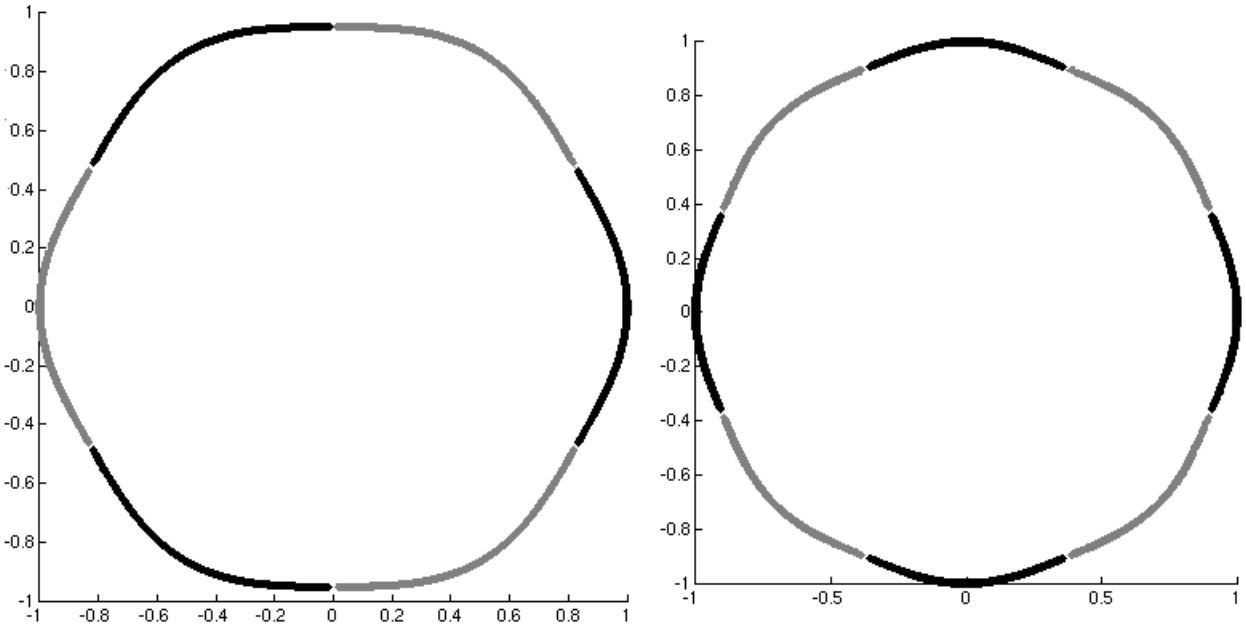

Figure 4.4: The six- and eight-body two-dimensional periodic SBC orbits.

CHAPTER 5. LINEAR STABILITY OF THE EQUAL-MASS PLANAR ORIBT

5.1 INTRODUCTION

In this chapter we apply the method of Roberts to prove the linear stability of the singular periodic orbit in the symmetric planar equal mass problem as discussed in Chapter 4. The linear stability is determined for the regularized equations only and is reduced to the rigorous numerical computation of a single real number. Our linear stability analysis determines that the $2D$ singular periodic orbit is linear stable. These examples support and extend the conjecture made by Roberts [1] that the only linearly stable periodic orbits in the equal mass n-body problem are those that exhibit a time-reversing symmetry.

The results presented in this chapter were originally published as [27].

5.2 LINEAR STABILITY FOR THE 2D SYMMETRIC PERIODIC ORBIT

In Chapter 4, we proved the existence of a special type of planar periodic solution of $2n$ bodies with equal masses. In this section, we are going to consider the linear stability of this periodic solution when $n = 2$. (Other values of n may be considered, but the equations developed in Chapter 4 were only developed for $n = 2$, and would become more complicated for higher values of n.) We use the same regularization as in Chapter 4 for the orbit. The Hamiltonian in the regularized setting is given by

$$\Gamma = \frac{dt}{ds}(H-E) = \frac{1}{16}(P_1^2Q_2^2 + P_2^2Q_1^2) - \sqrt{2}(Q_1^2+Q_2^2) - \frac{\sqrt{2}Q_1^2Q_2^2}{\sqrt{Q_1^4+Q_2^4}} - EQ_1^2Q_2^2 \tag{5.1}$$

where E is the total energy of the Hamiltonian H. The differential equations in terms of the new coordinates $\{Q_1, Q_2, P_1, P_2\}$ are

$$Q_1' = \frac{1}{8}P_1Q_2^2, \tag{5.2}$$

$$Q_2' = \frac{1}{8}P_2Q_1^2, \tag{5.3}$$

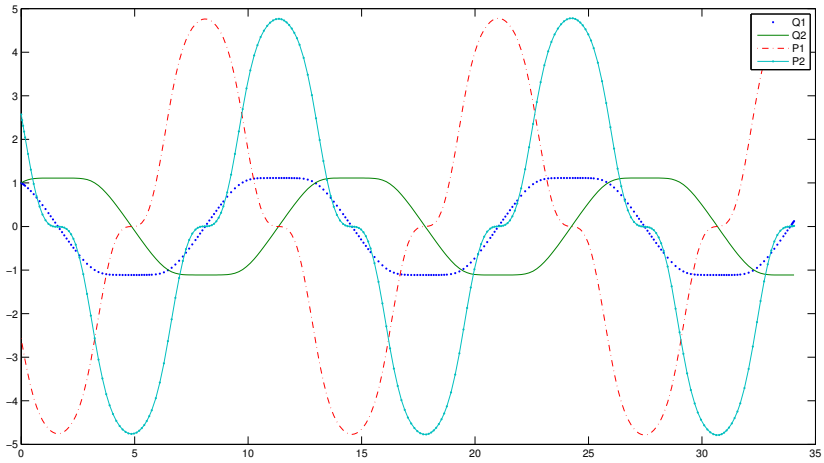

Figure 5.1: The periodic solution in the coordinate system Q_1, Q_2, P_1, P_2.

$$P_1' = -\frac{1}{8}P_2^2 Q_1 + 2\sqrt{2}Q_1 + \frac{2\sqrt{2}Q_1Q_2^2}{\sqrt{Q_1^4+Q_2^4}} - \frac{2\sqrt{2}Q_1^5Q_2^2}{(Q_1^4+Q_2^4)^{\frac{3}{2}}} + 2EQ_1Q_2^2, \tag{5.4}$$

$$P_2' = -\frac{1}{8}P_1^2 Q_2 + 2\sqrt{2}Q_2 + \frac{2\sqrt{2}Q_2Q_1^2}{\sqrt{Q_1^4+Q_2^4}} - \frac{2\sqrt{2}Q_2^5Q_1^2}{(Q_1^4+Q_2^4)^{\frac{3}{2}}} + 2EQ_2Q_1^2. \tag{5.5}$$

As shown in Chapter 4, for each $\zeta > 0$ there exists $v_0 > 0$ such that the initial conditions

$$Q_1(0) = \zeta, \;\; Q_2(0) = \zeta, \;\; P_1(0) = -4v_0, \;\; P_2(0) = 4v_0, \tag{5.6}$$

lead to a periodic solution with a minimal period T. From $\Gamma = 0$, the value of E is determined by this choice of ζ and v_0. By construction, this periodic orbit satisfies

$$Q_1(T/4) = -\zeta, \;\; Q_2(T/4) = \zeta, \;\; P_1(T/4) = -4v_0, \;\; P_2(T/4) = -4v_0.$$

Simultaneous binary collisions correspond to $s = T/8, 5T/8$ i.e., when $Q_1(s) = 0$, and to $s = 3T/8, 7T/8$, i.e., when $Q_2(s) = 0$. For $\zeta = 1$, we have (numerically) $4v_0 \approx 2.57487$, and $T/8 = 1.62047$. Figure 5.1 illustrates the coordinates (Q_1, Q_2, P_1, P_2) of this periodic solution.

5.2.1 Stability Reductions using Symmetry. We will reduce the stability analysis to the first eighth of the periodic orbit. The symmetric periodic 2D orbit

$$\gamma(t) = (Q_1(t), Q_2(t), P_1(t), P_2(t))$$

with period T has a time-reversing symmetry and a time-preserving symmetry. For

$$F = \begin{bmatrix} 0 & -1 \\ 1 & 0 \end{bmatrix}, \quad G = \begin{bmatrix} -1 & 0 \\ 0 & 1 \end{bmatrix},$$

the matrices

$$S_F = \begin{bmatrix} F & 0 \\ 0 & F \end{bmatrix}, \quad S_G = \begin{bmatrix} G & 0 \\ 0 & -G \end{bmatrix}$$

satisfy $S_F^{-1} = S_F^T$, $S_F^2 \neq I$, $S_F^3 \neq I$, $S_F^4 = I$, $S_G^2 = I$, $S_G^T = S_G$, and $(S_F S_G)^2 = I$. Since $\gamma(s + T/4)$ and $S_F\gamma(s) = (-Q_2(s), Q_1(s), -P_2(s), P_1(s))$ are solutions of (5.2) through (5.5) and share the same initial conditions when $s = 0$, uniqueness of solutions implies that

$$\gamma(s + T/4) = S_F\gamma(s) \text{ for all } s.$$

Thus S_F is a time-preserving symmetry of $\gamma(s)$. With $N = 4$, conditions (2), (3), and (4) of Lemma 3.1 are satisfied, so that Corollary 3.2 (with $k = 4$) and $S_F^4 = I$ imply that

$$X(T) = S_F^4 \left(S_F^T X(T/4)\right)^4 = \left(S_F^T X(T/4)\right)^4.$$

Since $\gamma(-s + T/4)$ and $S_G\gamma(s)$ are solutions of (5.2) through (5.5) and share the same initial conditions when $s = 0$, uniqueness of solutions implies that

$$\gamma(-s + T/4) = S_G\gamma(s) \text{ for all } s.$$

Thus S_G is a time-reversing symmetry for $\gamma(s)$. With $N = 4$, conditions (2), (3), and (4) of Lemma 3.3 are satisfied, and so Corollary 3.4 implies that

$$X(T/4) = S_G\,[X(T/8)]^{-1}\,S_G^T X(T/8) = S_G\,[X(T/8)]^{-1}\,S_G X(T/8).$$

Let

$$B = X(T/8).$$

Combining the factorization of $X(T)$ that involves S_F and the factorization of $X(T/4)$ that involves S_G gives the factorization

$$X(T) = \left(S_F^T S_G B^{-1} S_G B\right)^4.$$

Setting

$$Q = S_F^T S_G = \begin{bmatrix} 0 & 1 & 0 & 0 \\ 1 & 0 & 0 & 0 \\ 0 & 0 & 0 & -1 \\ 0 & 0 & -1 & 0 \end{bmatrix}$$

and $D = B^{-1} S_G B$ results in the factorization

$$X(T) = (QD)^4$$

where Q and D are both involutions. The symmetries S_F and S_G generate a D_4 symmetry group for the periodic orbit $\gamma(s)$.

5.2.2 A Good Basis. Let $Y(s)$ be the fundamental matrix solution to the linearized equations about the 2D periodic orbit $\gamma(s)$ with arbitrary initial conditions Y_0. Let

$$B = Y(T/8).$$

By remarks following Corollaries 3.2 and 3.4, the matrix $Y_0^{-1}Y(T)$, which is similar to the monodromy matrix $X(T) = Y(T)Y_0^{-1}$, satisfies

$$Y_0^{-1}Y(T) = (Y_0^{-1}S_F^T S_G Y_0 B^{-1} S_G B)^4 = (Y_0^{-1} Q Y_0 B^{-1} S_G B)^4.$$

The question of linear stability reduces to showing that the eigenvalues of

$$W = Y_0^{-1} Q Y_0 B^{-1} S_G B$$

are on the unit circle. Recall that

$$\Lambda = \begin{bmatrix} I & 0 \\ 0 & -I \end{bmatrix}.$$

Lemma 5.1. *There exists Y_0 such that*

1. *Y_0 is orthogonal and symplectic, and*
2. *$Y_0^{-1} Q Y_0 = \Lambda$.*

Proof. Choose the third column of Y_0 to be

$$\frac{\gamma'(0)}{\|\gamma'(0)\|} = \frac{1}{c}\begin{bmatrix} -a & a & b & b \end{bmatrix}^T$$

where $a = v_0\zeta^2/2$, $b = E\zeta^3 = (2v_0^2 - 2\sqrt{2} - 1)\zeta$ and $c = \sqrt{2a^2 + 2b^2}$. Let $\mathrm{col}_i(Y_0)$ denote the i^{th} column of Y_0. Define

$$\mathrm{col}_1(Y_0) = J \cdot \mathrm{col}_3(Y_0) = \frac{1}{c}\begin{bmatrix} b & b & a & -a \end{bmatrix}^T.$$

We now choose $\mathrm{col}_4(Y_0)$ such that $\mathrm{col}_4(Y_0)$ is orthogonal to $\mathrm{col}_3(Y_0)$, and $\mathrm{col}_4(Y_0)$ is one of the eigenvectors of Q with respect to its eigenvalue of -1. Since the eigenspace of Q corresponding

to its eigenvalue of -1 is

$$\operatorname{span}\left\{\begin{bmatrix} 1 & -1 & 0 & 0 \end{bmatrix}^T, \begin{bmatrix} 0 & 0 & 1 & 1 \end{bmatrix}^T\right\},$$

define

$$\operatorname{col}_4(Y_0) = \frac{1}{c}\begin{bmatrix} b & -b & a & a \end{bmatrix}^T$$

and

$$\operatorname{col}_2(Y_0) = J \cdot \operatorname{col}_4(Y_0) = \frac{1}{c}\begin{bmatrix} a & a & -b & b \end{bmatrix}^T.$$

The matrix

$$Y_0 = \frac{1}{c}\begin{bmatrix} b & a & -a & b \\ b & a & a & -b \\ a & -b & b & a \\ -a & b & b & a \end{bmatrix},$$

is both symplectic and orthogonal and it satisfies $Y_0^{-1} Q Y_0 = \Lambda$. □

Setting $D = B^{-1} S_G B$ and choosing Y_0 to be the matrix constructed in Lemma 5.1 gives $W = \Lambda D$. The matrices Λ and D are involutions (the latter because $S_G^2 = I$). Then $W^{-1} = D\Lambda$, and there is a 2×2 matrix K such that

$$\frac{1}{2}\left(W + W^{-1}\right) = \begin{bmatrix} K^T & 0 \\ 0 & K \end{bmatrix}.$$

We show that the first column of K is $[1\ 0]^T$. Since $S_G^T = S_G$, $Y_0^{-1} = Y_0^T$, it follows by the remark following Corollary 3.4 that

$$W = Y_0^{-1} S_F^T S_G Y_0 B^{-1} S_G B = Y_0^{-1} S_F^T Y(T/4) = Y_0^T S_F^T Y(T/4).$$

Set $v = Y_0^{-1}\gamma'(0)$. By the choice of the matrix Y_0,

$$v = Y_0^{-1}\gamma'(0) = Y_0^T\gamma'(0) = \begin{bmatrix} 0 \\ 0 \\ ||\gamma'(0)|| \\ 0 \end{bmatrix} = ||\gamma'(0)||e_3.$$

Because $\gamma'(s)$ is a solution to the linearized equation $\dot{\xi} = JD^2\Gamma(\gamma(s))\xi$ and $\gamma'(0) = Y(0)Y_0^{-1}\gamma'(0)$, then $\gamma'(s) = Y(s)Y_0^{-1}\gamma'(0)$ for all s. Hence,

$$Wv = Y_0^T S_F^T Y(T/4)v = Y_0^T S_F^T \gamma'(T/4). \tag{5.7}$$

Since γ satisfies $\gamma(s+T/4) = S_F\gamma(s)$ for all s and $S_F^{-1} = S_F^T$, it then follows that

$$\gamma'(s) = S_F^{-1}\gamma'(s+T/4) = S_F^T\gamma'(s+T/4).$$

Setting $s = 0$ in this gives $\gamma'(0) = S_F^T\gamma'(T/4)$, and consequently that

$$Y_0^T S_F^T \gamma'(T/4) = Y_0^T\gamma'(0) = Y_0^{-1}\gamma'(0) = v. \tag{5.8}$$

Equations (5.7) and (5.8) now combine to show that $Wv = v$, i.e, that 1 is an eigenvalue of W and e_3 is an eigenvector for W corresponding to this eigenvalue. The first column of K is as claimed. The rest of K comes from the formula for the inverse of a symplectic matrix and the definition of D:

$$K = \begin{bmatrix} 1 & * \\ 0 & c_2^T(S_G J c_4) \end{bmatrix},$$

where c_i is the i^{th} column of $B = Y(T/8)$.

5.2.3 Numerical Calculations. Having not fixed E, we use an invariant scaling of the coordinates and time in equations (5.2) through (5.5) to preselect a period T before numerically computing the initial conditions for a periodic simultaneous binary collision orbit. For $\varepsilon > 0$, if $Q_1(s)$, $Q_2(s)$, $P_1(s)$, $P_2(s)$ is a periodic simultaneous collision orbit of equations (5.2) through (5.5) for a certain value of E, then $\varepsilon Q_1(\varepsilon s)$, $\varepsilon Q_2(\varepsilon s)$, $P_1(\varepsilon s)$, $P_2(\varepsilon s)$ is also a periodic simultaneous binary collision orbit with energy $\varepsilon^{-2}E$ and period $\varepsilon^{-1}T$. Furthermore, it is straightforward to show that monodromy matrices for the periodic simultaneous binary collision orbits corresponding to values of $\varepsilon \neq 1$ are all similar to that for $\varepsilon = 1$. Thus the linear stability of a periodic simultaneous binary collision orbit for one $\varepsilon > 0$ implies the linear stability of the periodic simultaneous binary collision orbits for all $\varepsilon > 0$.

We rigorously computed the value of $c_2^T(S_G J c_4)$ for the periodic simultaneous binary collision orbit whose period is $T = 8$. This means that the first time of a simultaneous binary collision for this orbit is at $s = 1$. We set $Q_1(0) = Q_2(0) = \xi$ and $-P_1(0) = P_2(0) = \eta$, and defined a function $F(\xi, \eta)$ to be equal to the vector quantity $(Q_1(1), P_2(1))$. We used Newton's method and a good initial guess to find a root (ξ, η) of F. This involved computing the Jacobian of F which was done using the linearized equations. We find numerically that

$$Q_1(0) = Q_2(0) \approx 1.62047, \quad -P_1(0) = P_2(0) \approx 2.57487,$$

lead to a periodic solution with a period of $T = 8$, and a value of $E \approx -1.14233$. Using MATLAB and a Runge-Kutta-Fehlberg algorithm, we computed the columns of the matrix $Y(T/8)$. From this we get

$$c_2^T(S_G J c_4) \approx -0.68024.$$

Using the scaling of coordinates and time described above, the initial conditions for the periodic simultaneous binary collision orbit shown in Figures 4.1 and 5.1 are

$$Q_1(0) = Q_2(0) = 1, \quad -P_1(0) = P_2(0) \approx 2.57487$$

with a period T satisfying $T/8 \approx 1.62047$, and energy $E \approx -2.99968$.

For the periodic simultaneous binary collision orbit, the rigorous estimate of the eigenvalue $c_2^T(S_G J c_4)$ of K and its distinctiveness from the eigenvalue 1 of K combine with Lemma 3.5 to give the following stability result.

Theorem 5.2. *The periodic simultaneous binary collision orbit in the 2D-symmetric equal mass four-body problem is linearly stable.*

When $c_2^T(S_G J c_4)$ is real and between -1 and 1, it is the real part of an eigenvalue with unit modulus for W (see [1]). For the periodic simultaneous collision orbit, the real part of $\exp(3\pi i/4)$, that is $-(1/2)\sqrt{2}$, is fairly close to the rigorously estimated value of $c_2^T(S_G J c_4)$. Raising $\exp(3\pi i/4)$ to the fourth power gives $\exp(3\pi i) = -1$, and so two of the eigenvalues of the monodromy matrix of the periodic simultaneous binary collision orbit are close to -1. The symmetry reductions used to compute the eigenvalues over just one-eighth of the period and the rigorous estimate of $c_2^T(S_G J c_4)$ showing that it is clearly between -1 and 1, assures the linear stability of the periodic simultaneous binary collision orbit.

CHAPTER 6. THE PAIRWISE EQUAL-MASS PLANAR ORBIT

6.1 INTRODUCTION

In this chapter we extend the analytic existence of a symmetric periodic SBC orbit in the fully symmetric planar four-body equal mass problem [26] to the analytic existence of a symmetric periodic SBC orbit in the planar pairwise symmetric four-body problem, or PPS4BP for short. The results presented in this chapter were originally published as [28].

The positions of the four pairwise symmetric bodies in the plane are $(\pm x_1, \pm x_2)$ and $(\pm x_3, \pm x_4)$, where the two bodies at $(\pm x_1, x_2)$ have mass 1, and the others pair has mass m, with $0 < m \leq 1$. With t as the time variable and $\dot{} = d/dt$, the momenta for the four masses are $(\omega_1, \omega_2) = 2(\dot{x}_1, \dot{x}_2)$, $(\omega_3, \omega_4) = 2m(\dot{x}_3, \dot{x}_4)$, $-(\omega_1, \omega_2)$, and $-(\omega_3, \omega_4)$. The Hamiltonian for the PPS4BP is $H = K - U$, where

$$K = \frac{1}{4}\left[\omega_1^2 + \omega_2^2\right] + \frac{1}{4m}\left[\omega_3^2 + \omega_4^2\right],$$

and

$$\begin{aligned} U = &\frac{1}{2\sqrt{x_1^2 + x_2^2}} + \frac{2m}{\sqrt{(x_3 - x_1)^2 + (x_4 - x_2)^2}} \\ &+ \frac{2m}{\sqrt{(x_1 + x_3)^2 + (x_2 + x_4)^2}} + \frac{m^2}{2\sqrt{x_3^2 + x_4^2}}. \end{aligned}$$

The angular momentum for the PPS4BP is

$$A = x_1\omega_2 - x_2\omega_1 + x_3\omega_4 - x_4\omega_3.$$

The center of mass is fixed at the origin, and the linear momentum is zero. With

$$J = \begin{bmatrix} 0 & I \\ -I & 0 \end{bmatrix}$$

for I the 4×4 identity matrix, the vector field for the PPS4BP is $J\nabla H$, i.e., the Hamiltonian system of equations with Hamiltonian H are $\dot{x}_i = \partial H/\partial \omega_i,\ \dot{\omega}_i = -\partial H/\partial x_i,\ i = 1,2,3,4$. The PPS4BP presented here is the Caledonian symmetric four-body problem [42] with non-collinear initial positions.

The initial conditions for the orbits of interest has the first body of mass 1 located on the positive horizontal axis with its momentum perpendicular to the horizontal axis, and the first body of mass m located on the positive vertical axis with its momentum perpendicular to the vertical axis. Specifically, at $t = 0$ we have

$$x_1 > 0,\ x_2 = 0,\ x_3 = 0,\ x_4 > 0,\ \text{with } x_4 \le x_1,$$
$$\omega_1 = 0,\ \omega_2 > 0,\ \omega_3 > 0,\ \omega_4 = 0,\ \text{with } \omega_2 \le \omega_3,$$

at which H is defined. The first objective is to find, for $0 < m \le 1$, values of $x_1, x_4, \omega_2, \omega_3$ at $t = 0$ such that:

(i) $x_3 - x_1 = 0$ and $x_4 - x_2 = 0$ with $x_1^2 + x_2^2 \neq 0$ at some $t = t_0 > 0$,

(ii) $x_1 + x_3 = 0$ and $x_2 + x_4 = 0$ with $x_1^2 + x_2^2 \neq 0$ at some $t = t_1 > t_0$,

(iii) the orbit extends to a symmetric periodic orbit, and

(iv) the periodic orbit avoids all the other kinds of collisions.

Such an orbit experiences a SBC in the first and third quadrant at $t = t_0$, and then another SBC in the second and fourth quadrants at $t = t_1$, before returning to its initial conditions at some $t = t_2 > t_1$. The presence of collisions along the orbit necessarily imposes zero angular momentum on the orbit, thus requiring that $x_1\omega_2 - x_4\omega_3 = 0$ at $t = 0$. Examples of these symmetric periodic SBC orbits in the PPS4BP with masses 1, m, 1, m are illustrated in Figure 6.1 for $m = 1$ and $m = 0.539$. The second objective is to numerically investigate the linear stability of the symmetric periodic SBC orbits as m varies over interval $(0, 1]$.

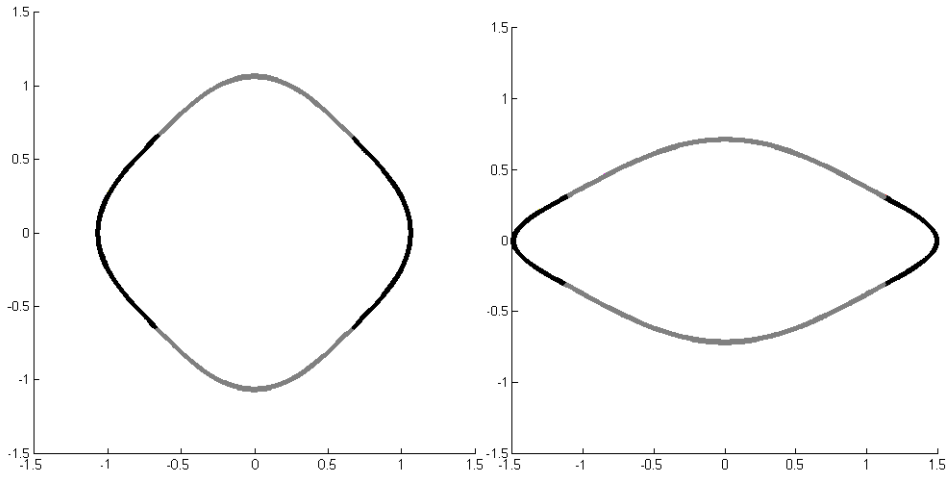

Figure 6.1: The symmetric periodic SBC orbit in the PPS4BP for $m = 1$ (left) and $m = 0.539$ (right). The two black curves are those traced out by $\pm(x_1(t), x_2(t))$, and the two gray curves are those traced out by $\pm(x_3(t), x_4(t))$.

The regularization of the SBCs, as described by (i) and (ii) above, in the Hamiltonian system of equations with Hamiltonian H plays a key role in achieving the two objectives. Section 6.2 details this regularization which consists of two canonical transformations followed by a scaling of time $t = \theta(s)$ with s as the regularizing time variable, producing a new Hamiltonian $\hat{\Gamma}$ for the PPS4BP in extended phase space. Section 6.3 describes a scaling of orbits of the Hamiltonian system of equations with Hamiltonian $\hat{\Gamma}$ which shows that any such periodic solution always belongs to a one-parameter family of periodic solutions for which the linear stability is the same for all periodic solutions in the family. Section 6.4 describes the symmetries of the Hamiltonian $\hat{\Gamma}$ which are used to construct periodic solutions with a D_4 symmetry group generated by a time-reversing symmetry and a time-preserving symmetry.

In Sections 6.5 and 6.6, we prove the analytic existence of a periodic SBC orbit $\gamma(s)$, with a D_4 symmetry group, for the Hamiltonian system of equations with Hamiltonian $\hat{\Gamma}$ with $m = 1$, and numerically investigate its stability. The proof extends the analytic existence of a symmetric periodic SBC orbit in the fully symmetric planar four-body equal mass problem, as found in Chapter 4, to the PPS4BP with equal masses. Our numerical estimates of the characteristic multipliers show that this periodic orbit is linearly stable.

6.2 REGULARIZATION

We adapt the regularization of Aarseth and Zare [19] to the PPS4BP to regularize SBCs as described in the first objective. This regularization differs from the one used in the Caledonian symmetric four-body problem [42] in that we only regularize the SBCs as described in the first objective of this chapter's introduction.

The first canonical transformation in our regularization is

$$(x_1, x_2, x_3, x_4, \omega_1, \omega_2, \omega_3, \omega_4) \to (g_1, g_2, g_3, g_4, h_1, h_2, h_3, h_4)$$

determined by the generating function

$$F_1(x_1, x_2, x_3, x_4, h_1, h_2, h_3, h_4) = h_1(x_1 - x_3) + h_2(x_2 - x_4) + h_3(x_1 + x_3) + h_4(x_2 + x_4).$$

So the first canonical transformation is determined by

$$\omega_i = \frac{\partial F_1}{\partial x_i}, \;\; g_i = \frac{\partial F_1}{\partial \omega_i}, \;\; i = 1, 2, 3, 4. \tag{6.1}$$

The new Hamiltonian is $\tilde{H} = \tilde{K} - \tilde{U}$, where

$$\tilde{K} = \frac{(h_1 + h_3)^2 + (h_2 + h_4)^2}{4} + \frac{(h_3 - h_1)^2 + (h_4 - h_2)^2}{4m},$$

and

$$\tilde{U} = \frac{1}{\sqrt{(g_1 + g_3)^2 + (g_2 + g_4)^2}} + \frac{2m}{\sqrt{g_1^2 + g_2^2}} + \frac{2m}{\sqrt{g_3^2 + g_4^2}} + \frac{m^2}{\sqrt{(g_1 - g_3)^2 + (g_2 - g_4)^2}}.$$

The second canonical transformation in our regularization,

$$(g_1, g_2, g_3, g_4, h_1, h_2, h_3, h_4) \to (u_1, u_2, u_3, u_4, v_1, v_2, v_3, v_4)$$

is determined by the generating function

$$F_2(h_1,h_2,h_3,h_4,u_1,u_2,u_3,u_4) = -\sum_{j=1}^{4} h_j f_j(u_1,u_2,u_3,u_4),$$

where

$$f_1 = u_1^2 - u_2^2,\ \ f_2 = 2u_1u_2,\ \ f_3 = u_3^2 - u_4^2,\ \ f_4 = 2u_3u_4.$$

So the second canonical transformation is determined by

$$g_i = -\frac{\partial F_2}{\partial h_i},\ \ v_i = -\frac{\partial F_2}{\partial u_i},\ \ i = 1,2,3,4. \tag{6.2}$$

The new Hamiltonian is $\hat{H} = \hat{K} - \hat{U}$, where

$$\begin{aligned}\hat{K} =& \frac{1}{16}\left(1+\frac{1}{m}\right)\left[\frac{(v_1^2+v_2^2)(u_3^2+u_4^2)+(v_3^2+v_4^2)(u_1^2+u_2^2)}{(u_1^2+u_2^2)(u_3^2+u_4^2)}\right] \\ &+\frac{1}{8}\left(1-\frac{1}{m}\right)\frac{(v_3u_3-v_4u_4)(v_1u_1-v_2u_2)+(v_3u_4+v_4u_3)(v_1u_2+v_2u_1)}{(u_1^2+u_2^2)(u_3^2+u_4^2)},\end{aligned}$$

and

$$\begin{aligned}\hat{U} =& \frac{1}{\sqrt{(u_1^2-u_2^2+u_3^2-u_4^2)^2+(2u_1u_2+2u_3u_4)^2}} + \frac{2m}{u_1^2+u_2^2} + \frac{2m}{u_3^2+u_4^2} \\ &+ \frac{m^2}{\sqrt{(u_1^2-u_2^2-u_3^2+u_4^2)^2+(2u_1u_2-2u_3u_4)^2}}.\end{aligned}$$

We introduce a new time variable s by the regularizing change of time

$$\frac{dt}{ds} = (u_1^2+u_2^2)(u_3^2+u_4^2).$$

To simplify notation, we set

$$
\begin{aligned}
M_1 &= v_1u_1 - v_2u_2, & M_2 &= v_1u_2 + v_2u_1,\\
M_3 &= v_3u_3 - v_4u_4, & M_4 &= v_3u_4 + v_4u_3,\\
M_5 &= u_1^2 - u_2^2 + u_3^2 - u_4^2, & M_6 &= 2u_1u_2 + 2u_3u_4,\\
M_7 &= u_1^2 - u_2^2 - u_3^2 + u_4^2, & M_8 &= 2u_1u_2 - 2u_3u_4.
\end{aligned}
$$

The Hamiltonian in the extended phase space with coordinates u_1, u_2, u_3, u_4, $\hat{E}$, v_1, v_2, v_3, v_4, t is

$$
\begin{aligned}
\hat{\Gamma} = \frac{dt}{ds}\big(\hat{H} - \hat{E}\big) =& \frac{1}{16}\left(1+\frac{1}{m}\right)\Big((v_1^2+v_2^2)(u_3^2+u_4^2) + (v_3^2+v_4^2)(u_1^2+u_2^2)\Big)\\
&+ \frac{1}{8}\left(1-\frac{1}{m}\right)\big(M_3M_1 + M_4M_2\big)\\
&- \frac{(u_1^2+u_2^2)(u_3^2+u_4^2)}{\sqrt{M_5^2+M_6^2}} - 2m\big(u_1^2+u_2^2+u_3^2+u_4^2\big)\\
&- \frac{m^2(u_1^2+u_2^2)(u_3^2+u_4^2)}{\sqrt{M_7^2+M_8^2}} - \hat{E}(u_1^2+u_2^2)(u_3^2+u_4^2).
\end{aligned}
$$

We will use $'$ to denote the derivative with respect to time s. In this notation, the Hamiltonian system of equations with Hamiltonian $\hat{\Gamma}$ is

$$
u_i' = \frac{\partial\hat{\Gamma}}{\partial v_i},\ \ v_i' = -\frac{\partial\hat{\Gamma}}{\partial u_i},\ \ i = 1,2,3,4, \tag{6.3}
$$

along with the auxiliary equations,

$$
\hat{E}' = \frac{\partial\hat{\Gamma}}{\partial t} = 0,\ \ t' = -\frac{\partial\hat{\Gamma}}{\partial\hat{E}} = (u_1^2+u_2^2)(u_3^2+u_4^2). \tag{6.4}
$$

On the level set $\hat{\Gamma} = 0$, the value of the Hamiltonian $\hat{H}$ (i.e., the energy) along solutions of the Hamiltonian system of equations with Hamiltonian $\hat{\Gamma}$ is $\hat{E}$. Independent of the values of $\hat{E}$ and $\hat{\Gamma}$, the angular momentum $A = x_1\omega_2 - x_2\omega_1 + x_3\omega_4 - x_4\omega_3$ in the coordinates $u_1, u_2, u_3, u_4, v_1, v_2, v_3, v_4$

simplifies to

$$A = \frac{1}{2}\big[- v_1 u_2 + v_2 u_1 - v_3 u_4 + v_4 u_3 \big]. \tag{6.5}$$

On the level set $\hat{\Gamma} = 0$, two simultaneous binary collisions in the PPS4BP have been regularized in the Hamiltonian system of equations with Hamiltonian $\hat{\Gamma}$. The simultaneous binary collision $x_3 - x_1 = 0$ and $x_4 - x_2 = 0$ with $x_1^2 + x_2^2 \neq 0$ corresponds to $u_1^2 + u_2^2 = 0$ with $u_3^2 + u_4^2 \neq 0$. These imply that $M_5^2 + M_6^2 = 4(x_1^2 + x_2^2) \neq 0$ and $M_7^2 + M_8^2 = 4(x_1^2 + x_2^2) \neq 0$. From $\hat{\Gamma} = 0$ it follows that

$$v_1^2 + v_2^2 = (32m^2)/(m+1). \tag{6.6}$$

Similarly, the simultaneous binary collision $x_3 + x_1 = 0$ and $x_4 + x_2 = 0$ with $x_1^2 + x_2^2 \neq 0$ corresponds to $u_3^2 + u_4^2 = 0$ with $u_1^2 + u_2^2 \neq 0$, and hence that $M_5^2 + M_6^2 = 4(x_1^2 + x_2^2) \neq 0$, $M_7^2 + M_8^2 = 4(x_1^2 + x_2^2) \neq 0$, and, from $\hat{\Gamma} = 0$, that

$$v_3^2 + v_4^2 = (32m^2)/(m+1).$$

On the level set $\hat{\Gamma} = 0$, the other singularities of the PPS4BP have not been regularized in the Hamiltonian system of equations with Hamiltonian $\hat{\Gamma}$. The binary collision $x_1 = 0$, $x_2 = 0$ with $x_3^2 + x_4^2 \neq 0$ corresponds to $M_5^2 + M_6^2 = 0$ and $M_7^2 + M_8^2 \neq 0$ with $u_1^2 + u_2^2 \neq 0$ and $u_3^2 + u_4^2 \neq 0$. The binary collision $x_3 = 0$, $x_4 = 0$ with $x_1^2 + x_2^2 \neq 0$ corresponds to $M_5^2 + M_6^2 \neq 0$ and $M_7^2 + M_8^2 = 0$ with $u_1^2 + u_2^2 \neq 0$ and $u_3^2 + u_4^2 \neq 0$. Because of the pairwise symmetry, there are no triple collisions. Total collapse $x_1 = 0$, $x_2 = 0$, $x_3 = 0$, $x_4 = 0$ corresponds to $u_1 = 0$, $u_2 = 0$, $u_3 = 0$, and $u_4 = 0$.

We establish next the correspondence between the original coordinates and the regularized coordinates for the initial conditions given in the introduction to this chapter, the proof of which is straightforward.

Lemma 6.1. *The conditions* $(at\ t = 0)$

$$x_1 > 0,\ x_2 = 0,\ x_3 = 0,\ x_4 > 0,\ \text{with } x_4 \le x_1,$$
$$\omega_1 = 0,\ \omega_2 > 0,\ \omega_3 > 0,\ \omega_4 = 0,\ \text{with } \omega_2 \le \omega_3,$$

correspond to the conditions $(at\ s = 0)$

$$u_3 = \pm u_1,\ u_4 = \mp u_2,\ \text{with } u_1u_2 < 0,\ |u_2| \le (\sqrt{2}-1)|u_1|,$$
$$v_3 = \mp v_1,\ v_4 = \pm v_2,\ \text{with } 0 < v_1u_2 + v_2u_1 \le v_2u_2 - v_1u_1.$$

6.3 A Scaling of Periodic Orbits and Linear Stability

A certain scaling of solutions of the Hamiltonian system of equations with Hamiltonian $\hat{\Gamma}$ produces more solutions. When applied to a periodic solution, this scaling leads to a one-parameter family of periodic solutions. The proof of the following result is a straight-forward verification.

Lemma 6.2. *If* $\gamma(s) = (u_1(s), u_2(s), u_3(s), u_4(s), v_1(s), v_2(s), v_3(s), v_4(s))$ *is a periodic solution of the Hamiltonian system of equations with Hamiltonian* $\hat{\Gamma}$ *on the level set* $\hat{\Gamma} = 0$ *with period* T *and energy* $\hat{E}$*, then for every* $\varepsilon > 0$*, the function*

$$\gamma_\varepsilon(s) = (\varepsilon u_1(\varepsilon s), \varepsilon u_2(\varepsilon s), \varepsilon u_3(\varepsilon s), \varepsilon u_4(\varepsilon s), v_1(\varepsilon s), v_2(\varepsilon s), v_3(\varepsilon s), v_4(\varepsilon s))$$

is a periodic solution of the Hamiltonian system of equations with Hamiltonian $\hat{\Gamma}$ *on the level set* $\hat{\Gamma} = 0$ *with period* $T_\varepsilon = \varepsilon^{-1}T$ *and energy* $\hat{E}_\varepsilon = \varepsilon^{-2}\hat{E}$.

6.4 SYMMETRIES

The Hamiltonian system of equations with Hamiltonian $\hat{\Gamma}$ has a group of symmetries isomorphic to the dihedral group $D_4 = \langle a, b : a^2 = b^4 = (ab)^2 = e \rangle$. With

$$F = \begin{bmatrix} -1 & 0 \\ 0 & 1 \end{bmatrix}, \quad G = \begin{bmatrix} 1 & 0 \\ 0 & 1 \end{bmatrix},$$

define the matrices

$$S_F = \begin{bmatrix} 0 & F & 0 & 0 \\ -F & 0 & 0 & 0 \\ 0 & 0 & 0 & F \\ 0 & 0 & -F & 0 \end{bmatrix}, \quad S_G = \begin{bmatrix} -G & 0 & 0 & 0 \\ 0 & G & 0 & 0 \\ 0 & 0 & G & 0 \\ 0 & 0 & 0 & -G \end{bmatrix}.$$

These matrices satisfy $S_F^2 = -I$, $S_F^4 = I$, $S_G^2 = I$, and $(S_F S_G)^2 = I$. Fixing the value of $\hat{E}$, these matrices satisfy $\hat{\Gamma} \circ S_F = \hat{\Gamma}$ and $\hat{\Gamma} \circ S_G = \hat{\Gamma}$, and so S_F and S_G are the generators of the D_4-symmetry group for $\hat{\Gamma}$. If

$$\gamma(s) = (u_1(s), u_2(s), u_3(s), u_4(s), v_1(s), v_2(s), v_3(s), v_4(s))$$

is a solution of the Hamiltonian system of equations with Hamiltonian $\hat{\Gamma}$, then $S_F\gamma(s)$, $S_F^2\gamma(s)$, and $S_G\gamma(-s)$ are also solutions of the Hamiltonian system of equations with Hamiltonian $\hat{\Gamma}$. This means that S_F is a time-preserving symmetry and that S_G is a time-reversing symmetry. The proof of the following follows the same procedure as similar proofs in Chapters 4 and 5.

Lemma 6.3. *If for some $s_0 > 0$ there is a nonsingular solution $\gamma(s)$, $s \in [0, s_0]$, of the Hamiltonian system of equations with Hamiltonian $\hat{\Gamma}$ such that for constants $\zeta_1 \neq 0$, $\zeta_2 \neq 0$, $\rho_1 \neq 0$, and $\rho_2 \neq 0$ there holds*

$$u_1(0) = \zeta_1,\ u_2(0) = \zeta_2,\ u_3(0) = \zeta_1,\ u_4(0) = -\zeta_2,$$
$$v_1(0) = \rho_1,\ v_2(0) = \rho_2,\ v_3(0) = -\rho_1,\ v_4(0) = \rho_2,$$

and

$$u_1(s_0) = 0,\ u_2(s_0) = 0,\ u_3(s_0) \neq 0,\ u_4(s_0) \neq 0,$$
$$v_1(s_0) \neq 0,\ v_2(s_0) \neq 0,\ v_3(s_0) = 0,\ v_4(s_0) = 0,$$

then $\gamma(s)$ *extends to a periodic orbit with period* $8s_0$ *and a symmetry group isomorphic to* D_4 *such that*

$$u_1(3s_0) \neq 0,\ u_2(3s_0) \neq 0,\ u_3(3s_0) = 0,\ u_4(3s_0) = 0,$$
$$v_1(3s_0) = 0,\ v_2(3s_0) = 0,\ v_3(3s_0) \neq 0,\ v_4(3s_0) \neq 0,$$

and

$$u_1(5s_0) = 0,\ u_2(5s_0) = 0,\ u_3(5s_0) \neq 0,\ u_4(5s_0) \neq 0,$$
$$v_1(5s_0) \neq 0,\ v_2(5s_0) \neq 0,\ v_3(5s_0) = 0,\ v_4(5s_0) = 0,$$

and

$$u_1(7s_0) \neq 0,\ u_2(7s_0) \neq 0,\ u_3(7s_0) = 0,\ u_4(7s_0) = 0,$$
$$v_1(7s_0) = 0,\ v_2(7s_0) = 0,\ v_3(7s_0) \neq 0,\ v_4(7s_0) \neq 0.$$

6.5 Analytic Existence in the Equal Mass Case

When $m = 1$, there is an additional symmetry in the positions of the four masses that reduces the PPS4BP with equal masses to the fully symmetric planar four-body equal mass problem. We exploit this reduction to prove the existence of a symmetric periodic simultaneous binary collision orbit in the equal mass case.

The additional symmetry is the Ansätz, $x_4 = x_1$, $x_3 = x_2$, with $|x_2| \leq x_1$. From this it follows that $\omega_4 = \omega_1$, $\omega_3 = \omega_2$, $x_1 - x_2 \geq 0$, $x_1 + x_2 \geq 0$. From the canonical transformations (6.1) and

(6.2), we have

$$\frac{2u_1^2}{1+\sqrt{2}} = x_1 - x_2 = \frac{2u_2^2}{-1+\sqrt{2}}, \quad \frac{2u_3^2}{1+\sqrt{2}} = x_1 + x_2 = \frac{2u_4^2}{-1+\sqrt{2}}.$$

Since $2u_1u_2 = g_2 = x_2 - x_1 \leq 0$ and $2u_3u_4 = g_4 = x_1 + x_2 \geq 0$, it follows that

$$u_2 = -(\sqrt{2}-1)u_1, \quad u_4 = (\sqrt{2}-1)u_3. \tag{6.7}$$

From the second canonical transformation (6.2), we have

$$\begin{aligned} v_1 &= \sqrt{2}(\omega_1 - \omega_2)u_1, & v_2 &= -(2-\sqrt{2})(\omega_1 - \omega_2)u_1, \\ v_3 &= \sqrt{2}(\omega_1 + \omega_2)u_3, & v_4 &= (2-\sqrt{2})(\omega_1 + \omega_2)u_3. \end{aligned}$$

These imply that

$$v_2 = -(\sqrt{2}-1)v_1, \quad v_4 = (\sqrt{2}-1)v_3. \tag{6.8}$$

Substitution into the Hamiltonian system of equations with Hamiltonian $\hat{\Gamma}$ (and with $m = 1$) gives

$$\begin{aligned} u_1' &= \frac{4-2\sqrt{2}}{4} v_1 u_3^2, & u_2' &= -\frac{(\sqrt{2}-1)(4-2\sqrt{2})}{4} v_1 u_3^2, \\ u_3' &= \frac{4-2\sqrt{2}}{4} v_3 u_1^2, & u_4' &= \frac{(\sqrt{2}-1)(4-2\sqrt{2})}{4} v_3 u_1^2, \end{aligned}$$

$\hat{E}' = 0$, and

$$
\begin{aligned}
v_1' =& -\frac{(4-2\sqrt{2})u_1 v_3^2}{4} + 4u_1 + \frac{4u_1 u_3^2}{\sqrt{u_1^4+u_3^4}} - \frac{4u_1^5 u_3^2}{\left(u_1^4+u_3^4\right)^{3/2}} + 2(4-2\sqrt{2})\hat{E}u_1 u_3^2,\\
v_2' =& -(\sqrt{2}-1)\Bigg[-\frac{(4-2\sqrt{2})u_1 v_3^2}{4} + 4u_1 + \frac{4u_1 u_3^2}{\sqrt{u_1^4+u_3^4}} - \frac{4u_1^5 u_3^2}{\left(u_1^4+u_3^4\right)^{3/2}}\\
&\qquad + 2(4-2\sqrt{2})\hat{E}u_1 u_3^2\Bigg],\\
v_3' =& -\frac{(4-2\sqrt{2})u_3 v_1^2}{4} + 4u_3 + \frac{4u_1^2 u_3}{\sqrt{u_1^4+u_3^4}} - \frac{4u_1^2 u_3^5}{\left(u_1^4+u_3^4\right)^{3/2}} + 2(4-2\sqrt{2})\hat{E}u_1^2 u_3,\\
v_4' =& (\sqrt{2}-1)\Bigg[-\frac{(4-2\sqrt{2})u_3 v_1^2}{4} + 4u_3 + \frac{4u_1^2 u_3}{\sqrt{u_1^4+u_3^4}} - \frac{4u_1^2 u_3^5}{\left(u_1^4+u_3^4\right)^{3/2}}\\
&\qquad + 2(4-2\sqrt{2})\hat{E}u_1^2 u_3\Bigg],\\
t' =& (4-2\sqrt{2})^2 u_1^2 u_3^2.
\end{aligned}
$$

Because of Equations (6.7) and (6.8), the equations in u_2', u_4', v_2', and v_4' duplicate those in u_1', u_3', v_1', and v_3'. The Ansätz $x_4 = x_1$, $x_3 = x_2$ with $|x_2| \leq x_1$, therefore leads to the reduced system of equations,

$$
\begin{aligned}
u_1' =& \frac{4-2\sqrt{2}}{4} v_1 u_3^2,\\
u_3' =& \frac{4-2\sqrt{2}}{4} v_3 u_1^2,\\
\hat{E}' =& 0,\\
v_1' =& -\frac{(4-2\sqrt{2})u_1 v_3^2}{4} + 4u_1 + \frac{4u_1 u_3^2}{\sqrt{u_1^4+u_3^4}} - \frac{4u_1^5 u_3^2}{\left(u_1^4+u_3^4\right)^{3/2}} + 2(4-2\sqrt{2})\hat{E}u_1 u_3^2,\\
v_3' =& -\frac{(4-2\sqrt{2})u_3 v_1^2}{4} + 4u_3 + \frac{4u_1^2 u_3}{\sqrt{u_1^4+u_3^4}} - \frac{4u_1^2 u_3^5}{\left(u_1^4+u_3^4\right)^{3/2}} + 2(4-2\sqrt{2})\hat{E}u_1^2 u_3,\\
t' =& (4-2\sqrt{2})^2 u_1^2 u_3^2.
\end{aligned}
$$

Scale the value of $\hat{E}$ by

$$\tilde{E} = \frac{\hat{E}}{4-2\sqrt{2}}, \tag{6.9}$$

and define

$$\tilde{\Gamma} = \frac{4-2\sqrt{2}}{8}\left(v_1^2u_3^2+v_3^2u_1^2\right) - 2(u_1^2+u_3^2) - \frac{2u_1^2u_3^2}{\sqrt{u_1^4+u_3^4}} - (4-2\sqrt{2})^2\tilde{E}u_1^2u_3^2.$$

It is straight-forward to check that the reduced system of equations satisfies

$$u_i' = \frac{\partial\tilde{\Gamma}}{\partial v_i},\ \ v_i' = -\frac{\partial\tilde{\Gamma}}{\partial u_i},\ \ i=1,2,\ \ \tilde{E}' = \frac{\partial\tilde{\Gamma}}{\partial t},\ \ t' = -\frac{\partial\tilde{\Gamma}}{\partial\tilde{E}}.$$

Thus the system of reduced equations is Hamiltonian.

We will simplify the Hamiltonian $\tilde{\Gamma}$ by a linear symplectic transformation with a multiplier $\mu \neq 1$. Define new coordinates $(Q_1, Q_2, E, P_1, P_2, \tau)$ by

$$u_1 = \frac{Q_1}{2^{1/4}}, \qquad v_1 = \frac{P_1}{2\sqrt{\sqrt{2}-1}}, \tag{6.10}$$

$$u_3 = \frac{Q_2}{2^{1/4}}, \qquad v_3 = \frac{P_2}{2\sqrt{\sqrt{2}-1}}, \tag{6.11}$$

$$\tilde{E} = \frac{2E}{(4-2\sqrt{2})^2}, \qquad t = 2^{3/4}(\sqrt{2}-1)^{3/2}\,\tau. \tag{6.12}$$

This is a linear symplectic change of coordinates with multiplier

$$\mu = \frac{1}{2^{5/4}\sqrt{\sqrt{2}-1}}. \tag{6.13}$$

Under this linear symplectic transformation and the accompanying scaling $\sigma = s/\mu$ of the independent variable s, the Hamiltonian $\tilde{\Gamma}$ becomes

$$\Gamma = \frac{1}{16}\left(P_1^2Q_2^2+P_2^2Q_1^2\right) - \sqrt{2}(Q_1^2+Q_2^2) - \frac{\sqrt{2}Q_1^2Q_2^2}{\sqrt{Q_1^4+Q_2^4}} - EQ_1^2Q_2^2.$$

The reduced system of equations is the Hamiltonian system of equations with Hamiltonian Γ,

$$\frac{dQ_i}{d\sigma} = \frac{\partial \Gamma}{\partial P_i}, \;\; \frac{dP_i}{d\sigma} = -\frac{\partial \Gamma}{\partial Q_i}, \;\; i = 1,2, \;\; \frac{dE}{d\sigma} = 0, \;\; \frac{d\tau}{d\sigma} = Q_1^2 Q_2^2. \tag{6.14}$$

The function Γ is a regularized Hamiltonian for the fully symmetric planar four-body equal mass problem with the bodies located at (x_1,x_2), (x_2,x_1), $(-x_1,-x_2)$, and $(-x_2,-x_1)$, giving the same setting as in Chapter 4. On the level set $\Gamma = 0$, the solutions have energy E. One regularized simultaneous binary collision occurs when $Q_1 = 0$ and $Q_2 \neq 0$, for which $\Gamma = 0$ implies $P_1^2 = 16\sqrt{2}$, and for which the transformation between Q_1, Q_2 and x_1, x_2 implies $x_1 - x_2 = 0$ and $x_1 + x_2 \neq 0$. The other regularized simultaneous binary collision occurs when $Q_1 \neq 0$ and $Q_2 = 0$, for which $\Gamma = 0$ implies $P_2^2 = 16\sqrt{2}$, and for which the transformation between Q_1, Q_2 and x_1, x_2 implies $x_1 - x_2 \neq 0$ and $x_1 + x_2 = 0$. Total collapse occurs when $Q_1 = 0$ and $Q_2 = 0$, and is the only singularity in Γ that is not regularized.

From Chapter 4 (notation slightly varied):

Lemma 6.4. *There exists $\vartheta > 0$, $\sigma_0 > 0$, and a nonsingular solution $Q_1(\sigma)$, $Q_2(\sigma)$, $P_1(\sigma)$, $P_2(\sigma)$, $\sigma \in [0, \sigma_0]$, of the Hamiltonian system of equations with Hamiltonian Γ on the level set $\Gamma = 0$ such that*

$$Q_1(0) = 1, \;\; Q_2(0) = 1, \;\; P_1(0) = -\vartheta, \;\; P_2(0) = \vartheta, \tag{6.15}$$

$$E = \frac{\vartheta^2 - 16\sqrt{2} - 8}{8} < 0, \;\; \tau(\sigma) = \int_0^\sigma Q_1^2(y) Q_2^2(y)\, dy, \tag{6.16}$$

and

$$Q_1(\sigma_0) = 0, \;\; Q_2(\sigma_0) > 0, \;\; P_1(\sigma_0) = -4(2^{1/4}), \;\; P_2(\sigma_0) = 0. \tag{6.17}$$

This Lemma gives the existence of a solution of a boundary value problem for the Hamiltonian system of equations with Hamiltonian Γ. It is this solution whose symmetric extension gives a symmetric periodic SBC orbit in the PPS4BP with equal masses.

Theorem 6.5. *Fix $m = 1$. For each $\hat{E} < 0$, there exists a time-reversible periodic regularized SBC*

orbit

$$\gamma(s) = (u_1(s), u_2(s), u_3(s), u_4(s), v_1(s), v_2(s), v_3(s), v_4(s))$$

with period $T > 0$, angular momentum $A = 0$, and a symmetry group isomorphic to D_4, for the Hamiltonian system of equations with Hamiltonian $\hat{\Gamma}$ on the level set $\hat{\Gamma} = 0$ such that distinct regularized SBCs occur at $s = T/8, 3T/8, 5T/8, 7T/8$. This periodic orbit corresponds to a symmetric periodic singular orbit

$$(x_1(t),\ x_2(t),\ x_3(t),\ x_4(t),\ \omega_1(t),\ \omega_2(t),\ \omega_3(t),\ \omega_4(t))$$

with energy $\hat{E}$ for the PPS4BP with equal masses $m = 1$ where for all t,

$$x_4(t) = x_1(t),\ x_3(t) = x_2(t),\ |x_2(t)| \leq x_1(t),\ \omega_4(t) = \omega_1(t),\ \omega_3(t) = \omega_2(t),$$

with initial conditions

$$x_1(0) > 0,\ x_2(0) = 0,\ \omega_1(0) = 0,\ \omega_2(0) > 0,$$

and period

$$R = \int_0^{T/2} \left(u_1^2(s) + u_2^2(s)\right)\left(u_3^2(s) + u_4^2(s)\right)\, ds,$$

where for $t \in [0, R]$, the only singularities are two distinct SBC's occurring at $t = R/4$ and $t = 3R/4$.

Proof. By Lemma 6.4, let $Q_1(\sigma)$, $Q_2(\sigma)$, $P_1(\sigma)$, $P_2(\sigma)$, $\sigma \in [0, \sigma_0]$, be the nonsingular solution of the Hamiltonian system of equations (6.14) with Hamiltonian Γ on the level set $\Gamma = 0$, whose properties are given in (6.15), (6.16), and (6.17). Using the scaling $\sigma = s/\mu$, set $s_0 = \mu\sigma_0$. By the linear symplectic transformation given in (6.10), (6.11), and (6.12) with multiplier μ (as given in (6.13)), we have

$$u_1(s) = \frac{Q_1(s/\mu)}{2^{1/4}},\ \ u_3(s) = \frac{Q_2(s/\mu)}{2^{1/4}},\ \ v_1(s) = \frac{P_1(s/\mu)}{2\sqrt{\sqrt{2}-1}},\ \ v_3(s) = \frac{P_2(s/\mu)}{2\sqrt{\sqrt{2}-1}}.$$

By Equations (6.7) and (6.8), we have

$$u_2(s) = \frac{-(\sqrt{2}-1)Q_1(s/\mu)}{2^{1/4}}, \;\; u_4(s) = \frac{(\sqrt{2}-1)Q_2(s/\mu)}{2^{1/4}},$$

$$v_2(s) = \frac{-\sqrt{\sqrt{2}-1}P_1(s/\mu)}{2}, \;\; v_4(s) = \frac{\sqrt{\sqrt{2}-1}P_2(s/\mu)}{2}.$$

Set $\gamma(s) = (u_1(s), u_2(s), u_3(s), u_4(s), v_1(s), v_2(s), v_3(s), v_4(s))$, $s \in [0, s_0]$. From the Equations (6.9), (6.12), (6.16) in E, $\hat{E}$, $\tilde{E}$, and ϑ, we obtain

$$\hat{E} = \frac{(2+\sqrt{2})\vartheta^2}{16} - 3 - \frac{5\sqrt{2}}{2} < 0.$$

With this value of $\hat{E}$, it follows that the value of $\hat{\Gamma}$ at $\gamma(0)$ is 0. Set

$$\zeta_1 = \frac{1}{2^{1/4}} > 0, \;\; \zeta_2 = \frac{-(\sqrt{2}-1)}{2^{1/4}} < 0,$$

$$\rho_1 = \frac{-\vartheta}{2\sqrt{\sqrt{2}-1}} < 0, \;\; \rho_2 = \frac{\vartheta\sqrt{\sqrt{2}-1}}{2} > 0.$$

With $Q_1(\sigma)$, $Q_2(\sigma)$, $P_1(\sigma)$, $P_2(\sigma)$, $\sigma \in [0, \sigma_0]$, being a nonsingular solution of the Hamiltonian system of equations with Hamiltonian Γ, we have $Q_1^4(\sigma) + Q_2^4(\sigma) \neq 0$ for all $\sigma \in [0, \sigma_0]$. From this it follows for all $s \in [0, s_0]$ that

$$M_5 = u_1^2(s) - u_2^2(s) + u_3^2(s) - u_4^2(s) = (2-\sqrt{2})\left[Q_1^2(s/\mu) + Q_2^2(s/\mu)\right] \neq 0,$$

and

$$M_8 = 2u_1(s)u_2(s) - 2u_3(s)u_4(s) = -(2-\sqrt{2})\left[Q_1^2(s/\mu) + Q_2^2(s/\mu)\right] \neq 0.$$

These imply that $M_5^2 + M_6^2 \neq 0$ and $M_7^2 + M_8^2 \neq 0$ for all $s \in [0, s_0]$. Thus the function $\gamma(s)$ is a nonsingular solution of the Hamiltonian system of equations (6.3) with Hamiltonian $\hat{\Gamma}$ on the level

set $\hat{\Gamma} = 0$ that satisfies

$$u_1(0) = \zeta_1, \;\; u_2(0) = \zeta_2 \;\; u_3(0) = \zeta_1, \;\; u_4(0) = -\zeta_2,$$

$$v_1(0) = \rho_1, \;\; v_2(0) = \rho_2, \;\; v_3(0) = -\rho_1, \;\; v_4(0) = \rho_2,$$

$$u_1(s_0) = 0, \;\; u_2(s_0) = 0, \;\; u_3(s_0) > 0, \;\; u_4(s_0) > 0,$$

$$v_1(s_0) < 0, \;\; v_2(s_0) > 0, \;\; v_3(s_0) = 0, \;\; v_4(s_0) = 0.$$

By Lemma 6.3, the solution $\gamma(s)$ extends to a $T = 8s_0$ periodic solution, call it $\gamma(s)$, with a D_4 symmetry group generated by the symmetries S_F and S_G, and four distinct regularized simultaneous binary collisions at $s = s_0, 3s_0, 5s_0, 7s_0$, for which

$$\begin{aligned}
&u_1^2(s_0) + u_2^2(s_0) = 0, \; u_3^2(s_0) + u_4^2(s_0) \neq 0, \\
&u_1^2(3s_0) + u_2^2(3s_0) \neq 0, \; u_3^2(3s_0) + u_4^2(3s_0) = 0, \\
&u_1^2(5s_0) + u_2^2(5s_0) = 0, \; u_3^2(5s_0) + u_4^2(5s_0) \neq 0, \\
&u_1^2(7s_0) + u_2^2(7s_0) \neq 0, \; u_3^2(7s_0) + u_4^2(7s_0) = 0.
\end{aligned}$$

Since $Q_1^4(\sigma) + Q_2^4(\sigma) \neq 0$ for all $\sigma \in [0, \sigma_0]$, it follows that $(u_1^2(s) + u_2^2(s))(u_3^2(s) + u_4^2(s)) \neq 0$ for $s \in [0, T]$ except $s = s_0, 3s_0, 5s_0, 7s_0$. The regularizing change of time (6.4),

$$\frac{dt}{ds} = (u_1^2(s) + u_2^2(s))(u_3^2(s) + u_4^2(s)),$$

defines t as an invertible differentiable function of s, i.e., $t = \theta(s)$ with $\theta(0) = 0$ and $\theta'(s) = 0$ when $s = (2k+1)s_0$ for $k \in \mathbb{Z}$. The symmetry S_F satisfies $S_F\gamma(s) = \gamma(s+2s_0)$ and $-\gamma(s) = S_F^2\gamma(s) = \gamma(s+4s_0)$. The symmetry S_G satisfies $S_G\gamma(s) = \gamma(2s_0 - s)$, and so $\gamma(s)$ has a time-reversing symmetry. The angular momentum (6.5) for $\gamma(s)$ at $s = 0$ is

$$A = \frac{1}{2}\big[-v_1u_2 + v_2u_1 - v_3u_4 + v_4u_3 \big] = \rho_2\zeta_1 - \rho_1\zeta_2 = 0.$$

The extended solution $\gamma(s)$ gives a singular symmetric solution

$$z(t) = (x_1(t), x_2(t), x_3(t), x_4(t), \omega_1(t), \omega_2(t), \omega_3(t), \omega_4(t)),$$

of the PPS4BP with $m = 1$. Under the Ansätz, the components of $z(t)$ satisfies $x_4(t) = x_1(t)$, $x_3(t) = x_2(t)$, $|x_2(t)| \le x_1(t)$, $\omega_4(t) = \omega_1(t)$, $\omega_3(t) = \omega_2(t)$, where

$$\begin{aligned}
x_1(t) &= \frac{u_1^2(s) - u_2^2(s) + u_3^2(s) - u_4^2(s)}{2}, \\
x_2(t) &= u_1(s)u_2(s) + u_3(s)u_4(s), \\
\omega_1(t) &= \frac{v_1(s)u_1(s) - v_2(s)u_2(s)}{2(u_1^2(s) + u_2^2(s))} + \frac{v_3(s)u_3(s) - v_4(s)u_4(s)}{2(u_3^2(s) + u_4^2(s))}, \\
\omega_2(t) &= \frac{v_1(s)u_2(s) + v_2(s)u_1(s)}{2(u_1^2(s) + u_2^2(s))} + \frac{v_3(s)u_4(s) + v_4(s)u_3(s)}{2(u_3^2(s) + u_4^2(s))},
\end{aligned}$$

for $s = \theta^{-1}(t)$. The components of the extended solution $\gamma(s)$ satisfy $u_3(0) = u_1(0)$, $u_4(0) = -u_2(0)$, $u_1(0)u_2(0) < 0$, $|u_2(0)| = (\sqrt{2}-1)|u_1(0)|$, $v_3(0) = -v_1(0)$, $v_4(0) = v_2(0)$,

$$v_1(0)u_2(0) + v_2(0)u_1(0) = \rho_1\zeta_2 + \rho_2\zeta_1 = \frac{\sqrt{\sqrt{2}-1}\,\vartheta}{2^{1/4}} > 0,$$

and

$$v_2(0)u_2(0) - v_1(0)u_1(0) = \rho_2\zeta_2 - \rho_1\zeta_1 = \frac{\sqrt{\sqrt{2}-1}\,\vartheta}{2^{1/4}}.$$

From Lemma 6.1, it follows that $x_1(0) > 0$, $x_2(0) = 0$, $\omega_1(0) = 0$, and $\omega_2(0) > 0$. Set $R = \theta(T/2)$. Since $\gamma(4s_0) = -\gamma(0)$, it follows that $x_1(R) = x_1(0)$, $x_2(R) = x_2(0)$, $\omega_1(R) = \omega_1(0)$, and $\omega_2(R) = \omega_2(0)$. Thus the singular symmetric solution $z(t)$ has period R. By the construction of the extension of $\gamma(s)$ given in Lemma 6.3, there holds

$$\int_{ks_0}^{(k+1)s_0} (u_1^2(s) + u_2^2(s))(u_3^2(s) + u_4^2(s))\, ds = \int_0^{s_0} (u_1^2(s) + u_2^2(s))(u_3^2(s) + u_4^2(s))\, ds$$

for all $k = 1, \ldots, 7$. This implies that $R/4 = \theta((k+1)s_0) - \theta(ks_0)$ for all $k = 0, 1, \ldots, 7$. The first

regularized SBC for $\gamma(s)$ occurs at $s = s_0$, and this corresponds to $t = \theta(s_0) = R/4$. The next regularized SBC for $\gamma(s)$ occurs at $s = 3s_0$, and this corresponds to

$$t = \theta(3s_0) = (\theta(3s_0) - \theta(2s_0)) + (\theta(2s_0) - \theta(s_0)) + \theta(s_0) = \frac{R}{4} + \frac{R}{4} + \frac{R}{4} = \frac{3R}{4}.$$

Similarly, the regularized SBCs for $\gamma(s)$ occurring at $s = 5s_0, 7s_0$ correspond to $t = 5R/4, 7R/4$. Hence, for $t \in [0, R]$, the periodic solution $z(t)$ has SBCs as its only singularities, and these occur at $t = R/4, 3R/4$.

For a fixed but arbitrary $\varepsilon > 0$, the value of $\varepsilon^{-2}\hat{E}$ is a fixed but arbitrary negative real number. By Lemma 6.2, the scaled extended solution

$$\gamma_\varepsilon(s) = (\varepsilon u_1(\varepsilon s), \varepsilon u_2(\varepsilon s), \varepsilon u_3(\varepsilon s), \varepsilon u_4(\varepsilon s), v_1(\varepsilon s), v_2(\varepsilon s), v_3(\varepsilon s), v_4(\varepsilon s))$$

is a periodic solution for the Hamiltonian system of equations (6.3) with Hamiltonian $\hat{\Gamma}$ on the level set $\hat{\Gamma} = 0$, having period $\varepsilon^{-1}T$ and energy $\varepsilon^{-2}\hat{E} < 0$. By an argument similar to above, $\gamma_\varepsilon(s)$ satisfies the required conditions. □

6.6 Numerical Estimates in the Equal Mass Case

In the equal mass case, there is by Theorem 6.5 a time-reversible periodic orbit $\gamma(s)$ for the Hamiltonian system of equations with Hamiltonian $\hat{\Gamma}$ on the level set $\hat{\Gamma} = 0$ with period T. The components $u_1(s)$, $u_2(s)$, $u_3(s)$, $u_4(s)$, $v_1(s)$, $v_2(s)$, $v_3(s)$, $v_4(s)$ of $\gamma(s)$ satisfy Equations (6.7) and (6.8). The D_4 symmetry group of $\gamma(s)$ is generated by $S_F\gamma(s) = \gamma(s + T/4)$ and $S_G\gamma(s) = \gamma(T/4 - s)$. Under the linear symplectic transformation (6.10), (6.11), and (6.12) with multiplier μ (as given by (6.13)), this gives a periodic orbit $Q_1(\sigma)$, $Q_2(\sigma)$, $P_1(\sigma)$, $P_2(\sigma)$ of the Hamiltonian system of equations (6.14) with Hamiltonian Γ on the level set $\Gamma = 0$, which by Lemma 6.4 satisfies $Q_1(0) = 1$, $Q_2(0) = 1$, $P_1(0) = -\vartheta$, $P_2(0) = \vartheta$, $Q_1(\sigma_0) = 0$, $Q_2(\sigma_0) > 0$, $P_1(\sigma_0) = -4(2^{1/4})$, and $P_2(\sigma_0) = 0$

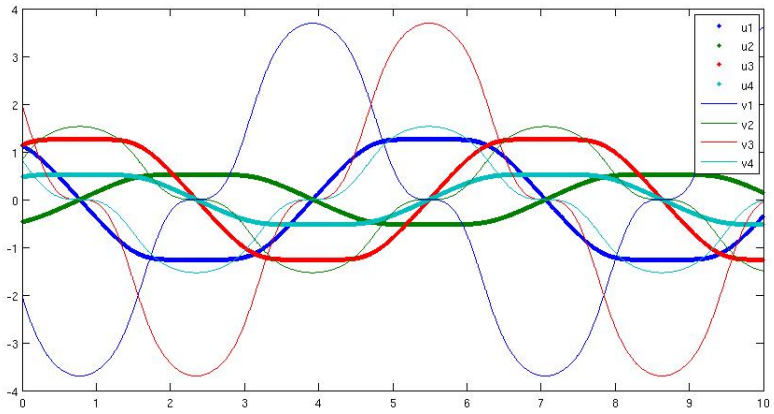

Figure 6.2: The u_1, u_2, u_3, u_4, v_1, v_2, v_3, v_4 coordinates of the symmetric periodic SBC orbit $\gamma_\varepsilon(s)$ for $m = 1$ and an $\varepsilon > 1$.

for some $\sigma_0 > 0$ and $\vartheta > 0$. In Chapter 5, we numerically estimated

$$\sigma_0 \approx 1.62047, \quad \vartheta \approx 2.57487.$$

The period of this periodic orbit is $8\sigma_0 \approx 12.96379$ and its energy is $E \approx -2.99968$. From the linear symplectic transformation (6.10), (6.11), and (6.12), with multiplier μ and from Equations (6.7) and (6.8), we have for the values of components of $\gamma(0)$ the exact quantities

$$u_1(0) = u_3(0) = 2^{-1/4}, \quad -u_2(0) = u_4(0) = (\sqrt{2}-1)2^{-1/4},$$

and the estimates

$$v_1(0) = -v_3(0) = -\frac{\vartheta}{2\sqrt{\sqrt{2}-1}} \approx -2.00038,$$
$$v_2(0) = v_4(0) = \frac{\vartheta\sqrt{\sqrt{2}-1}}{2} \approx 0.82859.$$

Since $\sigma = s/\mu$, the period of $\gamma(s)$ is $T \approx 8.46900$. From Equation (6.9), the value of the energy for $\gamma(s)$ is $\hat{E} \approx -5.12077$.

The components of the scaled periodic orbit $\gamma_\varepsilon(s)$ for an $\varepsilon > 1$, shown in Figure 6.2, satisfy the symmetries $S_F\gamma_\varepsilon(s) = \gamma_\varepsilon(s + T_\varepsilon/4)$ and $S_G\gamma_\varepsilon(s) = \gamma_\varepsilon(T_\varepsilon/4 - s)$. We choose ε so that $T_\varepsilon = 2\pi$, and check the linear stability of $\gamma_\varepsilon(s)$. Using a Runge-Kutta order 4 algorithm with a fixed time step of $2\pi/50000$, we computed $X_\varepsilon(2\pi)$. Two of the eigenvalues of $X_\varepsilon(2\pi)$ are 1. Numerical estimates of the remaining eigenvalues of $X_\varepsilon(2\pi)$ are

$$-0.98887 \pm 0.14876i,$$
$$-0.99736 \pm 0.07264i,$$
$$0.99991 \pm 0.01371i,$$

which all have modulus one. Thus numerically, the periodic orbits $\gamma_\varepsilon(s)$ are linearly stable for all $\varepsilon > 0$. The first complex conjugate pair of eigenvalues for $X_\varepsilon(2\pi)$ matches the complex conjugate pair of characteristic multipliers for the periodic orbit $Q_1(\sigma)$, $Q_2(\sigma)$, $P_1(\sigma)$, $P_2(\sigma)$ of the Hamiltonian system of equations (6.14) with Hamiltonian Γ, corresponding to $\gamma_1(s) = \gamma(s)$, where we computed [27] the real part of the complex conjugate pair of modulus one to be -0.9888840619. Because, by a lengthly computation, $J\nabla^2\hat{\Gamma}(\gamma_\varepsilon(s))$ is not block diagonal, the last two complex conjugate pairs of eigenvalues of $X_\varepsilon(2\pi)$ are not repeats of the characteristic multipliers of the periodic orbit $Q_1(\sigma)$, $Q_2(\sigma)$, $P_1(\sigma)$, $P_2(\sigma)$.

Figure 6.1 illustrates the curves in the physical plane that the four equal masses follow in the linearly stable SBC orbit $z(t) = (x_1(t), x_2(t), x_3(t), x_4(t), \omega(t), \omega_2(t), \omega_3(t), \omega_4(t))$ of the PPS4BP, corresponding to $\gamma_\varepsilon(s)$ with $\varepsilon = 1/(2 - \sqrt{2})$. The initial conditions for $z(t)$ are

$$x_1(0) = x_4(0) = 1, \;\; x_2(0) = x_3(0) = 0, \;\; \omega_1(0) = \omega_4(0) = 0, \;\; \omega_2(0) = \omega_3(0) \approx 1.28743.$$

The value of $\varepsilon = 1/\sqrt{2 - \sqrt{2}}$ here for the scaling is determined by the equation $x_1(0) = \varepsilon^2(u_1^2(0) - u_2^2(0))$ coming from Lemma 6.1 and the canonical transformations (6.1) and (6.2) applied to the scaled periodic solution $\gamma_\varepsilon(s)$, together with the initial condition $x_1(0) = 1$, where $t = 0$ corresponds to $s = 0$. The value of the Hamiltonian H along $z(t)$ is $\varepsilon^{-2}\hat{E} \approx -2.999682732$.

CHAPTER 7. LINEAR STABILITY OF THE PAIRWISE EQUAL-MASS PLANAR ORBIT

7.1 INTRODUCTION

The results presented in this chapter were originally published as [30]. We apply Roberts' symmetry reduction method to a one-parameter family of symmetric singular periodic orbits in the planar pairwise symmetric four-body problem (PPS4BP) where the parameter is a mass $m \in (0,1]$ and the singularities are regularizable simultaneous binary collisions (SBCs). We recall in Section 7.2 the notation we used in [28] for the PPS4BP. (The PPS4BP is the Caledonian symmetric four-body problem [42] without its collinear restrictions on the initial conditions.) To compute the nontrivial characteristic multipliers of these periodic orbits we numerically integrated the linearized regularized equations along each regularized periodic orbit over only one-eighth of its period. This shows that numerically these symmetric singular periodic orbits experience several changes in their linear stability type (linearly stable, spectrally stable, or linearly unstable) as m is varied over $(0,1]$.

In this case, we use Roberts' symmetry reduction method to analytically factor out two of the trivial characteristic multipliers, leaving the numerical computations to estimate the two pairs of nontrivial characteristic multipliers and one pair of trivial characteristic multipliers. The details of these computations are given in Section 7.3. Two surprises here are the intervals $[0.21, 0.22]$ and $[0.23, 0.26]$ where we have linear stability. Long-term numerical integrations of the regularized equations for these periodic orbits (starting at our numerical approximations of their initial conditions and over 100932 periods) suggest instability for m in these two intervals.

7.2 LINEAR STABILITY OF THE PPS4BP

We use the same notatons from Chapter 6 for the PPS4BP, its regularized Hamiltonian, and properties of the regularized one-parameter family of symmetric SBC period orbits.

We apply Roberts' symmetry reduction method [1] to the one-parameter family of periodic

orbits $\gamma(s;m)$, $0 < m \leq 1$, of fixed period 2π, in the regularized Hamiltonian system (6.3). Let $\nabla^2\hat{\Gamma}$ denote the symmetric matrix of second-order partials of $\hat{\Gamma}$ with respect to the components of z. It is easily shown, that if $Y(t)$ is the fundamental matrix solution of the linearized equations along $\gamma(s;m)$,

$$\xi' = J\nabla^2\hat{\Gamma}(\gamma(s))\xi, \;\; \xi(0) = Y_0,$$

for an invertible Y_0, then the eigenvalues of $Y_0^{-1}Y(2\pi)$ are indeed the characteristic multipliers of $\gamma(s;m)$.

7.2.1 Stability Reductions using Symmetries. We use the symmetries of $\gamma(s;m)$ to show that $Y_0^{-1}Y(2\pi)$ can be factored in part by terms of the form $Y(\pi/4)$, that is, one-eighth of the period of $\gamma(s;m)$. Thus the symmetries of $\gamma(s;m)$ will reduce the analysis of its linear stability type to the numerical computation of $Y(\pi/4)$.

Lemma 7.1. *For each $0 < m \leq 1$, there exists a matrix W such that $Y_0^{-1}Y(2\pi) = W^4$ where $W = \Lambda D$ for involutions Λ and D with $\Lambda = Y_0^{-1}S_F^T S_G Y_0$ and $D = B^{-1}S_G B$ for $B = Y(\pi/4)$.*

Proof. Each $\gamma(s;m)$ satisfies $S_F\gamma(s;m) = \gamma(s+\pi/2;m)$. Then (by [1], see also [27]), we have that

$$Y(k\pi/2) = S_F^k Y_0 (Y_0^{-1}S_F^T Y(\pi/2))^k$$

holds for all $k \in \mathbb{N}$. Since $S_F^4 = I$, taking $k = 4$ gives

$$Y(2\pi) = Y_0(Y_0^{-1}S_F^T Y(\pi/2))^4. \tag{7.1}$$

Furthermore, each $\gamma(s;m)$ satisfies $S_G\gamma(s;m) = \gamma(\pi/2 - s;m)$. Then (by [1], see also [27]), for

$$B = Y(\pi/4)$$

we have that

$$Y(\pi/2) = S_G Y_0 B^{-1} S_G^T B = S_G Y_0 B^{-1} S_G B, \tag{7.2}$$

where we have used $S_G^T = S_G$. Combining equations (7.1) and (7.2) gives the factorization

$$Y(2\pi) = Y_0(Y_0^{-1}S_F^T S_G Y_0 B^{-1} S_G B)^4.$$

By setting

$$Q = S_F^T S_G \text{ and } W = Y_0^{-1} Q Y_0 B^{-1} S_G B,$$

we obtain

$$Y_0^{-1}Y(2\pi) = (Y_0^{-1}QY_0B^{-1}S_GB)^4 = W^4,$$

where

$$\Lambda = Y_0^{-1}QY_0 \text{ and } D = B^{-1}S_GB$$

are both involutions, i.e., $\Lambda^2 = D^2 = I$. □

7.2.2 A Choice of Y_0. The matrix $Q = S_F^T S_G$ that appears in Λ is orthogonal since S_F and S_G are both orthogonal. Furthermore, Q is symmetric and its eigenvalues are ± 1, each of multiplicity 4. An orthogonal basis for the eigenspace $\ker(Q-I)$ is

$$\begin{bmatrix} 0 \\ 0 \\ 0 \\ 0 \\ 0 \\ 1 \\ 0 \\ 1 \end{bmatrix}, \begin{bmatrix} 0 \\ 0 \\ 0 \\ 0 \\ -1 \\ 0 \\ 1 \\ 0 \end{bmatrix}, \begin{bmatrix} 0 \\ -1 \\ 0 \\ 1 \\ 0 \\ 0 \\ 0 \\ 0 \end{bmatrix}, \begin{bmatrix} 1 \\ 0 \\ 1 \\ 0 \\ 0 \\ 0 \\ 0 \\ 0 \end{bmatrix},$$

and an orthogonal basis for the eigenspace $\ker(Q+I)$ is

$$\begin{bmatrix} 0 \\ 0 \\ 0 \\ 0 \\ 1 \\ 0 \\ 1 \\ 0 \end{bmatrix}, \begin{bmatrix} 0 \\ 1 \\ 0 \\ 1 \\ 0 \\ 0 \\ 0 \\ 0 \end{bmatrix}, \begin{bmatrix} 0 \\ 0 \\ 0 \\ 0 \\ 0 \\ -1 \\ 0 \\ 1 \end{bmatrix}, \begin{bmatrix} -1 \\ 0 \\ 1 \\ 0 \\ 0 \\ 0 \\ 0 \\ 0 \end{bmatrix}.$$

We look for an appropriate choice of Y_0 such that

$$\Lambda = Y_0^{-1} Q Y_0 = \begin{bmatrix} I & 0 \\ 0 & -I \end{bmatrix}. \tag{7.3}$$

Lemma 7.2. *There exists an orthogonal and symplectic Y_0 such that Equation (7.3) holds.*

Proof. Since the components of $\gamma(s;m)$ satisfy the relations

$$u_3(0;m) = u_1(0;m),\ u_4(0;m) = -u_2(0;m), \tag{7.4}$$

$$v_3(0;m) = -v_1(0;m),\ v_4(0;m) = v_2(0;m), \tag{7.5}$$

then using the Hamiltonian system (6.3) on the level set $\hat{\Gamma} = 0$, the components of $\gamma'(0;m)$ satisfy

$$u_3'(0;m) = -u_1'(0;m),\ u_4'(0;m) = u_2'(0;m),\ v_3'(0;m) = v_1'(0;m),\ v_4'(0;m) = -v_2'(0;m).$$

It is easily recognized that the vector $\gamma'(0;m)$ belongs to $\ker(Q+I)$. Now set

$$a = u_1'(0;m),\ b = u_2'(0;m),\ c = v_1'(0;m),\ d = v_2'(0;m),\ e = \|\gamma'(0;m)\|$$

and define Y_0 by

$$Y_0 = \frac{1}{e}\begin{bmatrix} c & d & a & b & a & -b & -c & d \\ d & -c & b & -a & b & a & -d & -c \\ c & d & a & b & -a & b & c & -d \\ -d & c & -b & a & b & a & -d & -c \\ -a & b & c & -d & c & d & a & b \\ -b & -a & d & c & d & -c & b & -a \\ a & -b & -c & d & c & d & a & b \\ -b & -a & d & c & -d & c & -b & a \end{bmatrix}. \tag{7.6}$$

Let $\mathrm{col}_i(Y_0)$ denote the i^{th} column of Y_0. Notice that $\mathrm{col}_5(Y_0) = \gamma'(0;m)/\|\gamma'(0;m)\|$. The last four columns of Y_0 form an orthonormal basis for $\ker(Q+I)$, while the first four columns of Y_0 form an orthonormal basis for $\ker(Q-I)$. Since Q is symmetric, its two eigenspaces are orthogonal, and so Y_0 is orthogonal. Note that $J\mathrm{col}_{4+i}(Y_0) = \mathrm{col}_i(Y_0)$ for $i = 1,2,3,4$; in other words, multiplication by J maps $\ker(Q-I)$ bijectively to $\ker(Q+I)$. For P_1 the lower right 4×4 submatrix of Y_0 and P_2 the upper right 4×4 submatrix of Y_0, we have

$$Y_0 = \left(J\begin{bmatrix} P_2 \\ P_1 \end{bmatrix}, \begin{bmatrix} P_2 \\ P_1 \end{bmatrix} \right) = \begin{bmatrix} P_1 & P_2 \\ -P_2 & P_1 \end{bmatrix},$$

where $P_1^T P_1 + P_2^T P_2 = I$ and $P_1^T P_2 = 0$. These implies that Y_0 is symplectic. □

7.2.3 The Existence of K. By Lemma 7.1 we have $Y_0^{-1} Y(2\pi) = W^4$ where $W = \Lambda D$ with $\Lambda = Y_0^{-1} Q Y_0$ and $D = B^{-1} S_G B$ for $B = Y(\pi/4)$. By Lemma 7.2, there exists an orthogonal and symplectic Y_0 such that Equation (7.3) holds. Choose Y_0 as given in Equation (7.6). The matrix $W = \Lambda D$ is then symplectic, i.e., $W^T J W = J$, because Λ is symplectic with multiplier -1, $\Lambda^T J \Lambda = -J$, and S_G is symplectic with multiplier -1, $S_G^T J S_G = -J$, and B is symplectic.

Lemma 7.3. *With the given choice of Y_0, there exists a matrix K uniquely determined by $B =$*

$Y(\pi/4)$ *such that*

$$\frac{1}{2}\left(W+W^{-1}\right)=\begin{bmatrix} K^T & 0 \\ 0 & K \end{bmatrix}.$$

Proof. Since $W=\Lambda D$ where Λ and D are involutions, it follows that

$$W^{-1}=D\Lambda.$$

By the choice of Y_0, the form of the matrix Λ is given in Equation (7.3). If we partition the symplectic matrix B into the four 4×4 submatrices,

$$B=\begin{bmatrix} A_1 & A_2 \\ A_3 & A_4 \end{bmatrix}, \tag{7.7}$$

then the form of the inverse of B is

$$B^{-1}=\begin{bmatrix} A_4^T & -A_2^T \\ -A_3^T & A_1^T \end{bmatrix}.$$

Set

$$H=\begin{bmatrix} -G & 0 \\ 0 & G \end{bmatrix}.$$

Then we have that

$$D=B^{-1}S_GB=\begin{bmatrix} K^T & L_1 \\ -L_2 & -K \end{bmatrix}$$

where $K=A_3^THA_2+A_1^THA_4$, $L_1=A_4^THA_2+A_2^THA_4$, and $L_2=A_3^THA_1+A_1^THA_3$. It follows that K is uniquely determined by B, that

$$W=\Lambda D=\begin{bmatrix} I & 0 \\ 0 & -I \end{bmatrix}\begin{bmatrix} K^T & L_1 \\ L_2 & -K \end{bmatrix}=\begin{bmatrix} K^T & L_1 \\ L_2 & K \end{bmatrix}, \tag{7.8}$$

and that

$$W^{-1} = D\Lambda = \begin{bmatrix} K^T & L_1 \\ L_2 & -K \end{bmatrix} \begin{bmatrix} I & 0 \\ 0 & -I \end{bmatrix} = \begin{bmatrix} K^T & -L_1 \\ -L_2 & K \end{bmatrix}.$$

Thus

$$\frac{1}{2}\left(W + W^{-1}\right) = \begin{bmatrix} K^T & 0 \\ 0 & K \end{bmatrix} \tag{7.9}$$

for a K uniquely determined by $B = Y(\pi/4)$ as was desired. □

7.2.4 The Form of K. We will show that one of the eigenvalues of K is 1, and the remaining three eigenvalues of K are determined by the lower right 3×3 submatrix of K. Let c_i denote the i^{th} column of $B = Y(\pi/4)$.

Lemma 7.4. *With the given choice of Y_0, the matrix K uniquely determined by $B = Y(\pi/4)$ is*

$$\begin{bmatrix} 1 & * & * & * \\ 0 & c_2^T S_G J c_6 & c_2^T S_G J c_7 & c_2^T S_G J c_8 \\ 0 & c_3^T S_G J c_6 & c_3^T S_G J c_7 & c_3^T S_G J c_8 \\ 0 & c_4^T S_G J c_6 & c_4^T S_G J c_7 & c_4^T S_G J c_8 \end{bmatrix}.$$

Proof. We begin by showing that 1 is an eigenvalue of W by identifying a corresponding eigenvector. Since $Y(\pi/2) = S_G Y_0 B^{-1} S_G B$ (Equation 7.2) and $Q = S_F^T S_G$, it follows that

$$\begin{aligned} W &= Y_0^{-1} Q Y_0 B^{-1} S_G B \\ &= Y_0^{-1} S_F^T S_G Y_0 B^{-1} S_G B \\ &= Y_0^{-1} S_F^T Y(\pi/2). \end{aligned}$$

Set

$$v = Y_0^{-1} \gamma'(0; m).$$

The orthogonality of Y_0 and $\mathrm{col}_5(Y_0) = \gamma'(0;m)/\|\gamma'(0;m)\|$ imply that

$$v = Y_0^T \gamma'(0;m) = \|\gamma'(0;m)\| e_5,$$

where $e_5 = [0,0,0,0,1,0,0,0]^T$. Since $Y(s)$ is a fundamental matrix, then $\gamma'(s;m) = Y(s)Y_0^{-1}\gamma'(0;m)$. Hence,

$$\begin{aligned} Wv &= Y_0^{-1} S_F^T Y(\pi/2) v \\ &= Y_0^{-1} S_F^T Y(\pi/2) Y_0^{-1} \gamma'(0;m) \\ &= Y_0^{-1} S_F^T \gamma'(\pi/2;m). \end{aligned}$$

Since $S_F \gamma(s;m) = \gamma(s+\pi/2;m)$ and $S_F^{-1} = S_F^T$, we have that

$$\gamma'(s;m) = S_F^{-1}\gamma'(s+\pi/2;m) = S_F^T \gamma'(s+\pi/2;m).$$

Setting $s = 0$ in this gives

$$\gamma'(0;m) = S_F^T \gamma'(\pi/2;m).$$

From this it follows that

$$\begin{aligned} Wv &= Y_0^{-1} S_F^T \gamma'(\pi/2;m) \\ &= Y_0^{-1} \gamma'(0;m) \\ &= v. \end{aligned}$$

Thus 1 is an eigenvalue of W and $v = \|\gamma'(0;m)\| e_5$ is a corresponding eigenvector.

Next, we show that the first column of K is $[1,0,0,0]^T$. Since $Wv = v$, then $We_5 = e_5$. From

the form of W given in Equation (7.8), it follows that

$$e_5 = We_5 = \begin{bmatrix} L_1[1,0,0,0]^T \\ K[1,0,0,0]^T \end{bmatrix}.$$

This implies that

$$K \begin{bmatrix} 1 \\ 0 \\ 0 \\ 0 \end{bmatrix} = \begin{bmatrix} 1 \\ 0 \\ 0 \\ 0 \end{bmatrix}.$$

from which it follows that the first column of K is $[1,0,0,0]^T$.

Finally we show that the lower right 3×3 submatrix of K has the prescribed entries. Since Y_0 is symplectic, the matrix $B = Y(\pi/4)$ is symplectic. Hence B satisfies $J = B^T JB$, and so

$$B^{-1} = -JB^T J.$$

For $W = \Lambda D$ with $D = B^{-1} S_G B$ where S_G satisfies $S_G J = -JS_G$ we then obtain

$$\begin{aligned} W &= \Lambda B^{-1} S_G B \\ &= \Lambda(-JB^T J) S_G B \\ &= -\Lambda JB^T J S_G B \\ &= -\Lambda JB^T (-S_G J) B \\ &= \Lambda JB^T S_G JB. \end{aligned}$$

Writing B in the block partition form given in Equation (7.7), it follows that

$$\Lambda JB^T = \begin{bmatrix} 0 & I \\ I & 0 \end{bmatrix} B^T = \begin{bmatrix} 0 & I \\ I & 0 \end{bmatrix} \begin{bmatrix} A_1^T & A_3^T \\ A_2^T & A_4^T \end{bmatrix} = \begin{bmatrix} A_2^T & A_4^T \\ A_1^T & A_3^T \end{bmatrix}. \tag{7.10}$$

Let $\mathrm{col}_i(S_G JB)$ denote the i^{th} column of $S_G JB$. Then $\mathrm{col}_i(S_G JB) = S_G J c_i$ where c_i is the i^{th} column of $B = Y(\pi/4)$. This and Equation (7.10) imply that the (i,j) entry of W is then $c_i^T S_G J c_j$. But Equation (7.8) implies that the $(6,6)$ entry of W is the $(2,2)$ entry of K. Continuing in this manner we find the remaining entries of the lower right 3×3 submatrix of K to be given as prescribed. $\square$

7.2.5 A Stability Theorem. The characteristic multipliers of $\gamma(s;m)$ are the eigenvalues of W^4 which are the fourth powers of the eigenvalues of W. As was shown in the proof of Lemma 7.4, an eigenvalue of K is 1. Because of Equation (7.9), an eigenvalue of W is 1 with algebraic multiplicity (at least) 2. This accounts for two of the four known eigenvalues of 1 for W^4. Our numerical calculations show that -1 is an eigenvalue of K and hence of W for all $0 < m \leq 1$. This accounts for the remaining two known eigenvalues of 1 for W^4.

A symplectic matrix is called *spectrally stable* if:

1. All of its eigenvalues must have modulus one.

2. It has a pair of eigenvalues which are equal and that do not correspond to the invariant quantities from Chapter 2.

This condition is weaker than linear stability, which requires that no repeated eigenvalues occur, other than the repeated ± 1 eigenvalues from the conserved quantities.

When W is spectrally stable, the eigenvalues of K are the real parts of the eigenvalues of W. If 0 is an eigenvalue of K, then $\pm i$ are eigenvalues of W and so the algebraic multiplicity of 1 as an eigenvalue of W^4 is at least 6. If $1/\sqrt{2}$ is an eigenvalue of K, then $1/\sqrt{2} \pm i/\sqrt{2}$ are eigenvalues of W, and if $-1/\sqrt{2}$ is and eigenvalue of K, then $-1/\sqrt{2} \pm i/\sqrt{2}$ are eigenvalues of W; both these imply that -1 is a repeated eigenvalue of W^4. So when the remaining two eigenvalues λ_1 and λ_2 of K are real, distinct, have absolute value strictly smaller than one, and none of them are equal to 0 or $\pm 1/\sqrt{2}$, then the symmetric periodic SBC orbit is linearly stable, i.e., W, and hence W^4, is spectrally stable as well as semisimple when restricted to the four dimensional W-invariant subspace of $\mathbb{R}^8$ determined by the two distinct modulus one complex conjugate pairs of eigenvalues of W. On the other hand, if one of λ_1 or λ_2 is real with absolute value bigger than 1, or

is complex with a nonzero imaginary part, then the symmetric periodic SBC orbit is not spectrally stable, but is linearly unstable. The proof of the following result about the linear stability type for the symmetric periodic SBC orbits in the PPS4BP follows from all of the Lemmas and subsequent comments presented in this Section.

Theorem 7.5. *The symmetric periodic SBC orbit $\gamma(s;m)$ of period $T = 2\pi$ and energy $\hat{E}(m)$ is spectrally stable in the PPS4BP if and only if λ_1 and λ_2 are real and have absolute value smaller or equal to 1. If λ_1 and λ_2 are real, distinct, have absolute value strictly smaller than 1, and none of them are equal to 0 or $\pm 1/\sqrt{2}$, then $\gamma(s;m)$ is linearly stable in the PPS4BP.*

7.3 Numerical Results

We computed $Y(\pi/4)$ using our trigonometric polynomial approximations of $\gamma(s;m)$ for each m starting at $m = 1$ and decreasing by 0.01 until we reached $m = 0.01$, and the Runge-Kutta order 4 algorithm coded in MATLAB, with a fixed time step of

$$\frac{\pi/4}{50000} = \frac{\pi}{200000}.$$

From the needed columns of $Y(\pi/4)$, we computed the entries of the lower right 3×3 submatrix of K as given in Lemma 7.4, and then computed the eigenvalues λ_1, λ_2, and λ_3 of this 3×3 matrix. We have plotted these three eigenvalues, when real, as functions of m in Figure 7.3. One of these eigenvalues is real and stays close to -1 for all $m \in (0,1]$ except at $m = 0.20$; label this eigenvalue λ_3.

The remaining two eigenvalues λ_1 and λ_2 of K that determine the linear stability type of $\gamma(s;m)$ are for $m = 0.01$ near 1 and not shown, respectively, in Figure 7.3. The values of λ_1 and λ_2 at $m = 0.01$ are (approximately) 0.97431, and -50.70044 respectively. As m increases from 0.01, the value of λ_1 decreases, crossing $1/\sqrt{2}$ for some m in $(0.09, 0.10)$, and crossing 0 for some m in $(0.26, 0.27)$, while λ_2 increases to the value -1.14602 at $m = 0.19$, momentarily disappearing at $m = 0.20$, reappearing at $m = 0.21$ with a value of -0.86414, continuing to increase, crossing

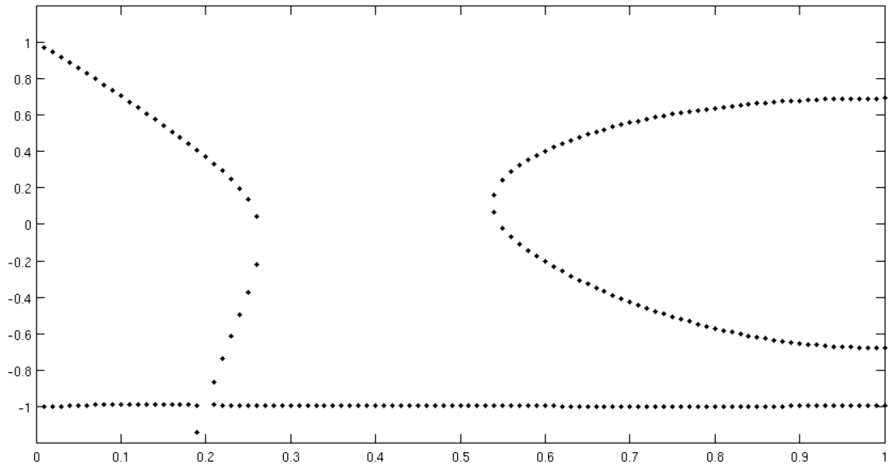

Figure 7.1: The eigenvalues λ_1, λ_2, λ_3, when real, of the 3×3 lower right submatrix of K over $0 < m \leq 1$.

$-1/\sqrt{2}$ for a value of m in $(0.22, 0.23)$, until at some value of m in $(0.26, 0.27)$, we have $\lambda_1 = \lambda_2 <$ 0. For m in $[0.27, 0.53]$, the eigenvalues λ_1 and λ_2 form a complex conjugate pair with nonzero imaginary part, and thus disappear in Figure 7.3. For some value of m in $(0.53, 0.54)$, we have λ_1 and λ_2 reappearing in Figure 7.3, with $\lambda_1 = \lambda_2 > 0$. As m increases from there, λ_1 increases and λ_2 decreases, with λ_1 crossing 0 for a value of m in $(0.54, 0.55)$, and with the values of λ_1 and λ_2 at $m = 1$ being respectively,

$$0.69414, -0.68022, \tag{7.11}$$

where the first of these is slightly smaller than $1/\sqrt{2}$, and the latter is slighter larger than $-1/\sqrt{2}$. These changes in the values of λ_1 and λ_2 account for the changes in the linear stability type of $\gamma(s;m)$ as m varies over $(0, 1]$.

From the numerical results and Theorem 7.5, we conclude that the periodic orbit $\gamma(s;m)$ is linearly stable when m is in $[0.21, 0.22]$, or m is in $[0.23, 0.25]$, $m = 0.54$, or m is in $[0.55, 1]$. We have linear instability when m is in $[0.01, 0.19]$ or in $[0.27, 0.53]$. We have at least spectral stability when $m = 0.20$ where λ_3 disappears momentarily along with λ_2 to form the complex conjugate

pair with nonzero imaginary part,

$$-0.99726 \pm 0.00865i.$$

This appears numerically to be a repeated eigenvalue of -1 for K. We also have at least spectral stability for a value of m in $(0.22, 0.23)$, and for a value of m in $(0.54, 0.55)$.

We have confirmed that numerically the equal mass symmetric periodic SBC orbit $\gamma(s;1)$ is linearly stable in the PPS4BP. From the eigenvalues of K, which are 1, -1, and those listed in (7.11), the characteristic multipliers of $\gamma(s;1)$ are 1 with algebraic multiplicity 4, and the two distinct complex conjugate pairs of modulus one,

$$-0.98887 \pm 0.14877,$$
$$-0.99736 \pm 0.07265i.$$

These agree numerically with the eigenvalues of the monodromy matrix for $\gamma(s;1)$ of Chapter 6.

To get a better estimate of the value of m between 0.54 and 0.55 at which the orbit $\gamma(s;m)$ loses spectral stability as m decreases, we numerically computed $Y(\pi/4)$ for the values of $m = 0.531, 0.532, \ldots, 0.538, 0.539$, and then computed the values of λ_1 and λ_2. These show for $m = 0.531$ through $m = 0.538$ that $\gamma(s;m)$ is linearly unstable because λ_1 and λ_2 form a complex conjugate pair with nonzero imaginary part. For $m = 0.539$, we have that $\gamma(s;m)$ is linearly stable because

$$\lambda_1 = 0.14253, \ \lambda_2 = 0.08595,$$

which are real, distinct, have absolute value smaller than 1, and are not equal to 0 or $\pm 1/\sqrt{2}$. These eigenvalues of K imply that the characteristic multipliers of $\gamma(s;0.539)$ are 1 with algebraic

multiplicity 4, and the two complex conjugate pairs

$$0.84079 \pm 0.54136i,$$

$$0.94134 \pm 0.33747i,$$

with each one of these having modulus 1. Thus the value of m in $[0.53, 0.54]$ at which $\gamma(s;m)$ is at least spectrally stable, lies in the interval $(0.538, 0.539)$.

CHAPTER 8. THE RHOMBOIDAL ORBIT AND ITS LINEAR STABILITY

8.1 INTRODUCTION

The chief aim of this chapter is to give stability results, including linear stability, for the symmetric mass rhomboidal orbit in both a four-degrees-of-freedom (4DF) and a two-degrees-of-freedom (2DF) setting at the same time. With our choice of coordinates in the 4DF setting, the linearized phase space of the regularized equations has an elegant decomposition into two invariant subspaces. The linear stability analysis in the 2DF setting corresponds to one of these subspaces. Additionally, we are able to use analytic techniques to reduce the linear stability analysis of the numerical calculation of three entries of a 4×4 matrix K related to the monodromy matrix. Chief among these techniques is using angular momentum, which is not "factored out" by a coordinate transformation, to give relations among the entries of K.

The results presented in this chapter were originally published as [31].

The remainder of this chapter is as follows: In Section 8.2, we describe the orbit and some of its properties. In 8.2.1, we give formal notation describing the orbit. We also perform the coordinate transformation that regularizes the collisions. Section 8.2.2 gives an analytic proof of the existence of the orbit in the regularized 4DF setting. Section 8.3 describes the symmetries of the orbit, which are needed to perform the stability analysis in 8.4. Section 8.4.1 describes all of the remaining linear stability analysis that can be done before any numerical work, including the decomposition into two invariant sets mentioned earlier.

Lastly, in Section 8.5, we present the results obtained from the numerical calculations. As mentioned, the 4DF stability result will immediately give a stability result in a 2DF invariant set. In 8.5.1, we detail the result in both cases. In the linearly stable 2DF setting, we perform further analysis with a Poincaré section in 8.5.2.

8.2 THE RHOMBOIDAL SYMMETRIC-MASS PROBLEM

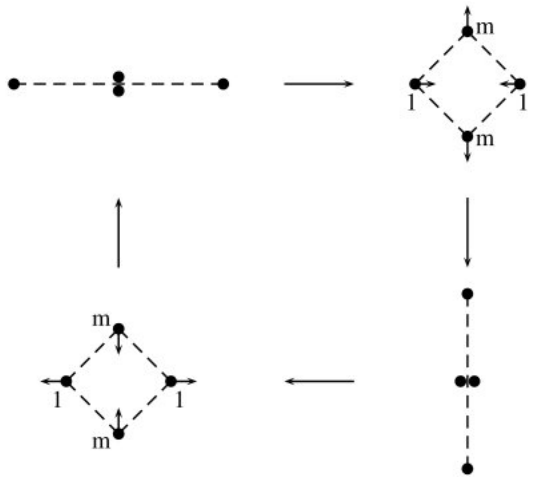

Figure 8.1: The rhomboidal four-body orbit.

8.2.1 Setting and Regularization. We consider the planar Newtonian 4-body problem with bodies located at

$$(x_1,x_2),(x_3,x_4),(-x_1,-x_2),(-x_3,-x_4) \tag{8.1}$$

and masses 1, m, 1, m respectively for some $m \in (0,1]$. (Throughout the chapter, we will often refer to this as the four-degrees-of-freedom, or 4DF, setting.) For the periodic orbit, the bodies travel along the x and y axes, forming the vertices of a rhombus at all times away from collision. At the time of collision between the two bodies on the x-axes, the other two bodies have zero momentum. Similarly, at the time of collision between the two bodies on the y-axes, the other two bodies have zero momentum. (See Figure 8.1.)

The Hamiltonian for this system is given by $H = K - U$, where

$$K = \frac{1}{4}\left(w_1^2 + w_2^2\right) + \frac{1}{4m}\left(w_3^2 + w_4^2\right)$$

where the w_i are the conjugate momenta defined by

$$w_1 = 2\dot{x}_1,\ w_2 = 2\dot{x}_2,\ w_3 = 2m\dot{x}_3,\ w_4 = 2m\dot{x}_4,$$

and

$$U = \frac{1}{2\sqrt{x_1^2+x_2^2}} + \frac{m^2}{2\sqrt{x_3^2+x_4^2}} \qquad + \frac{2m}{\sqrt{(x_3-x_1)^2+(x_4-x_2)^2}} + \frac{2m}{\sqrt{(x_3+x_1)^2+(x_4+x_2)^2}}.$$

The angular momentum for the system is given by

$$A = x_1 w_2 - x_2 w_1 + x_3 w_4 - x_4 w_3.$$

We can regularize the system under a change of spatial variables and a re-scaling of time. Define

$$F = w_1(Q_1^2 - Q_2^2) + 2w_2 Q_1 Q_2 + 2w_3 Q_3 Q_4 + w_4(Q_4^2 - Q_3^2).$$

As a generating function, F induces the canonical change of variables $(x_i, w_i) \leftrightarrow (Q_i, P_i)$ given by

$$\begin{aligned} x_1 &= Q_1^2 - Q_2^2 & P_1 &= 2w_1 Q_1 + 2w_2 Q_2 \\ x_2 &= 2Q_1 Q_2 & P_2 &= -2w_1 Q_2 + 2w_2 Q_1 \\ x_3 &= 2Q_3 Q_4 & P_3 &= 2w_3 Q_4 - 2w_4 Q_3 \\ x_4 &= Q_4^2 - Q_3^2 & P_4 &= 2w_3 Q_3 + 2w_4 Q_4. \end{aligned}$$

Each of the P_i is linear in w_i. Solving the resulting system of equations yields

$$\begin{bmatrix} w_1 \\ w_2 \end{bmatrix} = \frac{1}{2(Q_1^2+Q_2^2)} \begin{bmatrix} Q_1 & -Q_2 \\ Q_2 & Q_1 \end{bmatrix} \begin{bmatrix} P_1 \\ P_2 \end{bmatrix}$$

and

$$\begin{bmatrix} w_3 \\ w_4 \end{bmatrix} = \frac{1}{2(Q_3^2+Q_4^2)} \begin{bmatrix} Q_4 & Q_3 \\ -Q_3 & Q_4 \end{bmatrix} \begin{bmatrix} P_3 \\ P_4 \end{bmatrix}.$$

Setting $\mathbf{Q} = Q_1^2 Q_3 Q_4 - Q_2^2 Q_3 Q_4 - Q_1 Q_2 Q_3^2 + Q_1 Q_2 Q_4^2$, we now have

$$K = \frac{1}{16}\left(\frac{P_1^2 + P_2^2}{Q_1^2 + Q_2^2}\right) + \frac{1}{16m}\left(\frac{P_3^2 + P_4^2}{Q_3^2 + Q_4^2}\right), \tag{8.2}$$

$$\begin{aligned} U = {} & \frac{1}{2(Q_1^2 + Q_2^2)} + \frac{m^2}{2(Q_3^2 + Q_4^2)} \\ & + \frac{2m}{\sqrt{(Q_1^2 + Q_2^2)^2 + (Q_3^2 + Q_4^2)^2 - 4\mathbf{Q}}} + \frac{2m}{\sqrt{(Q_1^2 + Q_2^2)^2 + (Q_3^2 + Q_4^2)^2 + 4\mathbf{Q}}}, \end{aligned} \tag{8.3}$$

and

$$A = \frac{1}{2}\left(Q_1 P_2 - Q_2 P_1 + Q_3 P_4 - Q_4 P_3\right). \tag{8.4}$$

Finally, to regularize the collisions at the origin we multiply by a change of time satisfying $\frac{dt}{ds} = (Q_1^2 + Q_2^2)(Q_3^2 + Q_4^2)$. This gives regularized Hamiltonian Γ in extended phase space:

$$\Gamma = \frac{dt}{ds}(H - E), \tag{8.5}$$

where $H = K - U$, with K and U as given in Equations 8.2 and 8.3. At the time of collision between the two bodies of mass 1, we have $Q_1 = Q_2 = 0$. The condition $\Gamma = 0$ then yields

$$(Q_3^2 + Q_4^2)\left(\frac{P_1^2 + P_2^2}{16} - \frac{1}{2}\right) = 0$$

and so at collision the momenta P_1 and P_2 are both finite and satisfy $P_1^2 + P_2^2 = 8$. Similarly, when $Q_3 = Q_4 = 0$, we get

$$(Q_1^2 + Q_2^2)\left(\frac{P_3^2 + P_4^2}{16m} - \frac{m^2}{2}\right) = 0$$

so the momenta P_3 and P_4 are both finite and satisfy $P_3^2 + P_4^2 = 8m^3$.

8.2.2 Analytic Existence of the Orbit. We will next demonstrate the existence of the orbit that we described in Section 8.2.1. Portions of the proof depend on arguments given by Yan [24],

Shibayama [13], and Martinez [25]. Each of these studied the orbit in a two-degrees-of-freedom (2DF) configuration.

Theorem 8.1. *The periodic rhomboidal symmetric-mass orbit described in Section 8.2.1 analytically exists for the Hamiltonian system given by* Γ.

Proof. Let $\mathcal{A}$ denote the set where

$$x_2 = x_3 = w_2 = w_3 = 0, x_1 \geq 0, \text{ and } x_4 \geq 0.$$

This corresponds to the regularized coordinates

$$Q_2 = Q_3 = P_2 = P_3 = 0. \tag{8.6}$$

Then, when $\mathcal{A}$ holds, the four bodies and their respective momenta lie on the x- and y-axes. We also have

$$Q_i^2 = x_i, \quad w_i = \frac{P_i}{2Q_i}, \quad \text{for } i = 1,4,$$

which are the same coordinate transformations used in [24]. Furthermore, we have

$$\dot{Q}_2\big|_{\mathcal{A}} = \dot{Q}_3\big|_{\mathcal{A}} = \dot{P}_2\big|_{\mathcal{A}} = \dot{P}_3\big|_{\mathcal{A}} = 0,$$

so $\mathcal{A}$ is invariant. Furthermore, if we consider $\Gamma|_{\mathcal{A}}$, with Γ as defined in (8.5), we get exactly the same regularized Hamiltonian as in [24] (with the mass parameter m added). Also, we have

$$\Gamma|_{\mathcal{A}} = \frac{dt}{ds}(H|_{\mathcal{A}} - E)$$

for the same value of E as in (8.5). This is precisely the same regularized 2DF Hamiltonian as in [24] (with the mass parameter m added). Since analytic existence of the 2DF problem in the equal-mass case was given in [24], and in the 1, m, 1, m case was given in [13], analytic existence in the 4DF setting follows from the invariance of $\mathcal{A}$. □

As a further consequence of the invariant set $\mathcal{A}$, initial conditions for the periodic orbit in the 2DF setting automatically give the initial conditions for the 4DF setting. This is very useful numerically as it reduces the number of calculations required to find initial conditions.

8.3 Symmetries of the Orbit

In order to utilize the techniques developed by Roberts, it is necessary to first identify the symmetries of the periodic orbit.

Lemma 8.2. *The regularized Hamiltonian Γ has symmetry group isomorphic to the Klein four group.*

Proof. Let

$$G = \begin{bmatrix} 1 & 0 \\ 0 & -1 \end{bmatrix},$$

and define the block matrix

$$S = \begin{bmatrix} -G & 0 & 0 & 0 \\ 0 & -G & 0 & 0 \\ 0 & 0 & G & 0 \\ 0 & 0 & 0 & G \end{bmatrix}, \tag{8.7}$$

where 0 represents the 2×2 zero matrix. Then we have

$$S^2 = (-S)^2 = I$$

Hence, S and $-S$ generate a group isomorphic to the Klein four group. For fixed values of m and E, let $\gamma = (Q_1, Q_2, Q_3, Q_4, P_1, P_2, P_3, P_4)$. Then we have

$$\Gamma \circ (\pm S\gamma) = \Gamma(\gamma),$$

as the changes of sign prescribed by S leave K from Equation 8.2 invariant and switch the roles of

$-4\mathbf{Q}$ and $+4\mathbf{Q}$ in Equation 8.3. So $\pm S$ generate a Klein-four symmetry group for Γ as well. □

Symmetries for Γ also help to determine symmetries for the periodic orbit.

Theorem 8.3. *Let γ be a solution to the Hamiltonian system defined by Γ for some fixed values of $m \in (0,1]$ and $E < 0$ such that*

$$\gamma(0) = (0,0,0,\zeta_4,\sqrt{8},0,0,0)$$

and

$$\gamma(s_0) = (\zeta_1,0,0,0,0,0,0,\sqrt{8m^3}).$$

(In other words, $\gamma(0)$ corresponds to collision between the two bodies of mass 1, and $\gamma(s_0)$ corresponds to collision between the two bodies of mass m. Furthermore, the non-colliding bodies have zero momentum at the time of collision of the other two bodies.) Then γ extends to a $T = 4s_0$-periodic solution of the same Hamiltonian system, wherein S and $-S$ are time-reversing symmetries for the orbit.

Proof. Note that if $\gamma(s)$ is a T-periodic solution to the regularized equations of motion resulting from 8.5, a standard calculation shows that both $-S\gamma(T/2-s)$ and $S\gamma(T-s)$ are solutions as well. Existence and uniqueness of solutions then imply that

$$-S\gamma(T/2-s) = \gamma(s) = S\gamma(T-s)$$

for all s. Hence the symmetry group for the rhomboidal four-body orbit is isomorphic to the Klein four group, with S and $-S$ as generators. □

8.4 Stability Reduction using Symmetries

Note that the matrix S given in (8.7) satisfies all the hypotheses of Lemma 3.3. Applying Corollary 3.4 with $N = 2$, S as defined in (8.7), and noting that $S^T = S$ yields

$$Y(T/2) = SY_0Y(T/4)^{-1}SY(T/4).$$

Similarly, if $N = 1$, since $S^2 = I$, we get

$$\begin{aligned} Y(T) &= -SY_0Y(T/2)^{-1}(-S)Y(T/2) \\ &= SY_0[SY_0Y(T/4)^{-1}SY(T/4)]^{-1}S[SY_0Y(T/4)^{-1}SY(T/4)] \\ &= SY_0Y(T/4)^{-1}SY(T/4)Y_0^{-1}SY_0Y(T/4)^{-1}SY(T/4). \end{aligned}$$

This yields

$$\begin{aligned} Y_0^{-1}Y(T) &= Y_0^{-1}SY_0Y(T/4)^{-1}SY(T/4)Y_0^{-1}SY_0Y(T/4)^{-1}SY(T/4) \\ &= [Y_0^{-1}SY_0Y(T/4)^{-1}SY(T/4)]^2 \\ &= W^2 \end{aligned}$$

with $W = Y_0^{-1}SY_0Y(T/4)^{-1}SY(T/4)$. Hence, in order to analyze the stability of the orbit, we need only compute the entries of Y along a quarter of the orbit.

We now show that there is an appropriate choice of Y_0 for which W has the required form, further reducing the stability calculations for the orbit. If we let

$$\Lambda = \begin{bmatrix} I & 0 \\ 0 & -I \end{bmatrix}, \tag{8.8}$$

then setting

$$Y_0 = \left[\begin{array}{cccc|cccc} 0 & 0 & 0 & 0 & 1 & 0 & 0 & 0 \\ 0 & 0 & 1 & 0 & 0 & 0 & 0 & 0 \\ 0 & 0 & 0 & 0 & 0 & 1 & 0 & 0 \\ 0 & 0 & 0 & 1 & 0 & 0 & 0 & 0 \\ \hline -1 & 0 & 0 & 0 & 0 & 0 & 0 & 0 \\ 0 & 0 & 0 & 0 & 0 & 0 & 1 & 0 \\ 0 & -1 & 0 & 0 & 0 & 0 & 0 & 0 \\ 0 & 0 & 0 & 0 & 0 & 0 & 0 & 1 \end{array}\right] \tag{8.9}$$

yields $-Y_0^{-1} S Y_0 = \Lambda$. (The lines here are provided for ease in reading. Much of our later analysis will involve breaking 8×8 matrices down into 4×4 blocks.) Furthermore, it is easy to check that Y_0 is both orthogonal and symplectic. If we set $D = -B^{-1} S B$ for $B = Y(T/4)$, we then have

$$W = \Lambda D.$$

Also, since $\Lambda^2 = D^2 = I$, we know immediately that

$$W^{-1} = D\Lambda.$$

Since $B = Y(T/4)$ is symplectic, setting

$$B = \begin{bmatrix} B_1 & B_2 \\ B_3 & B_4 \end{bmatrix} \text{ and } S = \begin{bmatrix} S_1 & 0 \\ 0 & -S_1 \end{bmatrix}$$

gives

$$\begin{aligned} D &= -B^{-1}SB \\ &= -\begin{bmatrix} K^T & L_1 \\ -L_2 & K \end{bmatrix}, \end{aligned}$$

where L_1, L_2, and K are 4×4 matrices satisfying $L_1 = B_4^T S_1 B_2 + B_2^T S_1 B_4$, $L_2 = B_3^T S_1 B_1 - B_1^T S_1 B_3$, and $K = -B_2^T S_1 B_2 - B_1^T S_1 B_4$. Thus,

$$W = \Lambda D = \begin{bmatrix} K^T & L_1 \\ L_2 & K \end{bmatrix}.$$

Similarly, we find that

$$W^{-1} = D\Lambda = \begin{bmatrix} K^T & -L_1 \\ -L_2 & K \end{bmatrix}.$$

Thus, we have

$$\frac{1}{2}\left(W + W^{-1}\right) = \begin{bmatrix} K^T & 0 \\ 0 & K \end{bmatrix}. \tag{8.10}$$

Remark. The given matrix Y_0 in (8.9) is not unique. Different choices of Y_0 are possible, but our particular choice is helpful for much of our later analysis. It is also worth noting that our choice of Y_0 is independent of the value of m for this orbit, which is not always true (see Chapter 7.)

We can give formulas for the entries of K in terms of W. Since B is symplectic, we have $J = B^T JB$, and hence

$$B^{-1} = -JB^T J.$$

Using $W = \Lambda D$ for $D = -B^{-1}SB$ and the relation $-SJ = JS$, we find

$$\begin{aligned} W &= \Lambda(-B^{-1}SB) \\ &= \Lambda JB^T JSB \\ &= -\Lambda JB^T SJB. \end{aligned}$$

Directly computing ΛJ and using the block form of B, we find that

$$(\Lambda J)B^T = -\begin{bmatrix} 0 & I \\ I & 0 \end{bmatrix}\begin{bmatrix} B_1^T & B_3^T \\ B_2^T & B_4^T \end{bmatrix} = -\begin{bmatrix} B_2^T & B_4^T \\ B_1^T & B_3^T \end{bmatrix}.$$

Define $\mathrm{col}_i(-SJB)$ to be the ith column of the matrix $-SJB$. Then we have $\mathrm{col}_i(-SJB) = -SJc_i$ where c_i is the ith column of B. Using the above two formulas, this implies that the (i,j) entry of W is given by $-c_i^T SJC_j$. Equation (8.10) shows that the (i,j) entry of K is the $(i+4, j+4)$ entry of W. Hence,

$$K = \begin{bmatrix} -c_1^T SJc_5 & -c_1^T SJc_6 & -c_1^T SJc_7 & -c_1^T SJc_8 \\ -c_2^T SJc_5 & -c_2^T SJc_6 & -c_2^T SJc_7 & -c_2^T SJc_8 \\ -c_3^T SJc_5 & -c_3^T SJc_6 & -c_3^T SJc_7 & -c_3^T SJc_8 \\ -c_4^T SJc_5 & -c_4^T SJc_6 & -c_4^T SJc_7 & -c_4^T SJc_8 \end{bmatrix}. \tag{8.11}$$

Remark. Computing the entries of K this way will allow us to bypass computing W^{-1}. This is preferred as a numerical method as W may be very poorly conditioned.

8.4.1 Entries of K from Invariant Quantities. Before any numerical work is done, we can determine many of the values of entries of K by using properties of the orbit. We first introduce

some notation to simplify the analysis. Let $\mathcal{M}$ denote the set of matrices of the form

$$\begin{bmatrix} m_{11} & 0 & 0 & m_{14} \\ 0 & m_{22} & m_{23} & 0 \\ 0 & m_{32} & m_{33} & 0 \\ m_{41} & 0 & 0 & m_{44} \end{bmatrix}$$

where all of the listed $m_{ij} \in \mathbb{R}$ ($m_{ij} = 0$ is permitted). Further, let $\mathcal{M}_2$ denote the set of 8×8 matrices whose 4×4 blocks are in $\mathcal{M}$. That is to say, $\mathcal{M}_2$ consists of matrices of the form

$$\begin{bmatrix} M_1 & M_2 \\ M_3 & M_4 \end{bmatrix}$$

where each of the $M_i \in \mathcal{M}$. It is easy to check that $\mathcal{M}$ forms a ring with the standard definitions of matrix addition and multiplication. Furthermore, each element of $\mathcal{M}$ with nonzero determinant has its inverse in $\mathcal{M}$ as well. The same ring structure exists for $\mathcal{M}_2$.

The following two lemmas will help establish an important theorem about the form of K:

Lemma 8.4. *If $M \in \mathcal{M}_2$, then the system of differential equations given by*

$$\eta' = M(s)\eta$$

and initial conditions

$$\eta(0) = (*, 0, 0, *, *, 0, 0, *)^T$$

has solutions of the form

$$\eta(s) = (f_1(s), 0, 0, f_4(s), f_5(s), 0, 0, f_8(s))^T$$

Proof. We verify that $M\eta$ has the proper form. Note that

$$\left[\begin{array}{cccc|cccc} * & 0 & 0 & * & * & 0 & 0 & * \\ 0 & * & * & 0 & 0 & * & * & 0 \\ 0 & * & * & 0 & 0 & * & * & 0 \\ * & 0 & 0 & * & * & 0 & 0 & * \\ \hline * & 0 & 0 & * & * & 0 & 0 & * \\ 0 & * & * & 0 & 0 & * & * & 0 \\ 0 & * & * & 0 & 0 & * & * & 0 \\ * & 0 & 0 & * & * & 0 & 0 & * \end{array}\right] \left[\begin{array}{c} * \\ 0 \\ 0 \\ * \\ * \\ 0 \\ 0 \\ * \end{array}\right] = \left[\begin{array}{c} * \\ 0 \\ 0 \\ * \\ * \\ 0 \\ 0 \\ * \end{array}\right].$$

Hence, the zeros in the 2nd, 3rd, 6th, and 7th are preserved under multiplication by M. Thus, we can find equations $f_1(s)$, $f_4(s)$, $f_5(s)$, and $f_8(s)$ that are solutions to the four-equation system restricted to the starred entries in the first, fourth, fifth, and eighth rows and columns. Inserting the zero solution in the remaining entries yields

$$\eta(s) = (f_1(s), 0, 0, f_4(s), f_5(s), 0, 0, f_8(s))^T$$

is a solution of $\eta' = M(s)\eta$. □

Lemma 8.5. *If $M \in \mathcal{M}_2$, then the system of differential equations given by*

$$\eta' = M(s)\eta$$

and initial conditions

$$\eta(0) = (0, *, *, 0, 0, *, *, 0)^T$$

has solutions of the form

$$\eta(s) = (0, f_2(s), f_3(s), 0, 0, f_6(s), f_7(s), 0)^T.$$

Theorem 8.6. *If Y_0 is given by (8.9), then $K \in \mathcal{M}$.*

Proof. Using a computer algebra system, we find that the matrix $JD^2\Gamma$ is of the form

$$\begin{bmatrix} O & I \\ -I & O \end{bmatrix} \left[\begin{array}{cccc|cccc} * & a & a & * & 0 & 0 & a & * \\ a & * & * & a & 0 & 0 & a & a \\ a & * & * & a & a & a & 0 & 0 \\ * & a & a & * & * & a & 0 & 0 \\ \hline 0 & 0 & a & * & * & 0 & 0 & 0 \\ 0 & 0 & a & a & 0 & * & 0 & 0 \\ a & a & 0 & 0 & 0 & 0 & * & 0 \\ * & a & 0 & 0 & 0 & 0 & 0 & * \end{array}\right] = \left[\begin{array}{cccc|cccc} 0 & 0 & a & * & * & 0 & 0 & 0 \\ 0 & 0 & a & a & 0 & * & 0 & 0 \\ a & a & 0 & 0 & 0 & 0 & * & 0 \\ * & a & 0 & 0 & 0 & 0 & 0 & * \\ \hline * & a & a & * & 0 & 0 & a & * \\ a & * & * & a & 0 & 0 & a & a \\ a & * & * & a & a & a & 0 & 0 \\ * & a & a & * & * & a & 0 & 0 \end{array}\right].$$

Here, the zeros denote entries for which the mixed partials evaluate to zero identically, and the entries denoted a are entries for which the mixed partials evaluate to zero assuming the conditions given by (8.6) which hold along the periodic orbit $\gamma(s)$. Under such conditions, we have $JD^2\Gamma \in \mathcal{M}_2$. If $\xi(0) \in \mathcal{M}_2$, then each of the columns of $\xi(0)$ has the same form as in either Lemma 8.4 or 8.5. Hence, the solution to the system of linearized equations given by (3.3) satisfies $\xi(s) \in \mathcal{M}_2$ for all s. Since $Y_0 \in \mathcal{M}_2$, $\xi(s) \in \mathcal{M}_2$ for all s. This gives $B \in \mathcal{M}_2$, where B is as defined in Corollary 3.4. Then, $B^{-1} \in \mathcal{M}_2$ by the closure of inverses within $\mathcal{M}_2$. Hence $D \in \mathcal{M}_2$, and $\Lambda \in \mathcal{M}_2$ by construction, with D defined following (8.9) and Λ as in (8.8). Since $W = \Lambda D$, we then have W and W^{-1} are also in $\mathcal{M}_2$. Lastly, Equation (8.10) gives $K \in \mathcal{M}$ as claimed. □

Remark. (i) In terms of the 4DF Rhomboidal orbit, the structure of $\mathcal{M}_2$ very nicely decomposes phase space into a direct sum of $\mathcal{A} = \{Q_2 = Q_3 = P_2 = P_3 = 0\}$ and $\mathcal{A}^\perp = \{Q_1 = Q_4 = P_1 = P_4 = 0\}$. This decomposition is due in part to the coordinate transformation we chose. The choice of notation for $\mathcal{A}^\perp$ is appropriate in that $\mathcal{A}^\perp$ and $\mathcal{A}$ are orthogonal complements in $\mathbb{R}^8$. The two are also skew-orthogonal: if $a_1 \in \mathcal{A}$ and $a_2 \in \mathcal{A}^\perp$, then $a_1^T J a_2 = 0$.

(ii) Matrices of the form $\mathcal{M}$ and $\mathcal{M}_2$ are similar to the diamond product discussed in [43]. Specif-

ically, $\Sigma^{-1}M\Sigma = A_1 \diamond A_2$ for some matrices A_1 and A_2, where $M \in \mathcal{M}_2$ and Σ is the matrix

$$\Sigma = \begin{bmatrix} 0 & 1 & 0 & 0 & 0 & 0 & 0 & 0 \\ 0 & 0 & 1 & 0 & 0 & 0 & 0 & 0 \\ 0 & 0 & 0 & 1 & 0 & 0 & 0 & 0 \\ 0 & 0 & 0 & 0 & 1 & 0 & 0 & 0 \\ 0 & 0 & 0 & 0 & 0 & 1 & 0 & 0 \\ 0 & 0 & 0 & 0 & 0 & 0 & 1 & 0 \\ 0 & 0 & 0 & 0 & 0 & 0 & 0 & 1 \\ 1 & 0 & 0 & 0 & 0 & 0 & 0 & 0 \end{bmatrix}.$$

Furthermore, one of A_1 or A_2 corresponds to the 2DF setting.

(iii) The particular choice of Y_0 given in (8.9) is important for this argument.

In light of Theorem 8.6, we need only to find eight of the entries of the matrix K. We can, in fact, reduce this number further by using invariant properties of the orbit $\gamma(s)$. As is well-known, invariant quantities of the n-body problem are center of mass, net momentum, angular momentum, and energy (the Hamiltonian itself). Each of these correspond to trivial eigenvalues of the monodromy matrix. The center of mass and net momentum were "factored out" by our choice of coordinates at the beginning. The remaining two invariant quantities will be used to reduce the number of entries of K needed to find its eigenvalues.

Theorem 8.7. *The matrix K has a right eigenvector* $[1,0,0,0]^T$*, corresponding to eigenvalue* -1.

Proof. Let $v = Y_0^{-1}\gamma'(0)/||\gamma'(0)||$ or, equivalently, $Y_0^T\gamma'(0)/||\gamma'(0)||$. By Corollary 3.4, since Y_0 is orthogonal and S is symmetric, we have

$$W = Y_0^{-1}SY_0B^{-1}SB = Y_0^{-1}SY_0B^{-1}S^TB = Y_0^TY(T/2).$$

Since $\gamma'(s)$ is a solution of $\dot{\xi} = JD^2\Gamma(\gamma(s))\xi$ and $\gamma'(0) = Y(0)Y_0^{-1}\gamma'(0) = Y(0)v$, we also know

that $\gamma'(s) = Y(s)Y_0^{-1}\gamma'(0) = Y(s)v$. This implies

$$Y_0^{-1}\gamma'(T/2) = Y_0^T Y(T/2)v = Wv. \tag{8.12}$$

By the symmetry $\gamma(s) = -S\gamma(T/2-s)$, we also have $\gamma'(s) = S\gamma'(T/2-s)$. Setting $s=0$ in this setting tells us that $\gamma'(0) = S\gamma'(T/2)$. Since

$$\gamma'(0) = (\omega, 0, 0, 0, 0, 0, 0, 0)$$

for some real number ω, we have $-S\gamma'(0) = \gamma'(0)$. Thus

$$Y_0^{-1}\gamma'(T/2) = Y_0^T S\gamma'(0) = -Y_0^T\gamma'(0) = -v. \tag{8.13}$$

Combining (8.12) and (8.13) gives $Wv = -v$, and so -1 is an eigenvalue of W with eigenvector v. By definition, we have that

$$v = Y_0^T\gamma'(0)/||\gamma'(0)|| = (0,0,0,0,1,0,0,0).$$

From the form of W, this implies that

$$K\begin{bmatrix}1\\0\\0\\0\end{bmatrix} = \begin{bmatrix}-1\\0\\0\\0\end{bmatrix}.$$

So $[1,0,0,0]^T$ is an eigenvector of K with eigenvalue -1. Consequently, the first column of K must be $[-1,0,0,0]^T$.

□

Combining the results of the previous two theorems gives

$$K = \begin{bmatrix} -1 & 0 & 0 & * \\ 0 & a & b & 0 \\ 0 & c & d & 0 \\ 0 & 0 & 0 & e \end{bmatrix}. \tag{8.14}$$

Remark. Owing to the decomposition of linearized phase space into two invariant subspaces and the ordering of the coordinates, the position of e in the matrix K indicates that it should be an eigenvalue corresponding to the behavior of the orbit in $\mathcal{A}$. This eigenvalue, along with the trivial eigenvalue -1 from the $(1,1)$ position, completely classify linear stability in the 2DF setting. Hence, computing the linear stability of the 4DF orbit in the chosen coordinates automatically gives the stability of the 2DF orbit. (The results will be discussed further in Section 8.5.1.)

We can make use of the final invariant quantity, angular momentum, to further simplify our calculations. This is an extension of Roberts' method from [1], in which coordinate transformations "factor out" the angular momentum before linearization is performed. In the following theorem, we are able to show that this invariant quantity can be used to simplify linear stability calculations after linearization.

Theorem 8.8. *The matrix W has a left eigenvector $\nabla A(\gamma(0))Y_0$ with eigenvalue -1.*

Proof. This proof is based on ideas given in [37], p. 134, Lemma 7. Define $\hat{v}(s) = \nabla A(\gamma(s))$, where A represents the regularized angular momentum given in (8.4). Then

$$\hat{v} = \frac{1}{2}\left(P_2, -P_1, P_4, -P_3, -Q_2, Q_1, -Q_4, Q_3\right).$$

Since

$$\gamma(0) = (0,0,0,\zeta_4,\sqrt{8},0,0,0),$$

we know that

$$\hat{v}(0) = \frac{1}{2}\left(0, -\sqrt{8}, 0, 0, 0, 0, -\zeta_4, 0\right).$$

Let $\phi(s,z)$ be the general solution to the system of regularized differential equations with initial condition z. Then

$$A(\phi(s,z)) = A(z).$$

Differentiating with respect to z gives

$$\nabla A(\phi(s,z))\frac{\partial \phi}{\partial z}(s,z) = \nabla A(z)$$

or, equivalently

$$\hat{v}(s)X(s) = \hat{v}(0)$$

where $X(s)$ is the fundamental matrix solution. Setting $s = T/2$ and substituting $X(T/2) = Y_0(Y_0^{-1}Y(T/2))Y_0^{-1}$ gives

$$\hat{v}(T/2)Y_0(Y_0^{-1}Y(T/2))Y_0^{-1} = \hat{v}(0)$$

and so

$$\hat{v}(T/2)Y_0(Y_0^{-1}Y(T/2)) = (\hat{v}(T/2)Y_0)W = \hat{v}(0)Y_0.$$

By the symmetry of the orbit, $\gamma(T/2) = -\gamma(0)$, which gives

$$\hat{v}(T/2) = -\hat{v}(0),$$

and therefore

$$(\hat{v}(0)Y_0)W = -\hat{v}(0)Y_0.$$

Hence $\hat{v}(0)Y_0$ is a left eigenvector for W with eigenvalue -1. □

We readily compute $\hat{v}(0)Y_0 = \frac{1}{2}(0,-\zeta_4,\sqrt{8},0,0,0,0,0)$. From this, we know that

$$(0,-\zeta_4,\sqrt{8},0)K^T = -(0,-\zeta_4,\sqrt{8},0).$$

Since $K \in \mathcal{M}$, this requires that the additional -1 eigenvalue comes from the central 2×2 block

in K. Furthermore, this imposes some relations on the entries a,b,c,d in (8.14). In particular,

$$b = \frac{(a+1)\zeta_4}{\sqrt{8}},$$

$$c = \frac{(d+1)\sqrt{8}}{\zeta_4}.$$

Hence we have shown, through analytical techniques, that we only need to find three entries of the matrix K, namely a, d, and e, in order to determine the linear stability of the orbit.

Remark. (i) Since K is real-valued, this result, along with other results about the form of K, force all of the eigenvalues of K to be real.

(ii) This analysis is an improvement over work done in Chapter 7, in which the -1 eigenvalue corresponding to angular momentum showed up numerically but could not be factored out *a priori*. This improvement is due to the relative simplicity of the rhomboidal orbit.

8.5 RESULTS

8.5.1 Stability in Two Settings. As discussed in Section 8.2.2, in order to find the initial conditions for the 4DF orbit, we need only to find the initial conditions for the 2DF orbit. We found the initial conditions for $m = 0.01, 0.02, ..., 0.99, 1$ by adapting our technique used in [28] to the rhomboidal configuration. The details are discussed in Appendix A.

We numerically obtain the matrix W (hence K) by a numerical integration of the linearized systems and the initial conditions computed in Appendix A. The values of a, d, and e in the matrix K, as given in (8.14), are readily computed using (8.11). Knowing these, as well as the value of ζ_4 from Appendix A, we are able to determine the eigenvalues of K. The results are represented in Figures 8.2 and 8.3.

Following these calculations, we obtain the following:

Theorem 8.9. *The 4DF rhomboidal symmetric-mass orbit is linearly unstable for all m except for a small interval about* $m = 0.4$.

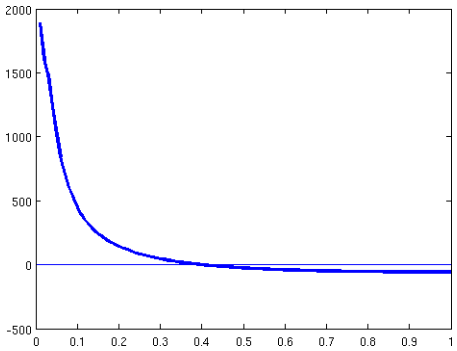

Figure 8.2: A plot of the nontrivial eigenvalue of the central 2×2 submatrix of K as a function of m. This eigenvalue crosses the horizontal axis for some value of $m \approx 0.4$.

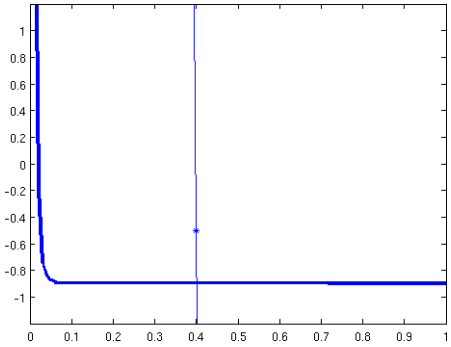

Figure 8.3: A plot of the nontrivial eigenvalues of K as functions of m. The thicker line represents the $(4,4)$ entry of K. The thinner line is the same curve as plotted in Figure 8.2 with the value at $m = 0.4$ emphasized.

We also note that there are five values of m for which we establish only spectral stability, due to repeated eigenvalues on the unit circle. For simplicity of explanation, let $f(m)$ denote the thicker of the two curves in Figure 8.3, and $g(m)$ the other. Roberts' argument (see [1]) demonstrates that each of the computed eigenvalues of K in $[-1,1]$ correspond to the real part of a square root of an eigenvalue on the complex unit circle. Accordingly, the value of $m = m_1$ where $f(m_1) = g(m_1)$ is a point with duplicated eigenvalues, hence the corresponding orbit has only spectral stability. Similarly, for m_2 and m_3 satisfying $g(m_2) = -1$ and $g(m_3) = 1$ give a pair of $(\pm 1)^2$ eigenvalues of W^2. For m_4 with $g(m_4) = 0$, we get $(\pm i)^2 = -1$ eigenvalues of W^2. Finally, there is a fifth value when $\cos(2f(m_5)) = \cos(2g(m_5))$, which arises by equating the real parts of $(e^{i\pi\theta_1})^2 = (e^{i\pi\theta_2})^2$ when $\theta_1 \neq \theta_2$.

In order to obtain a more precise interval of mass values for which the orbit is linearly stable (excluding the above-mentioned m_i), the initial conditions for mass values $m = 0.39$, 0.391, ..., 0.409, 0.41 were obtained using the same trigonometric polynomial approximation/optimization as used in Appendix A. The same linear stability calculations demonstrate that the 4DF rhomboidal orbit is linearly stable for m contained in some subinterval of $(0.395, 0.401)$. In other words, the orbit was found to be linearly unstable for $m = 0.395$ and $m = 0.401$, but linearly stable for all computed values in between, with the exclusion of the three critical mass values m_1, m_4, and m_5.

In [44], Bounemoura shows that in an n-dimensional Hamiltonian system, orbits beginning close to a linearly stable invariant torus generically remain "close" to the invariant torus for a super-exponential amount of time, eventually drifting away. The theory can also be applied to other cases, such as elliptic fixed points of maps. This analysis leads us to believe that, even though we have linear stability for some open interval containing $m = 0.4$, the orbit is likely to be unstable. Numerical perturbations off of $\mathcal{A}$ give evidence that this is the case.

We recall again that if we restrict to $\mathcal{A}$, then the eigenvalue of K given by the $(4,4)$ entry corresponds to linear stability of the 2DF orbit. This value stays in the interval $[-1,1]$ for $m = .02, .03, ..., .99, 1$. Hence,

Corollary 8.10. *The 2DF rhomboidal symmetric-mass orbit is linearly stable for all m in the interval* $(.01+\varepsilon, 1]$ *for some* $\varepsilon > 0$.

8.5.2 Poincaré Section Analysis in the 2DF Orbit. To numerically analyze nonlinear stability in the 2DF setting, we find a suitable Poincaré section for the orbit. This was done in the $m = 1$ case in [34]. Our more general Poincaré section is based on techniques presented in [14] and [15]. For any value of m, we seek a number α such that

$$\frac{x_1}{x_4} = \alpha$$

is maintained throughout the orbit, with x_1 and x_4 as defined in (8.1) earlier, and fixing $x_2 = x_3 = 0$. In other words, the value of α corresponds to the ratio of x_1 and x_4 in a homographic orbit where

the trajectories of the bodies correspond to total collapse (or ejection from total collapse). This is also a central configuration of the rhomboidal four-body problem. We find this value of α by solving the standard equations of motion (1.1) with the substitutions $x_1 = \alpha x_4$ and $\ddot{x_1} = \alpha \ddot{x_4}$. Doing so, we find that the required value of α for a given mass m is a root of the 12th-degree polynomial

$$(1+\alpha^2)^3(m\alpha^3-1)^2 - 64\alpha^6(1-m)^2 = 0. \tag{8.15}$$

A similar polynomial (in terms of the angle between the vertical mass, the horizontal mass, and the origin) is given by Waldvogel in [34]. Notice that if the ratio x_1/x_4 is constant throughout the orbit, then the ratio x_4/x_1 is also constant throughout. It can be verified by numerical integration that the roots of (8.15) corresponding to the ratio x_1/x_4 lie in the interval $[0,1]$. This will be preferred for ease of numerical calculation. The value of α as a function of m is plotted in Figure 8.4.

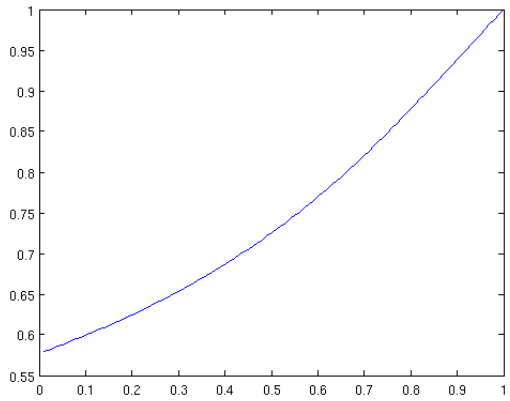

Figure 8.4: The value of α as a function of m.

For fixed $E = -1$, we define a Poincaré section Σ to be the two-dimensional surface given by $x_1 = \alpha x_4$ in the phase space defined by the variables x_1, x_4, $\dot{x}_1$, and $\dot{x}_4$. (Note that $\dot{x}_1$ and $\dot{x}_4$ are simply linear re-scalings of w_1 and w_4.) Restricting to $E = -1$, we find a bound on the possible values of x_1. Specifically, if $\dot{x_1} = \dot{x_4} = 0$ on Σ, the condition $E = -1$ requires that

$$x_1 = \frac{1}{2} + \frac{m^2\alpha}{2} + \frac{4m}{\sqrt{1+\frac{1}{\alpha^2}}} = r_{\max}.$$

For a set of initial conditions on Σ, the requirement $E = -1$ necessarily implies that $x_1 \leq r_{\max}$, and if either of $\dot{x}_1$ or $\dot{x}_4$ are non-zero, then the strict inequality $x_1 < r_{\max}$ holds.

We define coordinates (r, θ) on Σ by

$$r = \frac{x_1}{r_{\max}}, \quad \theta = \tan^{-1}\left(\frac{\dot{x}_1}{\alpha \dot{x}_4}\right).$$

Under this change of coordinates, the homographic orbit corresponds to the line $\theta = \pi/4$. For a 9×15 grid of equally spaced initial conditions in (r, θ) we numerically integrate the system for the corresponding initial conditions and record the first 200 intersections of the orbit with Σ. (Integration was preemptively terminated if any of Q_i, P_i exceeded 1000 in absolute value.) The results of this are shown in Figures 8.5 - 8.9. The observed concentric rings numerically match the predicted result of Moser's Invariant Curve Theorem in [5], and show that the rhomboidal symmetric-mass orbit is nonlinearly stable for $m = .02, .03, ..., .99, 1$.

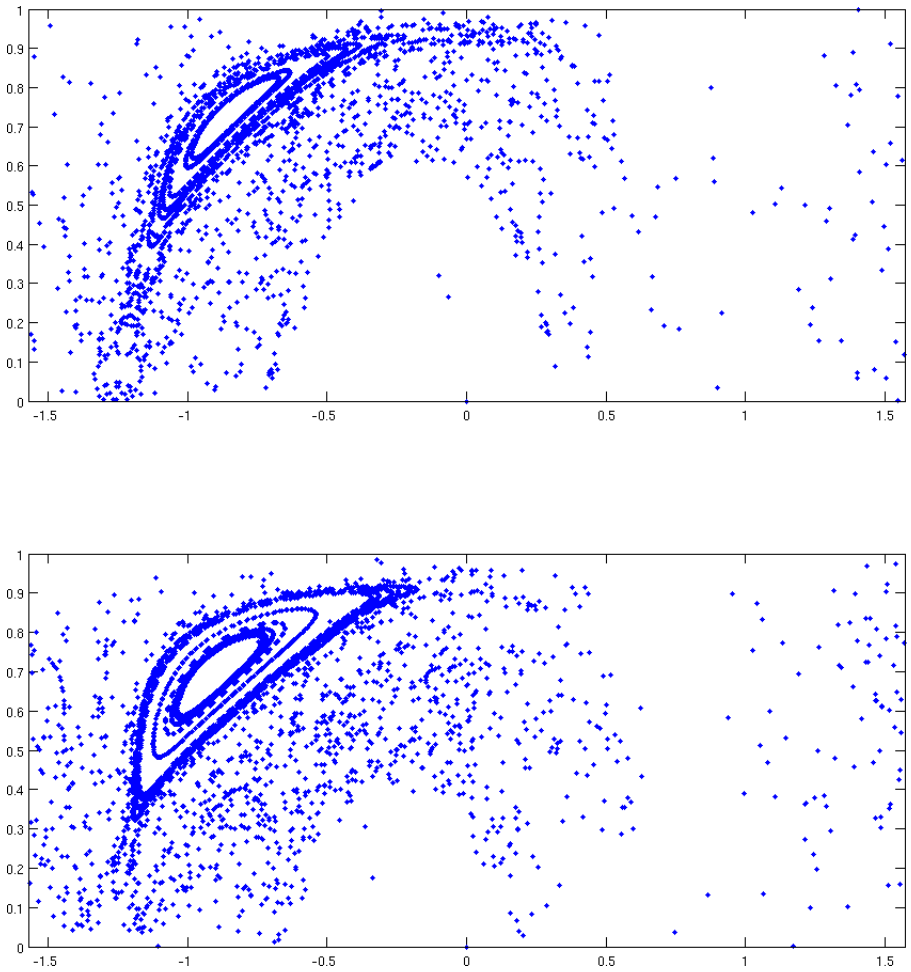

Figure 8.5: Poincaré sections plotted for $m = .1$ (top) and $m = .2$ (bottom). In these plots, r lies on the vertical axis. The homographic orbit at $\theta = \pi/4$ is not plotted for clarity.

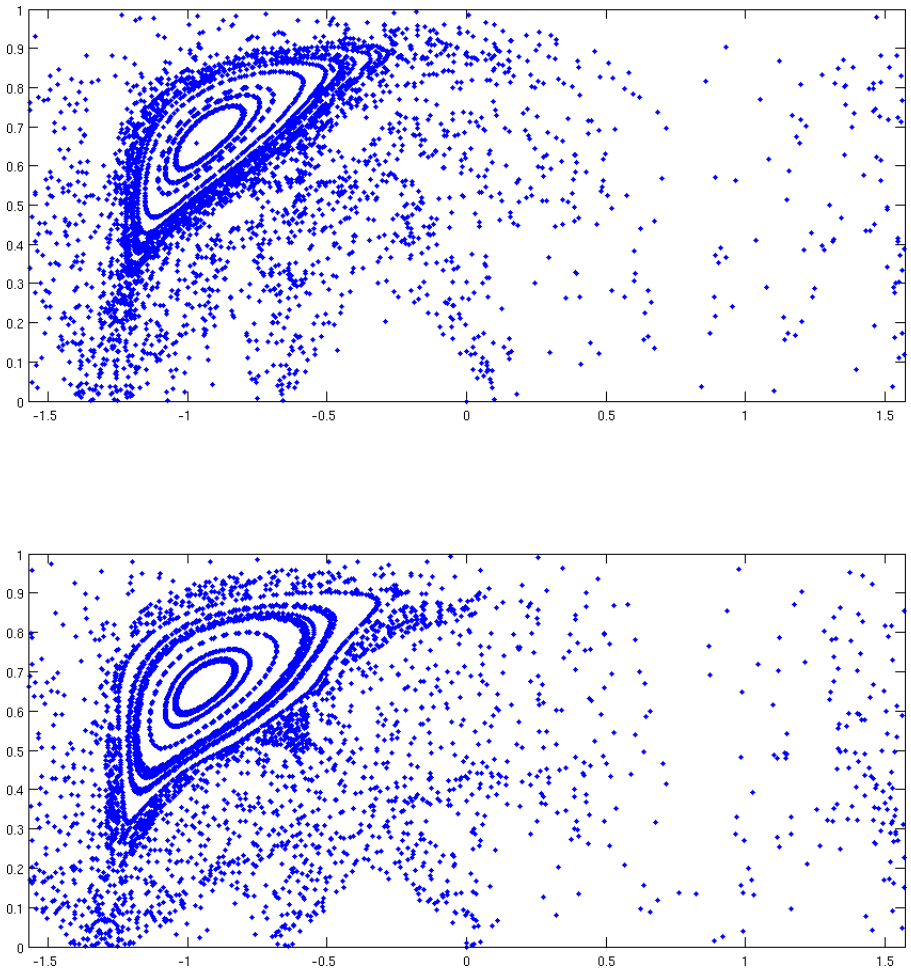

Figure 8.6: Poincaré sections plotted for $m = .3$ (top) and $m = .4$ (bottom).

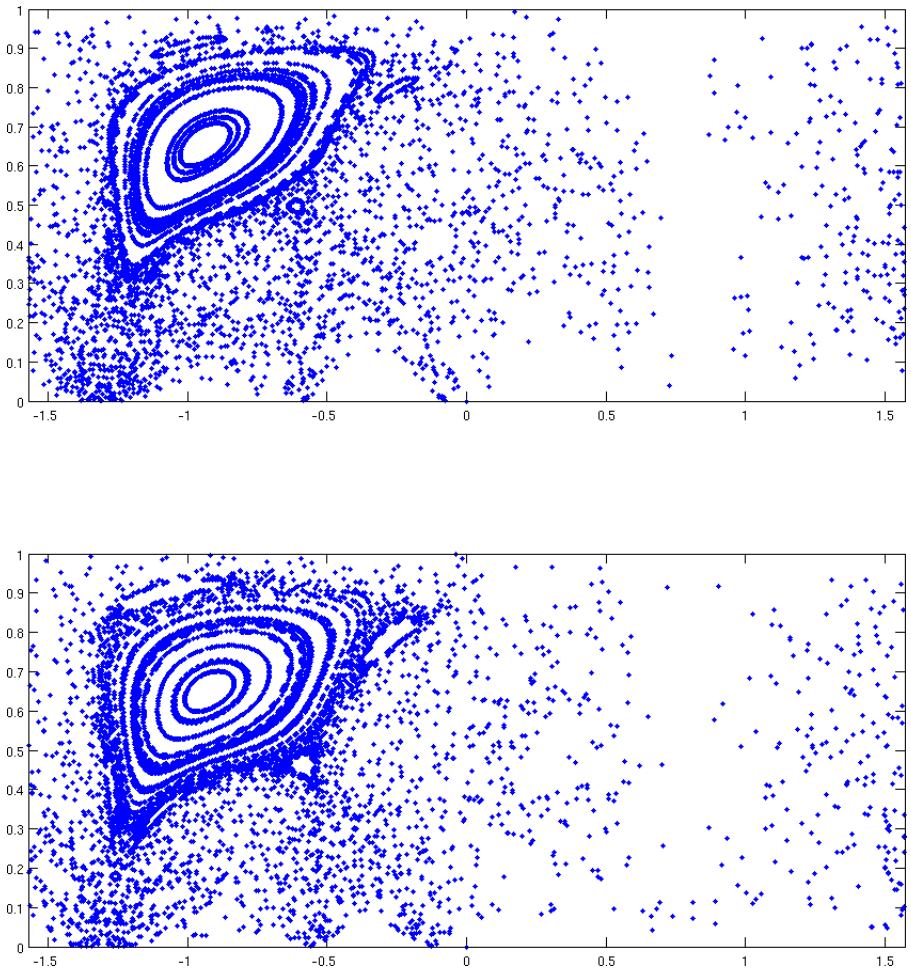

Figure 8.7: Poincaré sections plotted for $m = .5$ (top) and $m = .6$ (bottom).

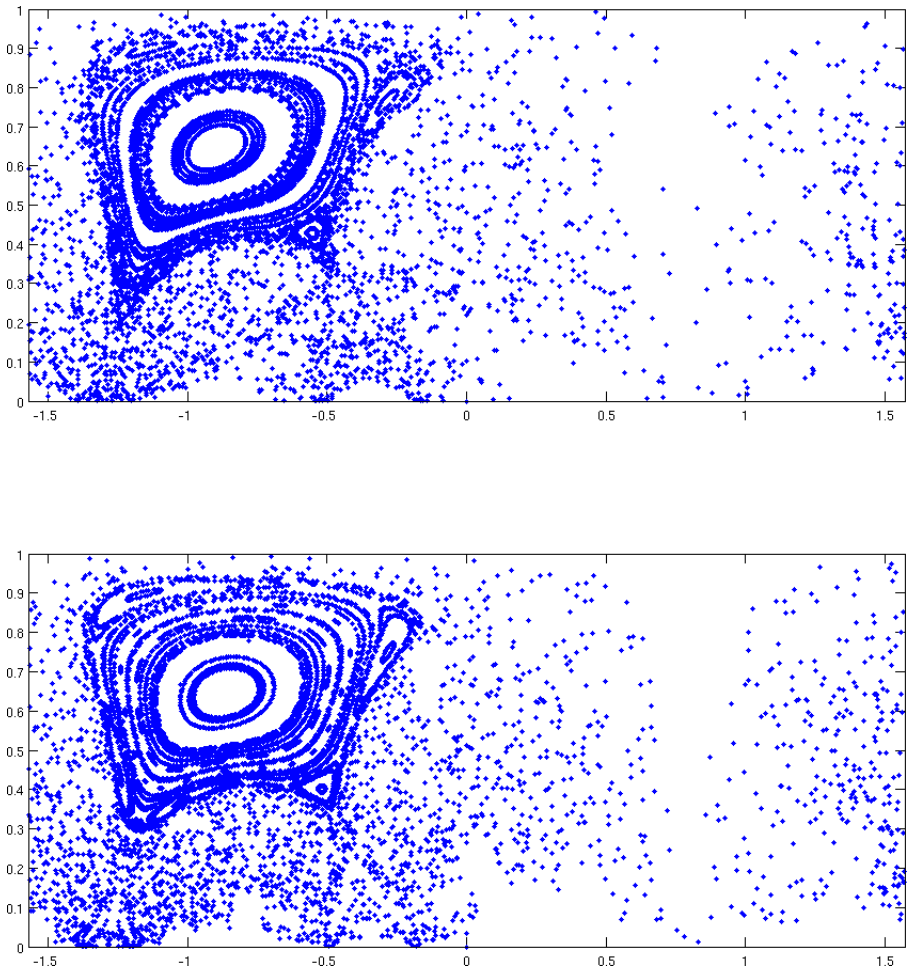

Figure 8.8: Poincaré sections plotted for $m = .7$ (top) and $m = .8$ (bottom).

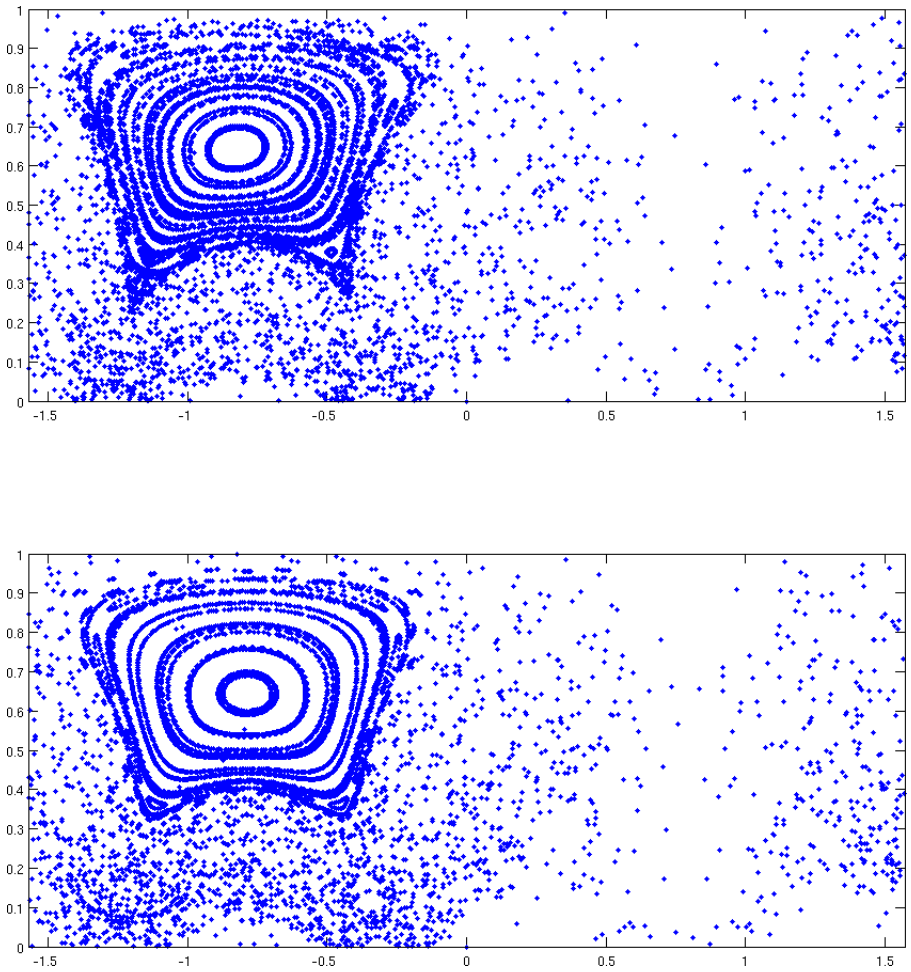

Figure 8.9: Poincaré sections plotted for $m = .9$ (top) and $m = 1$ (bottom).

CHAPTER 9. SEPARATING SURFACES IN GENERALIZED SITNIKOV PROBLEMS

9.1 INTRODUCTION

In 1960, Sitnikov [45] demonstrated the existence of a restricted three-body orbit which exhibits a remarkable chaotic behavior. This orbit consists of a periodic Kepler two-body orbit in the xy-plane with equal masses and a third, massless particle that runs along the z-axis, simultaneously remaining not bounded and not tending to infinity (oscillatory motion). The behavior is eventually extended to the case where the z-axis body has small finite mass. This orbit, and variations of it, have been the subject of much study since that time.

Analytic solutions of this orbit date back to before Sitnikov's time. In 1913, MacMillan [46] gave the explicit solution in the case where the Kepler orbit is circular in terms of elliptic functions. Finding analytic and numerical methods for computing solutions away from the circular case is still an active area of research (see [47], [48], and [49], for example). Additionally, numerical studies of the non-circular case have given some ideas of qualitative behavior of the orbit, including the nature of bifurcations as the eccentricity parameter varies. (See [50]).

In 2008 (with further work in 2010) the existence of an infinite family of non-trivial periodic orbits of the Sitnikov problem was demonstrated by Llibre and Ortega in [51] and Ortega and Rivera in [52]. It is demonstrated that there are orbits where p crossings of the massless particle through the origin occur for every N periods of the planar orbit, for any natural numbers p and N. Moreover, it is shown that these periodic orbits exist for any eccentricity in $[0,1)$ for the planar masses. Similar work was done independently by Marchesin and Castihlo in [53]. Existence results were extended to a generalized Sitnikov problem, which involves more than two masses in a planar configuration whose orbits are ellispses, by Rivera in 2013 (see [54]). Interestingly, the results of Rivera's work included an upper bound of 234 masses in the planar configuration needed for the results to hold.

Marchesin and Vidal consider a further departure from the general Sitnikov setting in [55]. In

their 2013 paper, they consider a rotating central configuration of four masses in two equal-mass pairs which geometrically form a rhombus. Under a certain transformation of coordinates, the masses become fixed points, as in the classical study of the restricted three-body problem. They are able to then derive many of the classical results known for the circular Sitnikov problem, including the non-existence of non-periodic oscillating motion. Additionally, they perform a stability analysis of the so-called "horizontal motion", wherein the massless particle is allowed to drift off of the z-axis. This is similar to the numerical stability analysis performed by Sidorenko in [56] for the circular Sitnikov problem.

Some other works, which we will not summarize here, but which lend further evidence to the volume of study given in this topic, include works by Alekseev ([57], [58], [59]), Moser ([60]), Liu and Sun ([61]), Perdios ([62]), Perdios and Markellos ([63]), and Soulis, Papadakis, and Bountis ([64]).

The work presented in this chapter originally arose out of a study of the rhomboidal four-body problem, in which two bodies of mass m_1 lie at $(\pm x, 0)$ for all time, and another pair of mass m_2 lie at $(0, \pm y)$. The periodic version of these orbits feature alternating horizontal and vertical collisions at the origin. Some relevant recent papers on this orbit include [34], [24], and [31]. Additionally, [25] and [13] include the rhomboidal four-body orbit as part of a larger class of periodic collision-based orbits. The $m_2 \to 0$ limiting case of this orbit is equivalent to the eccentricity-one version of the Sitnikov problem, featuring binary collision of the two non-zero masses at the origin. Since the zero-mass particles are symmetric for all time and exert no gravitational pull on each other, one may be ignored, giving the familiar Sitnikov setting. The results derived from research in this area readily generalized to the setting presented in this chapter.

The main portion of the chapter will be devoted to the proof of the following theorem:

Theorem 9.1. *There exists a four-branched, two-dimensional topological manifold $\mathcal{S}$ that separates Sitnikov-like $n+1$-body escape orbits from non-escape orbits. Moreover, each branch of $\mathcal{S}$ is either forward- or backward-invariant.*

The remainder of the chapter will be as follows: In Section 9.2, we establish the notation

that will be used throughout the chapter, as well as give the differential equations pertaining to the orbits which we are considering. Section 9.3 contains a theorem from topology that is a key ingredient to the proof of the Main Theorem. Section 9.4 contains the proof of the Main Theorem, broken into three parts. In Section 9.4.1, we build up some helpful results for the proof. Section 9.4.2 constitutes the bulk of the proof, and contains the majority of the construction of $\mathcal{S}$. Lastly, Section 9.4.3 completes the construction and gives some observations about $\mathcal{S}$. Section 9.5 focuses on numerical results pertaining to the Main Theorem. Section 9.5.1 gives a few more calculations that can be used to accelerate the pace of the numerical work. Sections 9.5.2 through 9.5.4 then give the results for various planar configurations. Lastly, Section 9.6 lists some open questions and gives some concluding remarks.

The results presented in this chapter were originally published as [65].

9.2 NOTATION

Consider any T-periodic planar configuration of n bodies whose coordinates are given by (x_1, y_1), ..., (x_n, y_n), and whose masses are given by m_1, ..., m_n. We will require that the configuration maintains a rotational symmetry throughout in the following sense: there is a fixed angle α which evenly divides 2π such that rotation of the plane through the angle α at any time yields the same physical setting (up to re-labeling of the bodies). For our purposes, no further restrictions need be placed on the planar bodies. In fact, no difficulty arises if planar orbits featuring regularized collisions are considered. Under the rotational symmetry condition, the acceleration of a massless particle on the z-axis will be in a direction parallel to the z-axis. Moreover, if the initial velocity of the particle on the z axis is also parallel to the z-axis, then the particle will remain on the z-axis for all time.

As the particular configuration of the planar masses will not be of much importance, we simplify notation slightly by setting

$$r_i = \sqrt{x_i^2 + y_i^2}$$

and consider only the distances from the origin of the bodies in the plane. Setting q to be the position of the massless particle on the z-axis with p its velocity, we have the following equations of motion:

$$\dot{q} = p, \tag{9.1}$$

$$\dot{p} = -\sum_{i=1}^{n} \frac{m_i q}{(r_i^2(t) + q^2)^{3/2}}, \tag{9.2}$$

where the dot represents the derivative with respect to time. It is important to remember that each of the r_i is time-dependent and T-periodic. At many points in our analysis, it will help to consider the time-independent system:

$$\dot{q} = p, \tag{9.3}$$

$$\dot{p} = -\sum_{i=1}^{n} \frac{m_i q}{\left(r_i^2(\theta) + q^2\right)^{3/2}}, \tag{9.4}$$

$$\dot{\theta} = 1 \tag{9.5}$$

and consider the behavior on $\mathbb{R} \times \mathbb{R} \times [0,T]$ with the $\theta = 0$ and $\theta = T$ planes identified. The flow given by equations 9.3 - 9.5 will be denoted ϕ_t, and points in this space will be given by ordered triples (p,q,θ). Note that changing the sign on both q and p also changes the sign of $\dot{q}$ and $\dot{p}$. Hence, understanding only half of the phase space is necessary to categorize the complete behavior of ϕ_t. For simplicity, we will consider the $q > 0$ region.

As the behavior near $q = \infty$ will be especially important for our analysis, we also define new variables Q and P by

$$Q = q^{-1/2},$$

$$P = p.$$

Note that under this change of variables, $Q = 0$ corresponds to $q = \infty$. In this setting, we have

$$\dot{Q} = -\frac{1}{2}Q^3 P, \tag{9.6}$$

$$\dot{P} = -\sum_{i=1}^{n} \frac{m_i Q^4}{\left(r_i^2(\theta)Q^4 + 1\right)^{3/2}}, \tag{9.7}$$

$$\dot{\theta} = 1. \tag{9.8}$$

We will use Φ_t to denote the flow on $[0,\infty) \times \mathbb{R} \times [0,T]$ as defined by 9.6 - 9.8, where the $\theta = 0$ and $\theta = T$ planes are again identified. Points in this coordinate setting will again be given by ordered triples (Q,P,θ).

Note that any point (Q,P,θ) with $Q = 0$ has a T-periodic orbit under Φ_t. These orbits correspond to orbits where the massless particle has escaped to infinity, de-coupling the system. Physically, the value of P is the velocity with which escape has occurred. In this setting, the new one-body system is not acted on by external force, and continues moving at its initial velocity in accordance with Newton's first law, while the planar configuration continues its periodic motion forever. If escape occurs with positive velocity, it is said to be *hyperbolic*. If escape occurs with zero velocity, it is said to be *parabolic*.

9.3 A Helpful Theorem

One tool that will be needed in our proof of the Main Theorem, but which is not directly related to the dynamics of the system, is presented below. It may be thought of as a topological version of the Closed Graph Theorem. However, to avoid confusion, we will refrain from referring to it as such. (This is presented as a problem in [66], p. 171.)

Theorem 9.2. *Let $f : X \to Y$, where Y is a compact Hausdorff space. Then f is continuous if and only if the graph Γ_f of f, defined as*

$$\Gamma_f = \{(x, f(x)) \ : \ x \in X\}$$

is closed in $X \times Y$.

We provide a proof for completeness.

Proof. Suppose that f is continuous, and let $\{x_n\} \to x$ in X. Then $f(x_n)$ converges to $f(x)$, and so the sequence of points $(x_n, f(x_n))$ converges to $(x, f(x))$. Since any sequence of points in Γ_f corresponds (via projection) to a sequence of points in x_n, we get that Γ_f is closed.

On the other hand, suppose that Γ_f is closed. Let V be any open neighborhood of $f(x_0)$ in Y, and let $V^c = Y - V$. Then $X \times V^c$ is closed, so $\Gamma_f \cap (X \times V^c)$ is closed. Since Y is compact, projecting the set $\Gamma_f \cap (X \times V^c)$ to X gives a closed set whose points correspond to the points mapped *outside* V by the function f. The complement of this set is therefore the open neighborhood required by the definition of continuity. □

9.4 Proof of the Main Theorem

9.4.1 Constructive Lemmas. In this section, we develop some results that will help to build up the surface described in the Main Theorem. We begin by making a number of important observations about the flow ϕ_t. The first is an observation from calculus.

Lemma 9.3. *There exists a positive number q_{mono} such that $\dot{p}$ is negative and monotonically increasing as a function of q for all $q > q_{mono}$ and for all θ.*

Proof. Recall that $\dot{p}$ is a sum of functions of the form

$$h_i(q) = -\frac{m_i q}{\left(r_i^2(\theta) + q^2\right)^{3/2}}.$$

For a fixed value of θ with $r_i^2(\theta) > 0$, the function $h_i(q)$ has the shape shown in Figure 9.1. (The $r_i(\theta) = 0$ case becomes the asymptotic curve $\dot{p} = q^{-3}$.)

Using basic calculus, we find the single critical point of h_i with $q > 0$ by evaluating $\partial\dot{p}/\partial q$. This value occurs when $q^2 = r_i^2/2$, or when $q = r_i/\sqrt{2}$. (Note that this still holds true for $r_i = 0$.) Since each r_i is continuous and periodic, each achieves a maximum value R_i over its period. So the

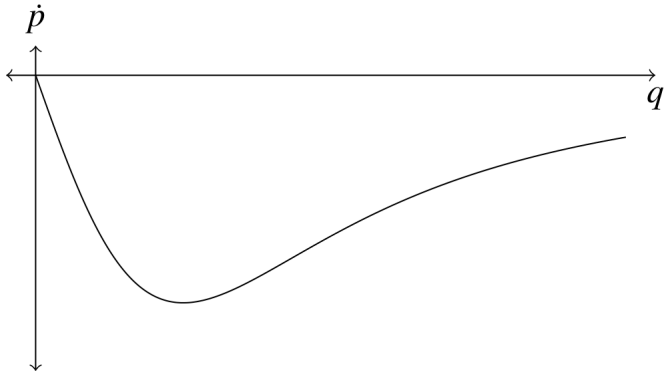

Figure 9.1: Typical shape of $h_i(q)$.

maximum value of q for which the above function can have its critical point is $R_i/\sqrt{2}$. So $h_i(q)$ is increasing for all $q > R_i/\sqrt{2}$ regardless of the value of θ. Setting q_{mono} to be the maximum of the values $R_i/\sqrt{2}$, then each $h_i(q)$ is increasing for $q > q_{\text{mono}}$ for any θ. Since $\dot{p}$ is simply the sum of all the h_i, $\dot{p}$ is increasing in q for all $q > q_{\text{mono}}$. □

Let $\phi_t^q(q_0, p_0, \theta_0)$ represent the value of the q variable under the flow ϕ_t with the prescribed initial conditions, and define ϕ_t^p and ϕ_t^θ similarly. It is worth noting that

$$\phi_t^\theta(q_0, p_0, \theta_0) = \theta_0 + t$$

for *any* initial conditions.

Lemma 9.4. *With q_{mono} as defined in Lemma 9.3, let q_1, q_2, p_1, and p_2 be positive numbers with $q_{mono} \leq q_1 \leq q_2$ and $p_1 \leq p_2$, and let $\theta_0 \in [0, T]$ be arbitrary. Let t_{final} be the (possibly infinite) maximum value of t for which both $\phi_t^p(q_1, p_1, \theta_0)$ and $\phi_t^p(q_2, p_2, \theta_0)$ are non-negative. Then, for $t \in (0, t_{final})$ we have that both $\phi_t^q(q_1, p_1, \theta_0) \leq \phi_t^q(q_2, p_2, \theta_0)$ and $\phi_t^p(q_1, p_1, \theta_0) \leq \phi_t^p(q_2, p_2, \theta_0)$.*

Proof. Define $\mathfrak{q} = \phi_t^q(q_2, p_2, \theta_0) - \phi_t^q(q_1, p_1, \theta_0)$ and $\mathfrak{p} = \phi_t^p(q_2, p_2, \theta_0) - \phi_t^p(q_1, p_1, \theta_0)$. Then, by assumption, both $\mathfrak{q} \geq 0$ and $\mathfrak{p} \geq 0$. It suffices to show that the set

$$\{(\mathfrak{q}, \mathfrak{p}) \ : \ \mathfrak{q} \geq 0, \mathfrak{p} \geq 0\}$$

is forward-invariant. We will do this by showing that the boundary of the region maps to the interior under the flow ϕ_t. Note that, by construction, $\dot{\mathfrak{q}} = \mathfrak{p}$. If $\mathfrak{q} = 0$ and $\mathfrak{p} > 0$, then $\dot{\mathfrak{q}} > 0$. On the other hand, if $\mathfrak{p} = 0$ and $\mathfrak{q} > 0$, then $\phi_t^q(q_2, p_2, \theta_0) > \phi_t^q(q_1, p_1, \theta_0)$. This implies that $\dot{\mathfrak{p}} > 0$ when $\mathfrak{p} = 0$ by Lemma 9.3. Lastly, if both $\mathfrak{q} = \mathfrak{p} = 0$, then $q_1 = q_2$ and $p_1 = p_2$, so $\mathfrak{q} = \mathfrak{p} = 0$ for all time by uniqueness of solution. Hence, the indicated set is forward-invariant. □

In a physical sense, Lemma 9.4 may be translated as the following: Consider the effect of placing two massless particles on the positive z-axis with some upward velocity. If their initial conditions are not identical and satisfy the conditions of Lemma 9.4, then:

- If both start at the same position, then the particle initially moving faster will be **both** moving faster **and** located farther away from the origin as long as both continue to move away from the origin.
- If both start with the same velocity, then the particle initially farther away from the origin will be **both** located farther away from the origin **and** moving faster as long as both continue to move away from the origin.
- If initial positions are not equal, and the particle farther from the origin also has greater velocity, then the particle farther from the origin will be **both** moving faster **and** be located farther away from the origin as long as both continue to move away from the origin.

Next, we give some analysis of some important behaviors of Φ_t. For this, we define functions Φ_t^Q and Φ_t^P in an analogous fashion to ϕ_t^q and ϕ_t^p.

Lemma 9.5. *Let $M = m_1 + \cdots + m_n$. Then, the set of all points (Q, P, θ) for which $P \geq \sqrt{2MQ}$ is forward-invariant.*

Two proofs of this Lemma will be given in this chapter. The first, presented here, is geometric in nature. A second, more analytic proof is presented as the proof of Theorem 9.12.

Proof. Let (Q, P, θ) be any point with $P \geq \sqrt{2MQ}$. Using equations 9.6 - 9.8 and projecting onto the QP-plane, we may think of this region as the area above a line. (See Figure 9.2.)

Now, note that

$$\begin{aligned}
|\dot{P}| &= \sum_{i=1}^{n} \frac{m_i Q^4}{\left(r_i^2(\theta)Q^4+1\right)^{3/2}} \\
&\leq \sum_{i=1}^{n} m_i Q^4 \\
&= MQ^4 \\
&= \left(\sqrt{\frac{M}{2}}Q^3\right)\left(\sqrt{2M}Q\right) \\
&\leq \sqrt{\frac{M}{2}}Q^3 P.
\end{aligned}$$

Then, we have that

$$\begin{aligned}
\left|\frac{\partial P}{\partial Q}\right| &= \left|\frac{\dot{P}}{\dot{Q}}\right| \\
&\leq \frac{\sqrt{\frac{M}{2}}Q^3 P}{\frac{1}{2}Q^3 P} \\
&= 2\sqrt{\frac{M}{2}} \\
&= \sqrt{2M}.
\end{aligned}$$

Geometrically, $\partial P/\partial Q$ represents the slope of a line in the P,Q plane. In our particular setting, this represents the directions that a trajectory of Φ_t^Q and Φ_t^P can take as t increases. Since both Φ_t^Q and Φ_t^P are decreasing, such trajectories must be decreasing in both variables. Moreover, since the maximum slope that such a trajectory can have is $\sqrt{2M}$ and the line $Q=0$ consists entirely of equilibria, it is impossible for a trajectory that begins in the $P \geq \sqrt{2M}Q$ region to escape it, as it cannot approach $P=\sqrt{2M}Q$.

□

9.4.2 The Core Construction. For this section, let $q_0 > q_{\text{mono}}$ be fixed, where q_{mono} is defined as in Lemma 9.3, and let $Q_0 = q_0^{-1/2}$ be the corresponding value in the inverted coordinate frame.

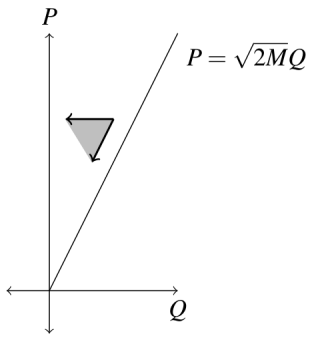

Figure 9.2: The "fan" of possible directions of a trajectory of Q and P at a given point.

The key step in the construction will be the following:

Theorem 9.6. *There exists a continuous function* $f(\theta) : [0,T] \to \mathbb{R}$ *such that*

$$\Phi_t^P(Q_0, f(\theta), \theta) \to 0 \text{ as } t \to \infty.$$

The remainder of this section will be the proof of this theorem. The function f will arise from the level set of another function g, which has to be defined in a piecewise fashion. Figure 9.3 will help to keep much of the notation straight.

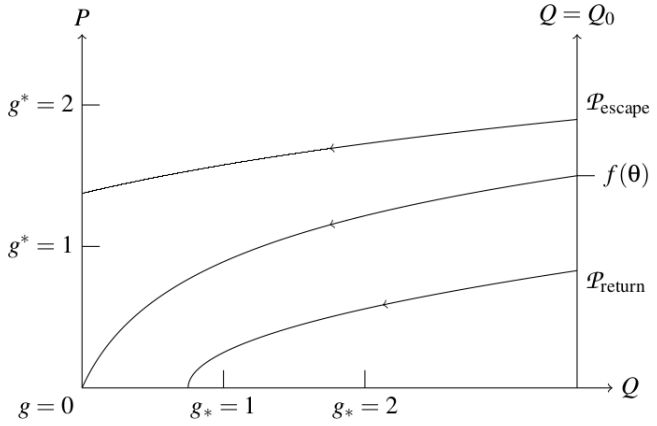

Figure 9.3: Simplified diagram for much of the notation in Section 9.4.2. The θ variable has been removed for ease of reading, but trajectories should be considered as taking place in (Q,P,θ) space.

To begin with, define the sets

$$\mathcal{P}_{\text{return}} = \{(Q_0,P,\theta) \ : \ P \geq 0, \ \theta \in [0,T], \ \Phi_t^P(Q_0,P,\theta) < 0 \text{ for some finite } t \geq 0\}$$

and

$$\mathcal{P}_{\text{escape}} = \{(Q_0, P, \theta) \ : \ P \geq 0, \ \theta \in [0, T], \ \lim_{t \to \infty} \Phi_t^P(Q_0, P, \theta)) > 0\}.$$

Physically, the set $\mathcal{P}_{\text{return}}$ corresponds to initial conditions that cause the massless particle to return to the origin, as the velocity P eventually becomes negative. On the other hand, $\mathcal{P}_{\text{escape}}$ corresponds to initial conditions that lead to the massless particle to escape to infinity with positive velocity (or hyperbolic escape). Certainly both sets are non-empty, as $(Q_0, 0, \theta) \in \mathcal{P}_{\text{return}}$ for any $\theta \in [0, T]$, and $\mathcal{P}_{\text{escape}}$ contains points for which Lemma 9.5 applies. Also, if $0 \leq P_1 < P_2$, then by Lemma 9.4:

- If $(Q_0, P_1, \theta) \in \mathcal{P}_{\text{escape}}$, then $(Q_0, P_2, \theta) \in \mathcal{P}_{\text{escape}}$, and
- If $(Q_0, P_2, \theta) \in \mathcal{P}_{\text{return}}$, then $(Q_0, P_1, \theta) \in \mathcal{P}_{\text{return}}$.

As the first step in building g, for all elements of $\mathcal{P}_{\text{return}}$, define

$$\tau(Q_0, P, \theta) = \max\{t \geq 0 \ : \ \Phi_t^P(Q_0, P, \theta) \geq 0\},$$

and define $g_* : \mathcal{P}_{\text{return}} \to \mathbb{R}$ by

$$g_*(Q_0, P, \theta) = \Phi^Q_{\tau(Q_0, P, \theta)}(Q_0, P, \theta).$$

In other words, g_* gives the position (in the inverted coordinate frame) at which the massless particle achieves its maximum before returning to the origin. Since τ is continuous by continuity with respect to initial conditions, then g_* is also continuous by composition.

By construction, the function g_* can take values only in the range $(0, Q_0]$. Moreover, by considering the backwards-time flow $\Phi_{-t}(Q, 0, \theta)$ over the set of points where $Q \in (0, Q_0]$ and $\theta \in [0, T]$, it is apparent that g_* is onto. Since $\mathcal{P}_{\text{return}}$ is the pre-image of the relatively open set set $(0, Q_0]$, then $\mathcal{P}_{\text{return}}$ is relatively open in the $Q = Q_0, P \geq 0$ plane. In fact, $g_*^{-1}((0, Q_0))$ is precisely $g_*^{-1}((0, Q_0])$ with the line $Q = Q_0$, $P = 0$ removed, and has two boundary curves – the aforementioned $Q = Q_0$, $P = 0$ line, and an upper ($P > 0$) yet-undetermined boundary.

We wish to extend this to a continuous function on $\overline{\mathcal{P}_{\text{return}}}$, where $\overline{\mathcal{P}_{\text{return}}}$ denotes the closure of $\mathcal{P}_{\text{return}}$. For any sequence of points in $\mathcal{P}_{\text{return}}$ that approach the open $P > 0$ boundary of $\mathcal{P}_{\text{return}}$, the sequence must eventually lie outside of $g_*^{-1}((\varepsilon, Q_0])$ for any $\varepsilon > 0$. Hence, defining g_* to be zero on the open boundary of $\mathcal{P}_{\text{return}}$ is a continuous extension of g_* to $\overline{\mathcal{P}_{\text{return}}}$.

We define a similar function $g^* : \mathcal{P}_{\text{escape}} \to \mathbb{R}$ by

$$g^*(Q_0, P, \theta) = \lim_{t \to \infty} \Phi_t^P(Q_0, P, \theta).$$

Physically, this function describes the velocity with which the massless particle escapes to infinity. By uniqueness of solutions to ODEs, this function is well-defined.

Lemma 9.7. *The function g^* as just defined is continuous and onto $(0, \infty)$.*

Proof. Recall from the proof of Lemma 9.5 that there is a limited interval of directions (thought of as slopes of lines) that trajectories in the (Q,P) plane can take under Φ_t. Using this, construct a truncated open "cone" $\mathcal{C}$ in the (Q,P) plane as pictured in Figure 9.4. Then, for any point (Q,P,θ) with $(Q,P) \in \mathcal{C}$, we know that $\Phi_t(Q,P,\theta) \in \mathcal{C} \times [0,T]$ for all $t > 0$. Let U be the union of all $\Phi_{-t}(\mathcal{C} \times [0,T])$ for $t \geq 0$. Then the set of all points in U with first coordinate Q_0 forms the relatively open set in $\mathcal{P}_{\text{escape}}$ required for the definition of continuity.

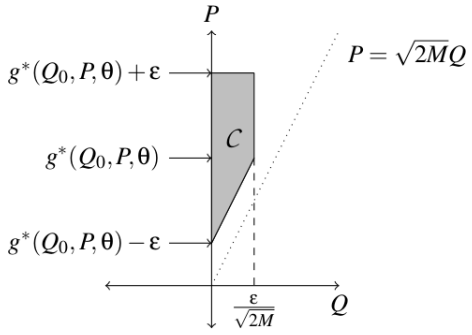

Figure 9.4: Construction of the truncated "cone" $\mathcal{C}$.

To show that g^* is onto, let L be any positive real number. Construct two non-intersecting "cones" $\mathcal{C}_1$ and $\mathcal{C}_2$ as in Figure 9.4, with a sufficiently small ε so that neither borders the point $(0,L)$, and so that $\mathcal{C}_1$ lies below the line $P = L$ and $\mathcal{C}_2$ lies above the line $P = L$. (See Figure 9.5.)

Then the pre-image of both $\mathcal{C}_i \times [0,T]$ under Φ_t intersecting $\mathcal{P}_{\text{escape}}$ contain two points which map to values of g^* which are above and below L. By continuity of g^*, there must then be a point at which $g^* = L$. □

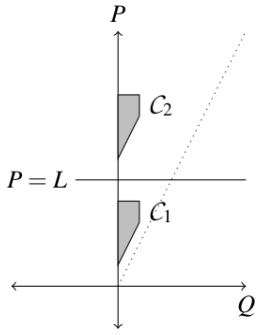

Figure 9.5: The function g^* is onto.

Similar to before, we now note that $\mathcal{P}_{\text{escape}}$ is open, as it is the continuous pre-image of the set $(0,\infty)$. We extend g^* to $\overline{\mathcal{P}_{\text{escape}}}$ by defining g^* to be zero on the boundary points. Such an extension is continuous. Finally, let $\mathcal{P} = \overline{\mathcal{P}_{\text{return}}} \cup \overline{\mathcal{P}_{\text{escape}}}$, and define $g : \mathcal{P} \to \mathbb{R}$ by

$$g(Q_0,P,\theta) = \begin{cases} g^*(Q_0,P,\theta) & : (Q_0,P,\theta) \in \overline{\mathcal{P}_{\text{escape}}} \\ -g_*(Q_0,P,\theta) & : (Q_0,P,\theta) \in \overline{\mathcal{P}_{\text{return}}} \end{cases}$$

It now remains to show that $\mathcal{P}$ is the set of all points with $Q = Q_0$ and $P \geq 0$.

Lemma 9.8. *For $Q = Q_0$ and a given θ_0, there is a single value of P satisfying $g(Q_0,P,\theta_0) = 0$.*

Proof. Suppose there are two values P_1 and P_2 with $P_1 < P_2$ so that

$$\Phi_t^P(Q_0,P_i,\theta_0) \to 0 \text{ as } t \to \infty$$

for $i = 1, 2$. Then, by Lemma 9.4 and the fact that both are assumed to escape to infinity, we must have $P_1 < P_2$ for all $t > 0$. Furthermore, by the proof of Lemma 9.4, the difference $P_2 - P_1$ must

be increasing for all t. Thus, it is impossible for

$$\lim_{t\to\infty} \Phi_t^P(Q_0, P_1, \theta_0) = 0 = \lim_{t\to\infty} \Phi_t^P(Q_0, P_2, \theta_0)$$

for $P_1 \neq P_2$. □

As a consequence, the upper boundary of $\mathcal{P}_{\text{return}}$ and the boundary of $\mathcal{P}_{\text{escape}}$ must be the same, as it is impossible for them to have an interval of any positive length separating them for any fixed value of θ. We can now define $f(\theta)$ to be the unique value such that $g(Q_0, f(\theta), \theta) = 0$. By construction of g, this gives the property

$$\Phi_t^P(Q_0, f(\theta), \theta) \to 0 \text{ as } t \to \infty$$

automatically. Since both of g_* and g^* are continuous in their respective domains, and they both take the value of 0 on their shared boundary, the new function g is continuous.

Lemma 9.9. *The function f is well-defined and continuous.*

Proof. We know f is well-defined by Lemma 9.8. Note that the set of all points $(Q_0, f(\theta), \theta)$ is closed, as it is precisely the set $g^{-1}(0)$. Then, by Theorem 9.2, we have that f is continuous, as the range of f is the compact interval $[0, \sqrt{2M}Q_0]$. □

9.4.3 The Final Parts. Here, we complete the proof of the Main Theorem and give some properties of the resulting surface $\mathcal{S}$. Let $\mathcal{G}$ be the set of all points $(Q_0, f(\theta), \theta)$, with Q_0 as defined in the previous section. Then the image of $\mathcal{G}$ under Φ_t for $t \in \mathbb{R}$ gives a topological 2-manifold $\mathcal{S}$ which is Φ_t-invariant and lies in the $q > 0$, $p > 0$ portion of phase space. Since changing the signs of q and p changes the sign of $\dot{q}$ and $\dot{p}$ in 9.1 and 9.2, the surface $\mathcal{S}$ is mirrored in the $q < 0$, $p < 0$ region "for free". Using the same coordinate changes for Q and P and running time backwards, we can construct an analogous surface $\mathcal{S}$ in the $q > 0$, $p < 0$ region and use symmetry to get the remaining two portions.

Theorem 9.10. *If $r_i(t) \neq 0$ for all i and for all t, then the p-coordinates of all points in $\mathcal{S}$ are bounded. In other words, $\mathcal{S}$ lies between the two planes $p = \pm B$ for some $0 < B < \infty$.*

Proof. Without loss of generality, consider the portion of $\mathcal{S}$ lying in the region $q > 0$, $p > 0$. (The $q > 0$, $p < 0$ region follows by reversing time. The $q < 0$ region then follows from symmetry.) Note that for any point $x = (q_0, p_x, \theta_x)$ in the set $\mathcal{G}$ described at the beginning of the section, forward images of x under ϕ_t will have decreasing values of p. Hence, only the backwards-time image of x need be considered to find a bound. In that case, the value of $\phi^p_{-t}(q_0, p_x, \theta_x)$ is increasing in t, but this rate of increase is bounded above by

$$\sum_{i=1}^{n} \frac{m_i q_0}{\sqrt{\varepsilon + q^2}} = \frac{M q_0}{\sqrt{\varepsilon + q^2}},$$

where $\varepsilon > 0$ is the minimum value of all the r_i on $[0, T]$. Furthermore, since $p_x > 0$, it must reach the $q = 0$ plane before $t = q_0/p_x$. Hence, the value of $\phi^p_{-t}(q_0, p_x, \theta_x)$ must be finite at the time the trajectory intersects the $q = 0$ plane, as it has a bounded rate of increase over a bounded time. Since mapping $\mathcal{G}$ to the $q = 0$ plane by ϕ_{-t} is continuous, the values of p on the intersection of $\mathcal{S}$ and $\{q = 0\}$ must be bounded. □

It is important to note that the $q > 0$ and $q < 0$ branches of $\mathcal{S}$ need not match up across the $q = 0$ plane. However, we can guarantee the existence of a few points where the two will match if the planar orbit satisfies certain symmetry properties.

Theorem 9.11. *Let t_0 be a real number for which all $r_i(t)$ satisfy $r_i(t_0 - t) = r_i(t_0 + t)$. Then there exists an orbit that escapes to infinity parabolically in both forward and reverse time which passes through the $q = 0$ plane when $\theta = t_0$ mod T.*

Proof. Let $(0, p_0, \theta_0)$ be a point with $\theta_0 = t_0 \bmod T$ such that $\phi_t(0, p_0, \theta_0) \in \mathcal{S}$ some for $t > 0$. Then $\phi_t(0, p_0, \theta_0) \in \mathcal{S}$ for all $t > 0$ by flow-invariance of $\mathcal{S}$. Since $r_i(t_0 - t) = r_i(t_0 + t)$, we then have $\phi^q_{-t}(0, p_0, \theta_0) = -\phi^q_t(0, p_0, \theta_0)$ and $\phi^p_{-t}(0, p_0, \theta_0) = -\phi^p_t(0, p_0, \theta_0)$. Since $\lim_{t\to\infty} \phi^q_t(0, p_0, \theta_0) = \infty$ and $\lim_{t\to\infty} \phi^p_t(0, p_0, \theta_0) = 0$ by construction, then we must have $\lim_{t\to\infty} \phi^q_{-t}(0, p_0, \theta_0) = -\infty$ and $\lim_{t\to\infty} \phi^p_{-t}(0, p_0, \theta_0) = 0$. □

In the case of the circular Sitnikov problem, such a time-reversing symmetry for the functions r_i exists for all t_0, and so the two branches of $\mathcal{S}$ will match exactly over $q = 0$. This is not too surprising, as this problem is completely integrable. For configurations with up to finitely many symmetries, the regions on which the two branches of $\mathcal{S}$ fail to line up on $q = 0$ give the "windows" through which any orbit passing from return to escape must pass. These will be the subject of the numerical investigations in the following section.

9.5 Numerical Investigations

9.5.1 A Numerical Catalyst. Before presenting any particular numerical worked examples, we present some theory that makes our numerical work simpler. Since $0 \leq r_i \leq R_i$ for all applicable i, then for $q > 0$, we have

$$q^3 \leq (r_i^2 + q^2)^{3/2} \leq (R_i^2 + q^2)^{3/2}.$$

Let $\mathfrak{R}$ be the maximum of $\{R_1, R_2, ..., R_n\}$. Then

$$q^3 \leq (r_i^2 + q^2)^{3/2} \leq (\mathfrak{R}_i^2 + q^2)^{3/2}.$$

Taking the reciprocal and multiplying by $m_i q$ gives

$$\frac{m_i}{q^2} \geq \frac{m_i q}{(r_i^2 + q^2)^{3/2}} \geq \frac{m_i q}{(\mathfrak{R}^2 + q^2)^{3/2}}.$$

Assuming further that $p > 0$, we then have that

$$\frac{-m_i p}{q^2} \leq \frac{-m_i qp}{(r_i^2 + q^2)^{3/2}} \leq \frac{-m_i qp}{(\mathfrak{R}^2 + q^2)^{3/2}}.$$

Since this holds for arbitrary i, it holds in the summation. We then have

$$\frac{-Mp}{q^2} \leq \sum_{i=1}^{n} \frac{-m_i qp}{(r_i^2 + q^2)^{3/2}} \leq \frac{-Mqp}{(\mathfrak{R}^2 + q^2)^{3/2}}.$$

The central quantity here is simply $p\dot{p}$. All of these expressions can be integrated explicitly with respect to t. Integrating over the interval $[t_a, t_b]$ gives

$$\frac{M}{q(t_b)} - \frac{M}{q(t_a)} \leq \frac{1}{2}p^2(t_b) - \frac{1}{2}p^2(t_a) \leq \frac{M}{\sqrt{\mathfrak{R}^2 + q^2(t_b)}} - \frac{M}{\sqrt{\mathfrak{R}^2 + q^2(t_a)}}. \tag{9.9}$$

Theorem 9.12. *If $q > 0$, $p > 0$, and*

$$E^* = \frac{1}{2}p^2(t_a) - \frac{M}{q(t_a)} > 0$$

at some time t_a, then $q(t) \to \infty$ as $t \to \infty$.

Proof. Re-arranging the right inequality in 9.9 gives

$$\frac{1}{2}(p(t_b))^2 \geq \frac{M}{q(t_b)} + E^*.$$

Hence, p is bounded below for all time $[t_a, t_b]$. As t_b was arbitrary and E^* only depends upon conditions at t_a, we have that p is bounded below for all time. Furthermore, p is bounded below uniformly by the value of E^*. Hence, q is increasing with its derivative bounded away from zero, so we must have $q \to \infty$ as $t \to \infty$. □

It is worth noting that in the inverted coordinates, the conditions of Theorem 9.12 become precisely those of Lemma 9.5. The geometric proof presented following Lemma 9.5 was useful for many of the details in Section 9.4. On the other hand, the proof of Theorem 9.12 can be more readily interpreted in terms of positions and velocities, giving a better physical intuition.

On the other hand, we also have

Theorem 9.13. *If $q > 0$, $p > 0$, and*

$$E_* = \frac{1}{2}p^2(t_a) - \frac{M}{\sqrt{\mathfrak{R}^2 + q^2(t_a)}} < 0$$

at some time t_a, then there is some future time t_b where $p(t_b) = 0$ and $q(t_b) < \infty$.

Proof. Rearranging the left inequality in 9.9, we have

$$\frac{1}{2}p^2(t_a) \leq \frac{M}{\sqrt{\mathfrak{R}^2 + q^2(t_b)}} + E_*.$$

Since the term on the left must be positive, the term on the right must be as well. This gives

$$-E_* \leq \frac{M}{\sqrt{\mathfrak{R}^2 + q^2(t_b)}}.$$

(Note that both sides here are positive.) Rearranging the equation then gives

$$q^2(t_b) \leq \left(\frac{M}{E_*}\right)^2 - \mathfrak{R}^2.$$

Since both numbers on the right are finite, we must have that q^2 is bounded, and so q is bounded as long as q and p are both positive. Then $\ddot{q}$ is negative and bounded away from zero on that same time interval, and so it must be the case that $\dot{q} = p = 0$ at some future time t_b. □

It is worth noting that if the inverted coordinates are used, the set $E_* = 0$ becomes the equation

$$P = \frac{\sqrt{2M}Q}{\sqrt[4]{R^2Q^4 + 1}}.$$

As $Q \to 0^+$, the derivative dP/dQ approaches $\sqrt{2M}$, which is the same as the boundary of the forward-invariant region given in Lemma 9.5. Since the invariant surface $\mathcal{S}$ must lie between the two, we can describe the linearized behavior of $\mathcal{S}$ near $Q = 0$–namely, $\mathcal{S}$ is locally approximated by $P = \sqrt{2M}Q$, independent of θ. Hence, we have a first-order approximation for a stable manifold of a degenerate fixed point (in the two-variable time-dependent system), similar to the work done by McGehee in [67].

Theorems 9.12 and 9.13 give readily verifiable conditions on q and p that determine whether the massless particle escapes to infinity or has a future point at which it again passes through the origin. The set of points in (q, p, θ) that satisfy these inequalities are not complements of each

other in $\mathbb{R}^3$, and the separating surface $\mathcal{S}$ must lie between them. It is also worth noting that these sets of points are merely forward-invariant under ϕ_t – there are points lying outside of these sets that eventually enter them under ϕ_t. This is helpful numerically, as we can obtain estimates of the intersection of $\mathcal{S}$ with the plane $q = q_0 \geq q_{\text{mono}}$, and hence find the value of $f(\theta)$, by fixing a value of θ and integrating initial conditions for various estimated values of p. Depending on which region they enter, we can adjust our guess upward or downward in a standard fashion (for instance, using the bisection method). This is very readily accomplished numerically in the inverted coordinate frame, as the intervals in which Q, P, and θ lie are all of finite length. Lastly, as described in Section 9.4.3, we can integrate to find the intersection of the image of this curve under ϕ_{-t} with the plane $q = 0$. These images can reveal some other interesting possible behaviors of the orbit of the massless particle.

9.5.2 A Non-circular Kepler Configuration. As a first example, we consider the classical Sitnikov problem with a non-circular Kepler orbit in the plane. Two bodies of mass 1 are initially placed at $(\pm 1, 0)$ with initial velocity $(0, \pm 1)$. This results in the intersecting ellipses shown in Figure 9.6.

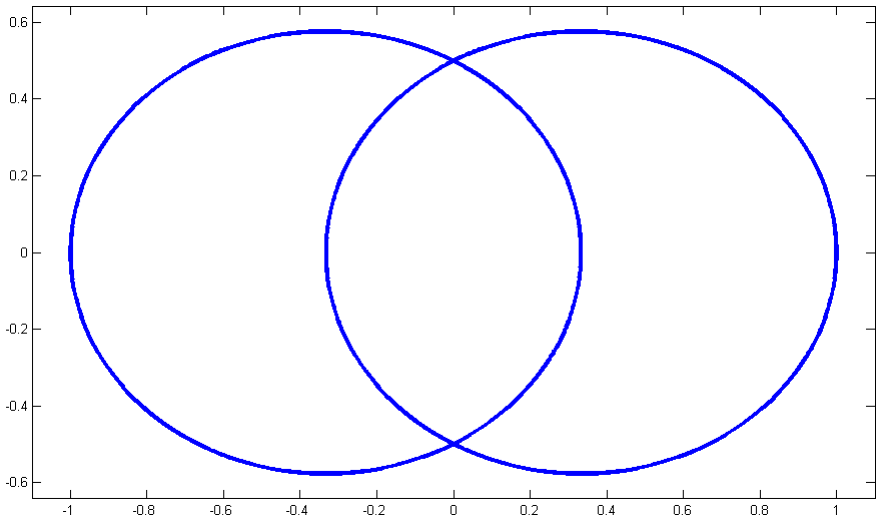

Figure 9.6: The planar two-body problem for Section 9.5.2 in the (x, y) plane.

This orbit has period $T \approx 2.4183$. The functions $r_1(t)$ and $r_2(t)$ satisfy $r_1(t) = r_2(t)$ for all t.

Further, with the initial conditions at the maximum distance from the origin, we have $r_1(T-t) = r_1(t)$. A similar symmetry $r_1(T/2+t) = r_1(T/2-t)$ exists at the point where the two bodies reach their minimum distance from the origin.

As $R_1 = R_2 = 1$ for this orbit, we choose the value of $q_0 = Q_0 = 1$ for convenience. Using the procedure described in Section 9.5.1 and the standard Runge-Kutta integration, we find the value of $P = f(\theta)$ for an evenly-spaced grid of points in the interval $\theta \in [0, T]$. The results of integrating these points back to the $q = 0$ plane are shown in Figure 9.7. It is worth noting that the peak value for parabolic escape occurs just before $t = T/2$. This is expected, as the gravitational pull along the z-axis of the planar orbit cannot be maximized at $T/2$ if $q = 0$.

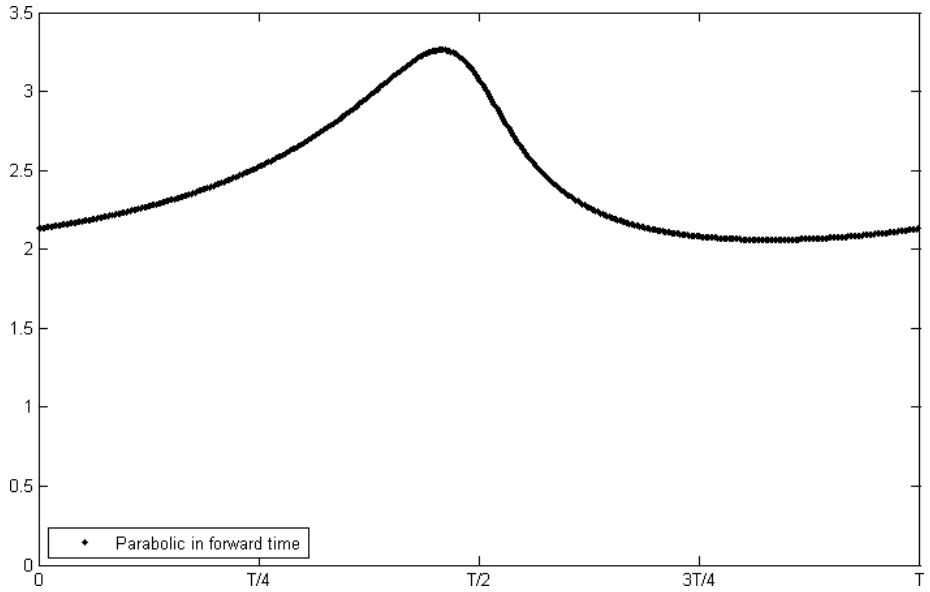

Figure 9.7: The limit of $\mathcal{S}$ on the $q = 0$ plane approaching from $q > 0$. Here, θ is plotted on the horizontal axis, and p is plotted on the vertical.

Let $\mathcal{S}_0^+$ denote the set of points shown in Figure 9.7. Owing to the time-reversing symmetry, we can also find the orbits which achieve parabolic escape in reverse time by reflecting the set $\mathcal{S}_0^+$ across the line $t = T$. Denote the resulting set $\mathcal{S}_0^-$. This is shown in Figure 9.8.

The set of points in the region where $\mathcal{S}_0^+$ lies below $\mathcal{S}_0^-$ $(T/2 < t < T)$ denotes initial conditions with $q = 0$ for which an orbit escapes hyperbolically in reverse time but returns at least once to the $q = 0$ plane in forward time. Similarly, points lying below $\mathcal{S}_0^+$ but above $\mathcal{S}_0^-$ $(0 < t < T/2)$

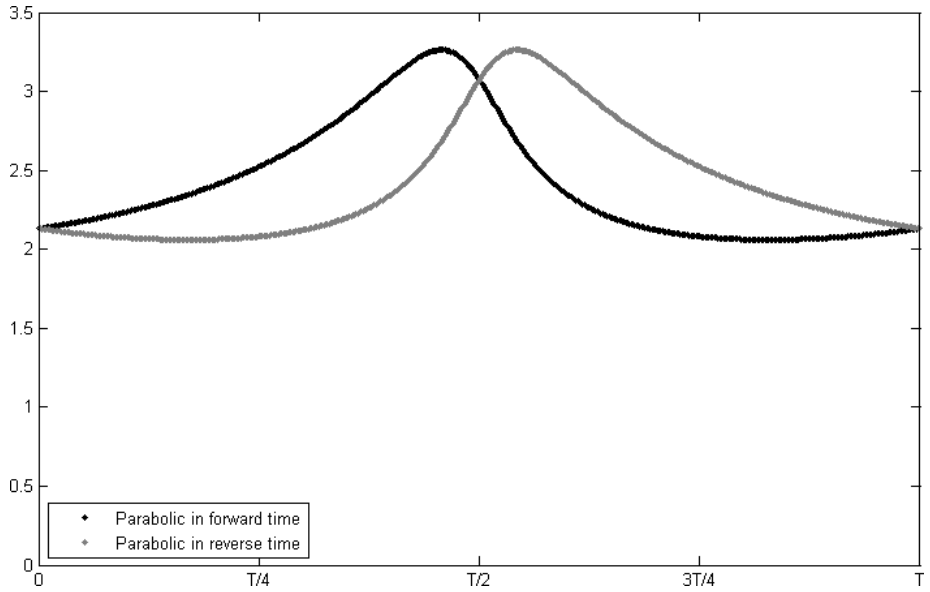

Figure 9.8: Figure 9.7 (darker), with the reverse-time parabolic escape orbit curve overlaid (lighter).

escape hyperbolically in forward time, but eventually return to $q = 0$ in reverse time. Points on either curve that lie above the other escape parabolically in either forward or reverse time, and hyperbolically in the other. The intersections of the two curves, which occur at $t = 0$ and $t = T/2$, correspond to the orbits which escape parabolically in both forward and reverse time.

We can observe more complicated behavior by integrating points that lie below the $\mathcal{S}_0^+$ curve and observing their next intersection with the $q = 0$ plane. Numerically, this can be slightly problematic, as behaviors near $q = \infty$ or $Q = 0$ involve high-order powers of very small terms. However, certain points far below $\mathcal{S}_0^+$ present no such problem. We show the results of one such integration in Figure 9.9. (It is worth noting that, strictly speaking, the starred points should have $p < 0$. However, since ϕ_t is symmetric with respect to $(q, p, \theta) \mapsto (-q, -p, \theta)$, an image similar to Figure 9.8 exists in the $q = 0$, $p < 0$ half-plane, and so we may consider the starred points in Figure 9.9 as the image of the corresponding points with $p < 0$.)

An interesting behavior is observed at the intersection of the curve of starred points and $\mathcal{S}_0^+$. This is another orbit that escapes parabolically in both forward and reverse time, but the number

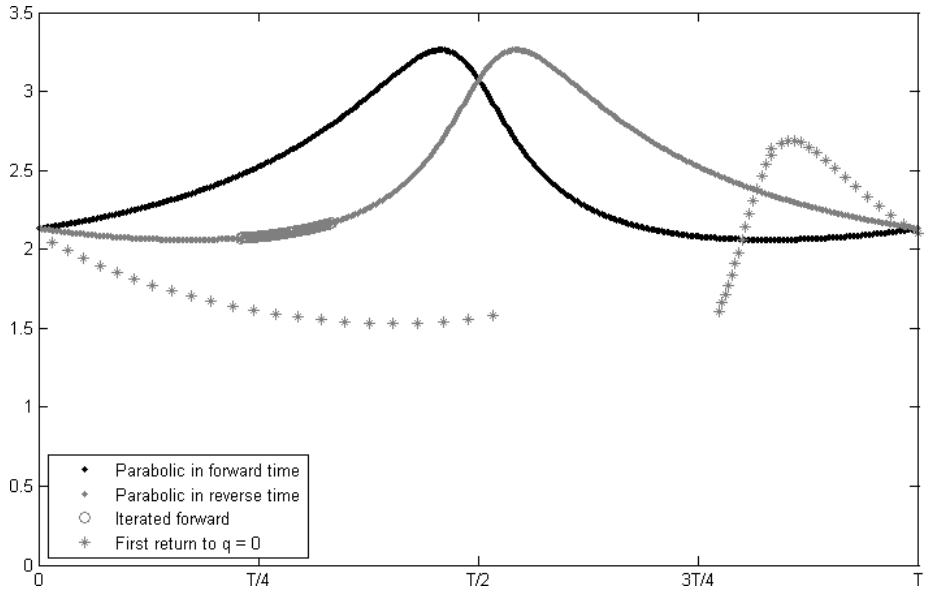

Figure 9.9: The indicated set of points on $\mathcal{S}_0^-$ integrated until they return to the $q = 0$ plane. The image under ϕ_t is denoted by the starred points.

of crossings through $q = 0$ varies. In this case, the forward-time orbit does not return to $q = 0$, but the reverse time orbit returns exactly once. Hence, this orbit connects a parabolic escape orbit at $q = \infty$ to a parabolic escape orbit at $q = \infty$ that passes through $q = 0$ exactly twice. In the $p < 0$ portion of the plane, the same phenomenon occurs, with an orbit connecting $q = -\infty$ to itself.

Again, due to the time-reversing symmetry, we obtain for free the result of the reverse-time image of the corresponding points on $\mathcal{S}_0^+$. The results are shown in Figure 9.10. Here, again, a new phenomenon occurs, with the intersection of the two starred curves, near the point $(T/2, 3/2)$. This point crosses $q = 0$ exactly once in forward and backward time, and then escapes parabolically. Hence, there is a parabolic orbit connecting $q = -\infty$ to $q = \infty$ and which passes through $q = 0$ exactly thrice.

9.5.3 A Configuration with Collision Singularities away from the Origin. In this section, we consider the planar orbit discussed in a series of papers ([26], [27], [28] and [29], see also [30]) that features simultaneous binary collisions away from the origin. Four bodies, each of mass $m = 1$, initially lie on the coordinate axes. Their initial velocities are perpendicular to the coordinate axes and equal in magnitude, leading to collisions as shown in Figure 9.11. It is shown in [26] that

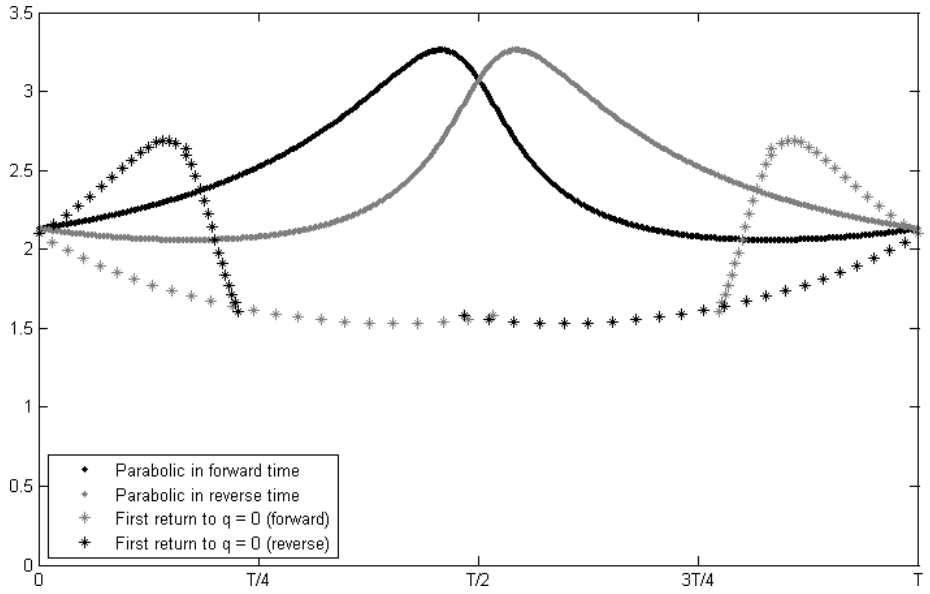

Figure 9.10: The symmetric image showing forward-time images of some points in $\mathcal{S}_0^-$ and reverse-time images of some points in $\mathcal{S}_0^+$.

the orbit exists as pictured, and is symmetric through rotation through the angle π. Moreover, the collisions in the orbit are regularizable. The regularization of the collisions of the four bodies involves changes in spatial coordinates, as well as a time change of the form $d\hat{t}/dt = u(x,y)$. The net effect of all of these changes is that the velocities of the four bodies is finite in the new coordinate frame, so the orbit may be continued past collision.

We may adapt the motion of the massless particle by performing the same time change on q and p, namely:

$$\dot{\hat{q}} = \frac{d\hat{t}}{dt}\dot{q}, \quad \dot{\hat{p}} = \frac{d\hat{t}}{dt}\dot{p}.$$

Similar transformations can be made to obtain inverted coordinates $\dot{\hat{Q}}$ and $\dot{\hat{P}}$. Then, replacing the time variable t by the fictional time variable τ, we obtain an equivalent system without singularities for the planar configuration and the massless particle. Specifically, the curves traced in $\mathbb{R}^4$ by $(x(t),y(t),q(t),p(t))$ and $(x(\hat{t}),y(\hat{t}),q(\hat{t}),p(\hat{t})$ are identical as sets of points, and differ only in the parameterization. Hence, we can perform our analysis in the regularized setting without any difficulty.

Placing the planar bodies at $(\pm 1,0)$ and $(0,\pm 1)$ with appropriate initial velocities yields a

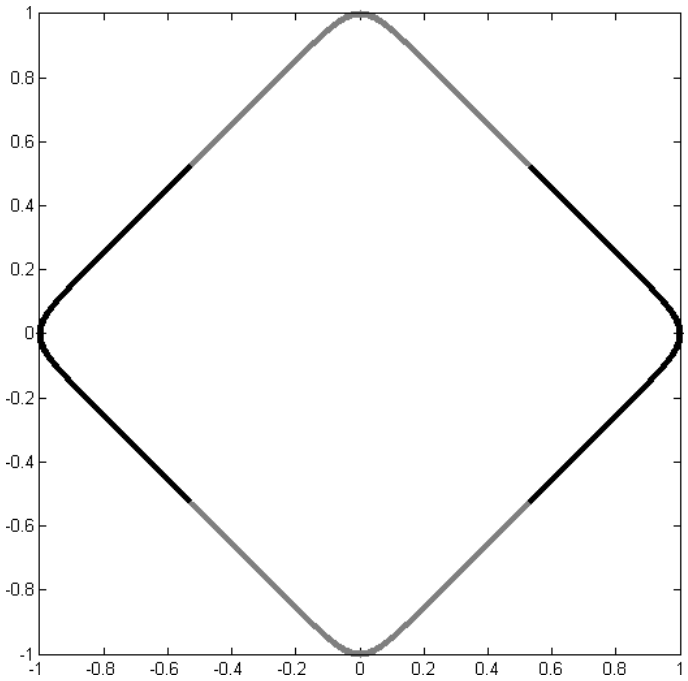

Figure 9.11: The simultaneous binary collision orbit featured in Section 9.5.3. At all times, the four bodies lie at positions (x,y), (y,x), $(-x,-y)$, and $(-y,-x)$. Collisions occur along the lines $y = x$ and $y = -x$.

planar orbit with period $\hat{t} \approx 6.4848$. Moreover, by the symmetry shown in Figure 9.11, we have that $r_1 = r_2 = r_3 = r_4$ for all time. For the first half of the period, we have all four bodies lying in the first and third quadrants, returning to the coordinate axes at the end of the interval. Then, over the second half, the four bodies lie in the second and fourth coordinates, repeating the same behavior up to reflection across either coordinate axis. Hence, each of the functions r_i is periodic with period $T \approx 3.2424$, as reflection across the coordinate axes does not change radial distance.

Figure 9.12 shows the result of repeating the numerical work as in Section 9.5.2. The central gap corresponds to the interval of time containing the collision. At this time, the value of $d\hat{t}/dt$ approaches zero, lengthening a momentary t-interval to a longer $\hat{t}$-interval. It is also important to note that the vertical scale is quite small, so the two curves are actually quite close to each other. For this reason, performing further numerical integration to obtain a figure similar to Figure 9.10 is problematic.

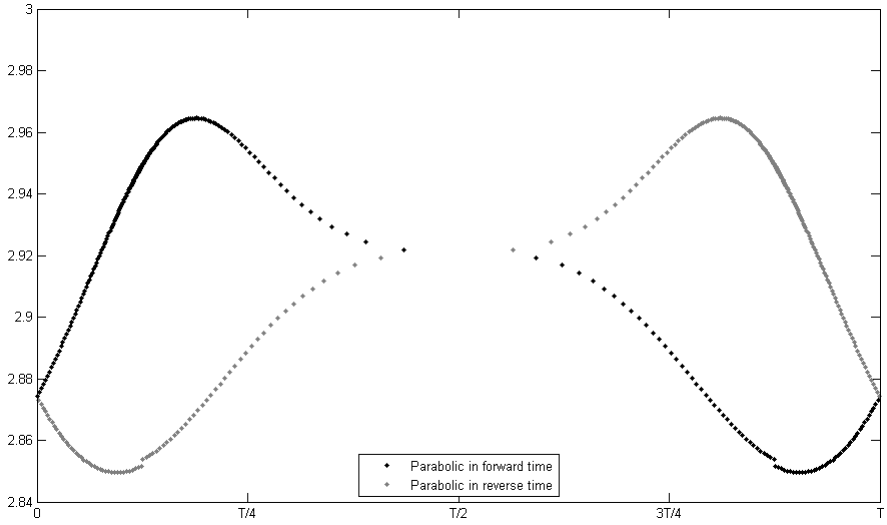

Figure 9.12: The $q = 0$ image corresponding to Figure 9.8 for the orbit of Section 9.5.3. Fictionalized time $\hat{t}$ lies on the horizontal axis, with p on the vertical. $T \approx 3.2424$.

9.5.4 The $e = 1$ Sitnikov Orbit, or the Restricted Rhomboidal Problem. As mentioned in the introduction, this work was the result of studying the Rhomboidal configuration as one pair of masses approaches $m = 0$. When $m = 0$, we have a collinear two-body configuration with collisions, and a pair of massless particles that are symmetric across the collinear configuration. Since the two massless particles have no influence over each other, removing one does not change the overall dynamics. In this setting, we have the Sitnikov problem with $e = 1$. For this, the solution of the planar orbit can be given explicitly, in both regularized and standard coordinates. In regularized time, we have that

$$r_1(\hat{t}) = r_2(\hat{t}) = \left| \frac{\sqrt{2}}{2} \sin\left(\frac{\hat{t}}{2}\right) \right|.$$

(This result comes from explicitly solving the regularized system presented in Chapter 2). This is 2π-periodic in $\hat{t}$. Since $r_i = 0$ for certain values of $\hat{t}$, Theorem 9.10 does not apply. We expect to see asymptotic "spikes" in the $q = 0$ plane corresponding to the times at which $r_i = 0$. Carrying out the same numerical studies as previous sections gives the result shown in Figure 9.13.

We can again produce the first-return map for the points corresponding to reverse-time parabolic orbit lying in $\theta > T/2$. In this instance, it is numerically feasible to perform this calculation for

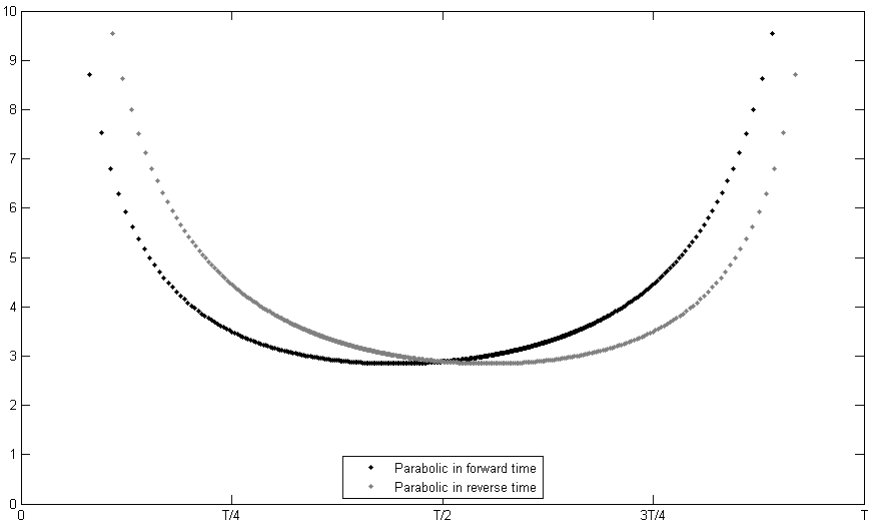

Figure 9.13: The $q = 0$ image corresponding to Figure 9.8 for the orbit of Section 9.5.4. Fictionalized time $\hat{t}$ lies on the horizontal axis, with p on the vertical. $T = 2\pi$.

nearly all such points. Prior to reduction mod T, asymptotic spikes appear at values of $\theta = nT$ for integer values of n. These are visible in Figure 9.14.

If we choose the interval $\theta \in [T, 2T]$ and overlay the corresponding points with Figure 9.13 (along with their reverse-time counterparts), we obtain the result shown in Figure 9.15. We could, of course, overlay any of the intervals $[nT, (n+1)T]$ and get a similar picture. In this case, the intersection of the return curves would correspond to orbits which escape parabolically in forward and reverse time, and cross through the $q = 0$ plane three times. By appropriate choice of n, we could specify an arbitrary number of periods through which the planar orbit passes between each of these three returns.

We could continue in similar fashion to obtain connecting parabolic orbits passing through $q = 0$ arbitrarily many times, with any finite integer sequence of periods completed between returns. It may be the case that the return times do not occur at exact integer multiples of the period, but counting only completed periods (e.g. counting collisions in the case of Sections 9.5.3 and 9.5.4) provides a more precise interpretation.

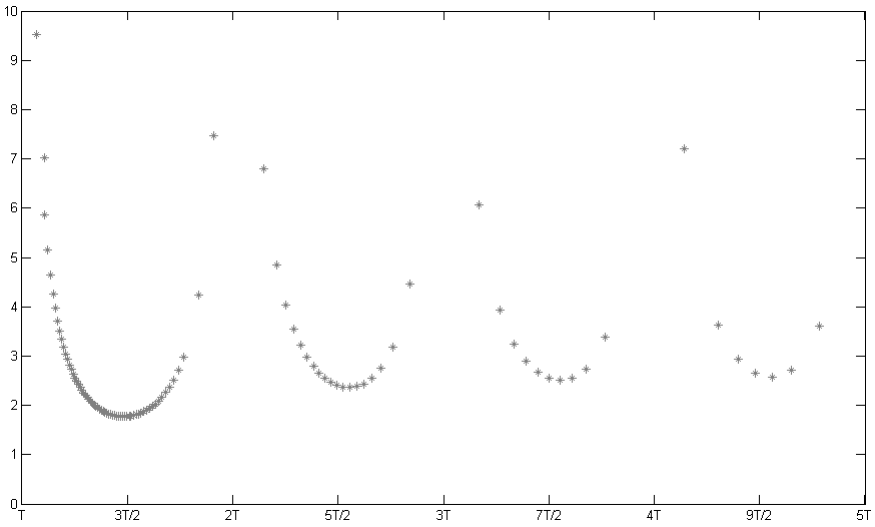

Figure 9.14: The $q = 0$ image corresponding to forward iteration of the "parabolic in reverse time" points lying below the "parabolic in forward time" curve, prior to reduction mod T. Fictionalized time $\hat{t}$ lies on the horizontal axis, with p on the vertical. $T = 2\pi$.

9.6 Concluding Remarks

9.6.1 Future Research. There are a few questions that we believe warrant further exploration. The foremost is the following:

Open Question 1. *Is $\mathcal{S}$ anything more than C^0? To what degree is this connected to the functions r_i?*

For example, the functions r_i of Sections 9.5.3 and 9.5.4 are merely continuous, with cusps at each collision time, whereas those of Section 9.5.2 are at least C^∞. Intuitively, we would expect this to cause a difference in the resulting surfaces $\mathcal{S}$ corresponding to each orbit.

Open Question 2. *Do the symbolic dynamics discussed in Section 9.5.4 hold for all orbits?*

We would expect that near the points in the $q = 0$ plane where forward- and reverse-time parabolic orbits intersect that there are return orbits with arbitrarily long return times. Since the planar orbits are periodic, this gives that an arbitrary number of periods can occur before the massless particle returns to the origin. The precise details of how these return regions overlap, however, will require much more work.

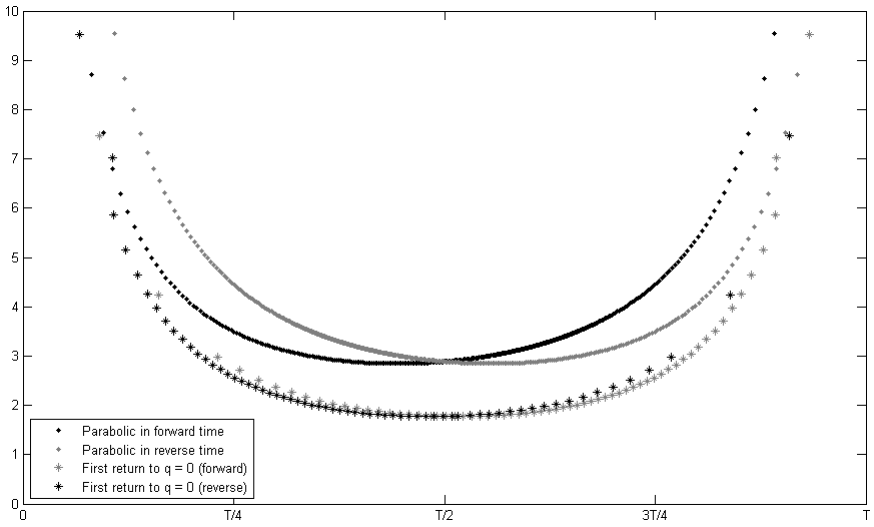

Figure 9.15: Analogue of Figure 9.10 for the orbit of Section 9.5.4. $T = 2\pi$.

APPENDIX A. A NUMERICAL ALGORITHM FOR FINDING PERIODIC ORBITS

The numerical determination of the initial conditions for all of the periodic orbits in this work all follow the same general technique. We will describe the algorithm in terms of the rhomboidal orbit of Chapter 8.

We restrict ourselves to the two-degrees-of-freedom case by setting $Q_2 = Q_3 = P_2 = P_3 = 0$ (e.g. remaining in $\mathcal{A}$). We model each of Q_1, Q_4, P_1, and P_4 by truncated trigonometric polynomials:

$$\tilde{Q}_1 = \sum_{i=0}^{n} a_i \sin((2i+1)s), \tag{A.1}$$

$$\tilde{Q}_4 = \sum_{i=0}^{n} b_i \sin((2i+1)(s+\pi/2)), \tag{A.2}$$

$$\tilde{P}_1 = \sum_{i=0}^{n} c_i \sin((2i+1)(s-\pi/2)), \tag{A.3}$$

$$\tilde{P}_4 = \sum_{i=0}^{n} d_i \sin((2i+1)s). \tag{A.4}$$

The choice of trigonometric polynomials is natural for modeling periodic behavior. A similar technique was carried out by Simó in [4]. The time shifts and choice of odd-only multiples of

s correspond to symmetries of the orbit. In particular, for these polynomials, the time-reversing symmetries shown earlier are built-in, and the non-colliding bodies have zero net momentum at collision time. For a fixed n, we numerically minimize the value of

$$\int_0^{2\pi} \left((Q_1' - \tilde{Q}_1')^2 + (Q_4' - \tilde{Q}_4')^2 + (P_1' - \tilde{P}_1')^2 + (P_4' - \tilde{P}_4')^2 \right) \, ds$$

where the minimization is taken over the space of coefficients $\{a_i, b_i, c_i, d_i\}$, and the non-approximated Q_i and P_i are evaluated at the approximated value. (Intuitively, this is a least-squares curve fit for the vector field determined by the differential equations.) We combine this with a root-finding technique to find the appropriate value of E for a 2π-periodic orbit. Once these trigonometric polynomials are determined, we can extract the initial conditions for the orbit by evaluating $\tilde{Q}_1, \tilde{Q}_4, \tilde{P}_1, \tilde{P}_4$ at any fixed time $s \in [0, 2\pi]$.

To obtain initial conditions for an interval of values of m, a "brute force" search for the first value must be performed first (unless initial conditions are available via some other technique). After that, a gradual "step-down" technique can be used to find the initial conditions for other nearby values of $m \in (0, 1]$, using the known values of the coefficients and E as an initial approximation.

BIBLIOGRAPHY

[1] Gareth E. Roberts. Linear stability analysis of the figure-eight orbit in the three-body problem. Ergodic Theory Dynam. Systems, 27(6):1947–1963, 2007.

[2] Cristopher Moore. Braids in classical dynamics. Phys. Rev. Lett., 70(24):3675–3679, 1993.

[3] Alain Chenciner and Richard Montgomery. A remarkable periodic solution of the three-body problem in the case of equal masses. Ann. of Math. (2), 152(3):881–901, 2000.

[4] C. Simó. New families of solutions in the n-body problem. Progress in Mathematics, 201:101–115, 2001.

[5] C. L. Siegel and J. K. Moser. Lectures on celestial mechanics. Classics in Mathematics. Springer-Verlag, Berlin, 1995.

[6] R. Martínez and C. Simó. The degree of differentiability of the regularization of simulaneous binary collisions in some n-body problems. Nonlinearity, 13:2107–2130, 2000.

[7] T. Ouyang and D. Yan. Simultaneous binary collision in the equal-mass collinear four-body problem. To appear in Electron. J. Differential Equations.

[8] M. S. Elbialy. On simultaneous binary collisions in the planar n-body problem. ZAMP, 44:880–890, 1993.

[9] J. Schubart. Numerische Aufsuchung periodischer Lösungen im Dreikörperproblem. Astr. Nachr., 283:17–22, 1956.

[10] M. Hénon. Stability of interplay orbits. Cel. Mech., 15:243–261, 1977.

[11] Andrea Venturelli. A variational proof of the existence of von Schubart's orbit. Discrete Contin. Dyn. Syst. Ser. B, 10(2-3):699–717, 2008.

[12] Richard Moeckel. A topological existence proof for the Schubart orbits in the collinear three-body problem. Discrete Contin. Dyn. Syst. Ser. B, 10(2-3):609–620, 2008.

[13] Mitsuru Shibayama. Minimizing periodic orbits with regularizable collisions in the n-body problem. Arch. Ration. Mech. Anal., 199(3):821–841, 2011.

[14] Jarmo Hietarinta and Seppo Mikkola. Chaos in the one-dimensional gravitational three-body problem. Chaos, 3(2):183–203, 1993.

[15] Winston L. Sweatman. The symmetrical one-dimensional Newtonian four-body problem: a numerical investigation. Celestial Mech. Dynam. Astronom., 82(2):179–201, 2002.

[16] Winston L. Sweatman. A family of symmetrical Schubart-like interplay orbits and their stability in the one-dimensional four-body problem. Celestial Mech. Dynam. Astronom., 94(1):37–65, 2006.

[17] M. Sekiguchi and K. Tanikawa. On the symmetric collinear four-body problem. Publ. Astron. Soc. Japan, 56:235–251, 2004.

[18] Tiancheng Ouyang and Duokui Yan. Periodic solutions with alternating singularities in the collinear four-body problem. Celestial Mech. Dynam. Astronom., 109(3):229–239, 2011.

[19] S.J. Aarseth and K. Zare. A regularization of the three-body problem. Celest. Mech. Dynam. Astron., 10:185–205, 1974.

[20] T. Ouyang and Z. Xie. Regularization of simultaneous binary collisions and solutions with singularities in the collinear four-body problem. Dis. Con. Dyn. Sys., 24(3):909–932, 2009.

[21] M. Saito and K. Tanikawa. The rectilinear three-body problem using symbol sequence i. role of triple collisions. Celest. Mech. Dynam. Astron., 98:95–120, 2007.

[22] M. Saito and K. Tanikawa. The rectilinear three-body problem using symbol sequence ii: Role of periodic orbits. Celest. Mech. Dynam. Astron., 103:191–207, 2009.

[23] M. Saito and K. Tanikawa. Non-schubart periodic orbits in the rectilinear three-body problem. Celest. Mech. Dynam. Astron., 107:397–407, 2010.

[24] Duokui Yan. Existence and linear stability of the rhomboidal periodic orbit in the planar equal mass four-body problem. J. Math. Anal. Appl., 388(2):942–951, 2012.

[25] Regina Martínez. On the existence of doubly symmetric "Schubart-like" periodic orbits. Discrete Contin. Dyn. Syst. Ser. B, 17(3):943–975, 2012.

[26] Tiancheng Ouyang, Duokui Yan, and Skyler Simmons. Periodic solutions with singularities in two dimensions in the n-body problem. Rocky Mtn. J. Math., 42(4):1601–1614, 2012.

[27] Lennard F. Bakker, Tiancheng Ouyang, Duokui Yan, Skyler Simmons, and Gareth E. Roberts. Linear stability for some symmetric periodic simultaneous binary collision orbits in the four-body problem. Celestial Mech. Dynam. Astronom., 108(2):147–164, 2010.

[28] Lennard F. Bakker, Tiancheng Ouyang, Duokui Yan, and Skyler Simmons. Existence and stability of symmetric periodic simultaneous binary collision orbits in the planar pairwise symmetric four-body problem. Celestial Mech. Dynam. Astronom., 110(3):271–290, 2011.

[29] Lennard F. Bakker, Tiancheng Ouyang, Duokui Yan, and Skyler Simmons. Erratum to: Existence and stability of symmetric periodic simultaneous binary collision orbits in the planar pairwise symmetric four-body problem [mr2821623]. Celestial Mech. Dynam. Astronom., 112(4):459–460, 2012.

[30] Lennard F. Bakker, Scott Mancuso, and Skyler C. Simmons. Linear stability for some symmetric periodic simultaneous binary collision orbits in the planar pairwise symmetric four-body problem. J. Math. Anal. Appl., 392(2):136–147, 2012.

[31] Lennard Bakker and Skyler Simmons. Stability of the rhomboidal symmetric-mass orbit. Disc. Cont. Dyn. Sys. A, 35(1):1–23, 2015.

[32] Anoop Sivasankaran, Bonnie A. Steves, and Winston L. Sweatman. A global regularisation for integrating the Caledonian symmetric four-body problem. Celestial Mech. Dynam. Astronom., 107(1-2):157–168, 2010.

[33] Archie E. Roy and Bonnie A. Steves. The Caledonian symmetrical double binary four-body problem. I. Surfaces of zero-velocity using the energy integral. Celestial Mech. Dynam. Astronom., 78(1-4):299–318 (2001), 2000.

[34] Jörg Waldvogel. The rhomboidal symmetric four-body problem. Celestial Mech. Dynam. Astronom., 113(1):113–123, 2012.

[35] I. S. Newton. Philosophiae naturalis principia mathematica. William Dawson & Sons, Ltd., London, undated.

[36] H Bruns. über die integrale des vielkörper-problems. Acta Math., 11:25–96, 1887-1888.

[37] Kenneth R. Meyer, Glen R. Hall, and Dan Offin. Introduction to Hamiltonian dynamical systems and the *N*-body problem, volume 90 of Applied Mathematical Sciences. Springer, New York, second edition, 2009.

[38] Zhihong Xia. The existence of the noncollision singularities in Newtonian system. ProQuest LLC, Ann Arbor, MI, 1989. Thesis (Ph.D.)–Northwestern University.

[39] T Levi-Civita. Sur la régularisation du problème de trois corpis. Acta Math., 42:99–144.

[40] G. Roberts. Linear stability analysis of the figure-eight orbit in the three-body problem. Ergod. Th. and Dynam. Sys., 27:1947–1963, 2007.

[41] Donald G. Saari. Collisions, rings, and other Newtonian *N*-body problems, volume 104 of CBMS Regional Conference Series in Mathematics. Published for the Conference Board of the Mathematical Sciences, Washington, DC; by the American Mathematical Society, Providence, RI, 2005.

[42] A. Sivasankaran, B. Steves, and W. Sweatman. A global regularisation for integrating the caledonian symmetric four-body problem. Celest. Mech. Dynam. Astron., 107:157–168, 2010.

[43] Yiming Long. Index theory for symplectic paths with applications, volume 207 of Progress in Mathematics. Birkhäuser Verlag, Basel, 2002.

[44] Abed Bounemoura. Generic super-exponential stability of invariant tori in Hamiltonian systems. Ergodic Theory Dynam. Systems, 31(5):1287–1303, 2011.

[45] K. Sitnikov. The existence of oscillatory motions in the three-body problems. Soviet Physics. Dokl., 5:647–650, 1960.

[46] W. MacMillan. An integrable case in the restricted problem of three bodies. Astron. J., 27:11–13, 1913.

[47] J. Hagel. A new analytic approach to the Sitnikov problem. Celestial Mech. Dynam. Astronom., 53(3):267–292, 1992.

[48] S. B. Faruque. Solution of the Sitnikov problem. Celestial Mech. Dynam. Astronom., 87(4):353–369, 2003.

[49] Johannes Hagel and Christoph Lhotka. A high order perturbation analysis of the Sitnikov problem. Celestial Mech. Dynam. Astronom., 93(1-4):201–228, 2005.

[50] Lidia Jiménez-Lara and Adolfo Escalona-Buendía. Symmetries and bifurcations in the Sitnikov problem. Celestial Mech. Dynam. Astronom., 79(2):97–117, 2001.

[51] Jaume Llibre and Rafael Ortega. On the families of periodic orbits of the Sitnikov problem. SIAM J. Appl. Dyn. Syst., 7(2):561–576, 2008.

[52] Rafael Ortega and Andrés Rivera. Global bifurcations from the center of mass in the Sitnikov problem. Discrete Contin. Dyn. Syst. Ser. B, 14(2):719–732, 2010.

[53] Marcelo Marchesin and César Castilho. Subharmonic solutions in the Sitnikov problem. Qual. Theory Dyn. Syst., 7(1):213–226, 2008.

[54] Andrés Rivera. Periodic solutions in the generalized Sitnikov $(N+1)$-body problem. SIAM J. Appl. Dyn. Syst., 12(3):1515–1540, 2013.

[55] Marcelo Marchesin and Claudio Vidal. Spatial restricted rhomboidal five-body problem and horizontal stability of its periodic solutions. Celestial Mech. Dynam. Astronom., 115(3):261–279, 2013.

[56] Vladislav V. Sidorenko. On the circular Sitnikov problem: the alternation of stability and instability in the family of vertical motions. Celestial Mech. Dynam. Astronom., 109(4):367–384, 2011.

[57] V. M. Alekseev. Quasirandom dynamical systems. II. One-dimensional nonlinear vibrations in a periodically perturbed field. Mat. Sb. (N.S.), 77 (119):545–601, 1968.

[58] V. M. Alekseev. Quasirandom dynamical systems. III. Quasirandom vibrations of one-dimensional oscillators. Mat. Sb. (N.S.), 78 (120):3–50, 1969.

[59] V. M. Alekseev. Quasirandom dynamical systems. I. Quasirandom diffeomorphisms. Mat. Sb. (N.S.), 76 (118):72–134, 1968.

[60] Jürgen Moser. Stable and random motions in dynamical systems. Princeton University Press, Princeton, N. J.; University of Tokyo Press, Tokyo, 1973. With special emphasis on celestial mechanics, Hermann Weyl Lectures, the Institute for Advanced Study, Princeton, N. J, Annals of Mathematics Studies, No. 77.

[61] Jie Liu and Yi Sui Sun. On the Sitnikov problem. Celestial Mech. Dynam. Astronom., 49(3):285–302, 1990.

[62] E. A. Perdios. The manifolds of families of 3D periodic orbits associated to Sitnikov motions in the restricted three-body problem. Celestial Mech. Dynam. Astronom., 99(2):85–104, 2007.

[63] E. Perdios and V. V. Markellos. Stability and bifurcations of Sitnikov motions. Celestial Mech., 42(1-4):187–200, 1987/88.

[64] P. S. Soulis, K. E. Papadakis, and T. Bountis. Periodic orbits and bifurcations in the Sitnikov four-body problem. Celestial Mech. Dynam. Astronom., 100(4):251–266, 2008.

[65] Lennard Bakker and Skyler Simmons. A separating surface for Sitnikov-like $n+1$-body problems. J. Differential Equations, 258(9):3063–3087, 2015.

[66] James R. Munkres. Topology: a first course, 2E. Prentice-Hall, Inc., Upper Saddle River, N.J., 2000.

[67] Richard McGehee. A stable manifold theorem for degenerate fixed points with applications to celestial mechanics. J. Differential Equations, 14:70–88, 1973.